

**Effect of Selective Up regulation of Prostacyclin Synthesis On Its Signaling And  
Vascular Protection**

---

A Dissertation Presented to  
The Department of Pharmacological and Pharmaceutical Sciences  
University of Houston

---

In Partial Fulfillment of  
The Requirement for the Degree of  
Doctor of Philosophy in Pharmacology

---

By  
Anita Janardhan Mohite

August 2011

## **ACKNOWLEDGEMENTS**

It is a pleasure to convey my gratitude to all of those who made this dissertation possible. I owe my deepest gratitude to my advisor, Dr. Ke-He Ruan, for his constant support, advice, guidance and encouragement through out the entire research. His ideas and his passion for research has always inspired me and enriched my growth as a student and a researcher. I would like to thank him for designing the superenzyme (triple catalytic enzyme-1) and for giving me a chance to work on this interesting project.

I am heartily thankful to all my committee members, Dr. Richard Bond, Dr. Louis Williams, Dr. Rong Yu and Dr. Xiaolian Gao for their time, constructive comments and suggestions on this dissertation. I am thankful that in the midst of all their activity, they accepted to be members of my dissertation committee. I am indebted to them, for the friendly support during the committee meeting and defense. I would like to express my special thanks to Dr. Williams for his fatherly support and encouragement.

I would also like to thank Dr. Brian Knoll and Dr. Vincent Lau for their administrative support. I would like to thank all the staff members of the PPS department for their hardwork in providing me all the knowledge during the courses. Thank you Dr. Bond for being such a wonderful teacher during the literature review course as this course has helped me develop my presentation skills as well as

confidence. I thank the department and University of Houston for giving me a chance to study and finish my graduate degree here.

I would like to thank all the graduate students for their continuous love and support. I am deeply indebted to Alice and Vanessa for being the most friendly, wonderful and supportive lab mates. I would like to thank Jaixin for his help in teaching me LC/MS. I would like to thank Alice for her contribution to this research work. I would also like to thank Cori and Manish for being there always whenever I needed help in my research. I would like to thank Anirudha for his support and guidance as a former lab mate.

I would like to thank the Animal House Committee members with special mention of Dr. Blasdel and Christina for their support in our animal related research. I would like to thank Dr. Gao, Qi and LC Sciences for the miRNA Microarray services. I would like to thank UT Health Science Center for the RNA illumina assay and MD Anderson for the transgenic mice.

My parents deserve special mention for their inseparable support and prayers. My Father and mother are the two persons who not only set the platform for my education but also who showed confidence in whatever decision I made. Thank you Achan and Mummy for everthing. Pramila, Pinki, Chinki, Vicky, thanks for being supportive and caring siblings.

Words fail me to express my appreciation towards my wonderful husband Samit whose dedication, love and persistent confidence in me, has taken the load off my shoulder. I owe him for being such a supportive and enthusiastic life partner. My PhD dissertation wasn't possible without you and thank you for everthing. I would also like to thank my in laws, Mummy, Papa, Ma, Daddy, Bhaiyya, Didi for their extended support throughout these years of research. I would like to specifically mention that I am extraordinarily fortunate to have a mother in law like mine whose motherly support, prayers and confidence has helped me to reach the stage of completion of my graduation. Thank you Piku, Didu and my sweet little kiddo, Neil. Last but not the least, I would like to thank my baby, Arnavi whose arrival in my life boosted my energy and gave me all the strength to finish my research work. Finally I would like to thank God for being there always.

**Effect of Selective Up regulation of Prostacyclin Synthesis On Its Signaling And  
Vascular Protection**

---

An Abstract of a Dissertation Presented to  
The Department of Pharmacological and Pharmaceutical Sciences  
University of Houston

---

In Partial Fulfillment of  
The Requirement for the Degree of  
Doctor of Philosophy in Pharmacology

---

By  
Anita Janardhan Mohite

August 2011

## ABSTRACT

Prostacyclin (PGI<sub>2</sub>) is a very important endogenous vascular protector. It provides vascular protection through actions like vasodilatation, platelet aggregation and vascular smooth muscle cell proliferation inhibition and smooth muscle differentiation regulation. Therefore since decades, there have been many ongoing attempts to use PGI<sub>2</sub> to treat vascular disorders such as pulmonary arterial hypertension, peripheral artery disease and thrombosis. However, the short half-life of PGI<sub>2</sub> has limited its therapeutic potential.

PGI<sub>2</sub> is synthesized endogenously from arachidonic acid using enzymes cyclooxygenase isoform 1/2(COX-1/2) and prostacyclin synthase (PGIS). Single gene therapy with either COX or PGIS through adenoviral vectors does not specifically overproduce PGI<sub>2</sub> and also is associated with inflammatory reactions. Thus to address these problems, our lab engineered a single hybrid gene (COX-1-10aa-PGIS) by fusing COX-1 with PGIS through transmembrane linker of 10 amino acids (10aa).

Adipose tissue derived cells have been used therapeutically in several vascular disorders due to their regenerative properties. Thus we isolated and cultured mature adipocytes (MA) from mouse adipose tissue and called it as prostanoid synthesizing fat cells (PSFC). Further, we engineered a novel adipose tissue-derived cell that constantly produces PGI<sub>2</sub>, through transfecting of the engineered cDNA of the hybrid enzyme

(human COX-1-10-aa-PGIS), which has superior triple catalytic functions in directly converting arachidonic acid into PGI<sub>2</sub>. The gene-transfected cells were further converted into a stable cell line, in which the cells constantly expressed the hybrid enzyme and were capable of overproducing specifically PGI<sub>2</sub> and thus we called this cell line as PGI<sub>2</sub> producing PSFC (PGI<sub>2</sub>-PSFC). When the results of the HPLC activity assay and LC/MS/MS were compared between just vector transfected (PSFC) and COX-1-10aa-PGIS gene transfected cells (PGI<sub>2</sub>-PSFC), it was observed that the majority of the endogenous AA metabolism shifted from that of unwanted PGE<sub>2</sub> (in PSFC) to that of the preferred PGI<sub>2</sub> (in PGI<sub>2</sub>-PSFC) with a PGI<sub>2</sub>/PGE<sub>2</sub> ratio change from 0.03 to 25. The PGI<sub>2</sub>-producing cell line not only exhibited an approximate 50-fold increase in PGI<sub>2</sub> biosynthesis, but also demonstrated superior anti-platelet aggregation *in vitro*, and increased reperfusion in the mouse ischemic hindlimb and thrombogenesis models *in vivo*.

PGI<sub>2</sub> regulates functions like vascular smooth muscle cell differentiation and proliferation and apoptosis. These actions are mediated through the PGI<sub>2</sub> receptor (IP) and nuclear receptor, peroxisome proliferator-activated receptors (PPAR). MicroRNAs (miRNAs), which are negative regulators of gene expression, also regulate similar functions like PGI<sub>2</sub>. PGI<sub>2</sub> regulates expression of genes by signaling through PPARs. Thus to find out if PGI<sub>2</sub> regulates gene expression by regulating miRNA expression by signaling through the IP and PPAR, a miRNA microarray analysis of the PGI<sub>2</sub>-PSFCs and PSFCs was performed. Analysis of the results obtained from miRNA study, revealed that PGI<sub>2</sub> is

involved in regulating cellular microRNA (miRNA) expression through its receptors in the mouse adipose tissue-derived primary culture cell line overexpressing COX-1-10aa-PGIS (PGI<sub>2</sub>-PSFC). The miRNA microarray analysis of the PGI<sub>2</sub>-PSFC revealed a significant up-regulation (711, 148b, and 744) and down-regulation of miRNAs of interest, which were reversed by antagonists to the IP and PPAR $\gamma$  receptors. Furthermore, we also found that the insulin-mediated lipid deposition was inhibited in the PGI<sub>2</sub>-PSFCs. The study also initiated a discussion, which suggested that the endogenous PGI<sub>2</sub> inhibition of lipid deposition in adipocytes could involve miRNA-mediated inhibition of expression of the targeted genes specifically of Akt1.

To translate the results of *in vitro* study, a transgenic mouse permanently expressing the COX-1-10aa-PGIS gene was generated. This genetic mouse animal model was used to study the effect of COX-1-10aa-PGIS overexpression on PGI<sub>2</sub> production *in vivo* and as well as its vascular protective effect. The transgenic mice was genotyped using polymerase chain reaction and further bred to develop a colony of homozygous transgenic mice. Quantitative PCR was performed to distinguish between the hemizygous and homozygous mice. PCR and immunoblot analysis of all the organs and tissues of mice revealed the expression of COX-1-10aa-PGIS in adipose tissue, brain, heart and uterus. LC/MS analysis of urine and plasma revealed approximately five-folds increase in PGI<sub>2</sub> biosynthesis permanently *in vivo*. The animals showed strong resistance to photochemical induced thrombosis. They produced healthy pups with a an increase

in live births when compared to the wild type without significant adverse effects in development and functions of major organs including brain, heart, kidneys. Tail cuff method was used to measure blood pressure of the mice which was similar to that in the wild type.

Thus PGI<sub>2</sub>-PSFCs (therapeutic cells) can be used as cell therapy as an alternative to adenoviral gene transfer to treat ischemic and vascular conditions. The cells, which have an ability to increase the biosynthesis of the vascular protector, PGI<sub>2</sub>, while reducing that of the vascular inflammatory mediator, PGE<sub>2</sub>, provide a dual effect on vascular protection, which is not available through any existing drug treatments. Thus, the current finding has potential to be an experimental intervention for PGI<sub>2</sub>-deficient diseases, such as pulmonary arterial hypertension. PGI<sub>2</sub> mediated gene expression regulation through miRNA expression regulation has unraveled a novel signaling mechanism for PGI<sub>2</sub>. This signaling could exist in broad pathophysiological processes involving PGI<sub>2</sub> (i.e. apoptosis, vascular inflammation, cancer, embryo implantation, and obesity). The results of the transgenic mice overexpressing COX-1-10aa-PGIS and producing PGI<sub>2</sub> provides the first evidences that risk of stroke and heart diseases could be reduced by the human transgene, as well as the insight into the possible future transgenic medicine to prevent and reduce the genetic risk of heart disease.

## TABLE OF CONTENTS

<b>Abstract</b>	<b>vii</b>
<b>List of Abbreviations</b>	<b>xviii</b>
<b>List of Tables</b>	<b>xxi</b>
<b>List of Figures</b>	<b>xxii</b>
<b>1. INTRODUCTION AND STATEMENT OF PROBLEM</b>	<b>1</b>
<b>2. REVIEW OF LITERATURE</b>	<b>10</b>
<b>2.1. Biosynthesis of Prostacyclin</b>	<b>10</b>
<b>2.2. Cyclooxygenase 1 and 2</b>	<b>11</b>
<b>2.3. Prostacyclin Synthase gene transfer studies</b>	<b>13</b>
<b>2.4. Prostacyclin pharmacology and signaling</b>	<b>15</b>
<b>2.5. Balance between PGI<sub>2</sub> and TXA<sub>2</sub> mediates vascular homeostasis</b>	<b>16</b>
<b>2.6. Role of PGI<sub>2</sub> in Pulmonary Hypertension</b>	<b>18</b>
<b>2.7. Role of PGI<sub>2</sub> in Atherosclerosis</b>	<b>19</b>
<b>2.8. Cell mediated gene therapy in peripheral vascular disease</b>	<b>21</b>
<b>2.9. Triple catalytic enzyme 1</b>	<b>26</b>
<b>2.10. MicroRNA</b>	<b>28</b>
<b>3. METHODS AND MATERIALS</b>	<b>30</b>

<b>3.1. Engineering of the cDNA plasmid encoding the hybrid enzyme COX-1-10aa-PGIS sequences</b>	<b>30</b>
<b>3.2. Establishing a primary cultured cell line derived from adipose tissue</b>	<b>30</b>
<b>3.3. Stable expression of the COX-1-10aa-PGIS in the cultured fat cells</b>	<b>31</b>
<b>3.4. Enzyme activity determination for the COX-1-10aa-PGIS using HPLC method</b>	<b>31</b>
<b>3.5. Determination of the endogenous AA metabolism in the cultured fat cells using LC/MS/MS analysis</b>	<b>32</b>
<b>3.6. Immunoblot Analysis</b>	<b>33</b>
<b>3.7. Anti-Platelet Aggregation Assays</b>	<b>33</b>
<b>3.8. Mouse Hindlimb Ischemia Model</b>	<b>34</b>
<b>3.9. Determination of the endogenous AA metabolisms in the mice using LC/MS/MS analysis</b>	<b>34</b>
<b>3.10. Mouse Running Time Model</b>	<b>35</b>
<b>3.11. Thrombotic occlusion model (Photochemical Vascular Injury)</b>	<b>35</b>
<b>3.12. MiRNA Microarray Analysis</b>	<b>36</b>
<b>3.13. Quantitative Real Time PCR (qRT-PCR)</b>	<b>37</b>
<b>3.14. Illumina gene expression assay</b>	<b>37</b>
<b>3.15. Akt1 Immunoblot</b>	<b>38</b>

<b>3.16. Lipid accumulation study in PSFCs and PGI<sub>2</sub>-PSFCs</b>	<b>39</b>
<b>3.17. Oil Red-O staining</b>	<b>39</b>
<b>3.18. Construction of the cDNA plasmid for generating the transgenic mice overexpressing COX-1-10aa-PGIS</b>	<b>40</b>
<b>3.19. Generation of transgenic mice overexpressing COX-1-10aa-PGIS</b>	<b>41</b>
<b>3.20. Identification of the transgenic mice by PCR analysis</b>	<b>42</b>
<b>3.21. Breeding of the transgenic mice</b>	<b>43</b>
<b>3.22. Identification of homozygous transgenic mice by qPCR</b>	<b>43</b>
<b>3.23. Bleeding time measurement</b>	<b>44</b>
<b>3.24. Determination of endogenous PGI<sub>2</sub> production in transgenic mice by LC/MS/MS analysis</b>	<b>44</b>
<b>3.25. Determination of COX-1-10aa-PGIS expression in different organs of the transgenic mice by PCR analysis</b>	<b>45</b>
<b>3.26. Immunoblot analysis of COX-1-10aa-PGIS in different organs of the transgenic mice</b>	<b>45</b>
<b>3.27. Blood pressure and heart rate measurement</b>	<b>46</b>
<b>3.28. Thrombotic occlusion model in transgenic mice</b>	<b>46</b>
<b>4. RESULTS</b>	<b>48</b>
<b>4.1. Isolation, culture, and conversion of the adipocytes into</b>	<b>48</b>

prostanoid-synthesizing fat cells (PSFCs)

<b>4.2. Engineering and cloning of the triple catalytic enzyme -1 (COX-1-10aa-PGIS)</b>	<b>52</b>
<b>4.3. Redirecting the PSFC line to specifically and constantly convert AA into PGI<sub>2</sub>, thereby forming the PGI<sub>2</sub>-PSFC line</b>	<b>53</b>
<b>4.4. PGI<sub>2</sub>-PSFCs inhibiting platelet aggregation in vitro</b>	<b>54</b>
<b>4.5. Effect of the PGI<sub>2</sub>-PSFCs on mouse thrombotic occlusion model</b>	<b>55</b>
<b>4.6. Effect of the PGI<sub>2</sub>-PSFCs on mouse ischemic hindlimb model</b>	<b>56</b>
<b>4.7. Determination of the endogenous AA metabolisms in the mouse urine using LC/MS/MS analysis</b>	<b>60</b>
<b>4.8. Determination of mouse running time in hindlimb ischemia model</b>	<b>60</b>
<b>4.9. Detection of miRNA expression in the PGI<sub>2</sub>-PSFCs</b>	<b>62</b>
<b>4.10. Profile of the miRNA that are upregulated by the endogenous PGI<sub>2</sub> in PGI<sub>2</sub>-PSFCs</b>	<b>62</b>
<b>4.11. Profile of the miRNAs that are downregulated by the endogenous PGI<sub>2</sub> in PGI<sub>2</sub>-PSFCs</b>	<b>63</b>
<b>4.12. Inhibition of upregulated miRNA expression in PGI<sub>2</sub>-PSFCs using PPAR<math>\gamma</math> antagonist</b>	<b>66</b>
<b>4.13. Inhibition of upregulated miRNA expression in PGI<sub>2</sub>-PSFCs using IP</b>	

antagonist	67
4.14. Quantitative determination of miRNA711 upregulated in PGI <sub>2</sub> -PSFCs using qRT-PCR approach	68
4.15. Inhibition of lipid accumulation in PGI <sub>2</sub> -PSFCs	71
4.16. Detection of downregulated Akt1 mRNA using illumina gene expression assay	71
4.17. Down-regulation of Akt1 protein expression in PGI <sub>2</sub> -PSFCs using immunoblot analysis	74
4.18. Generation of transgenic mice overexpressing COX-1-10aa-PGIS to increase endogenous PGI <sub>2</sub> level	75
4.19. Generation and characterization of homozygous transgenic mice	78
4.20. Endogenous production of PGI <sub>2</sub> is increased in COX-1-10aa-PGIS transgenic mice	78
4.21. Effect of increased endogenous PGI <sub>2</sub> production on haemodynamic parameters in COX-1-10aa-PGIS transgenic mice	81
4.22. The gene profile of the COX-1-10aa-PGIS expression in different tissues and organs	82
4.23. Effects of overproduction of PGI <sub>2</sub> on live birth from transgenic mice	84
4.24. Anatomical study of the organs of the transgenic mice	85

<b>4.25. Resistance to thrombosis in the transgenic mice using carotid artery thrombosis model</b>	<b>87</b>
<b>5. DISCUSSION</b>	<b>90</b>
<b>5.1. Stable expression of COX-1-10aa-PGIS in adipose tissue derived primary culture of mature adipocytes</b>	<b>90</b>
<b>5.2. Effect on hindlimb ischemia and thrombogenesis after treatment with PGI<sub>2</sub>-PSFCs in mice</b>	<b>93</b>
<b>5.3. Study of microRNA expression regulation in PGI<sub>2</sub>-PSFCs</b>	<b>96</b>
<b>5.4. Generation of the transgenic mice overexpressing COX-1-10aa-PGIS</b>	<b>101</b>
<b>6. SUMMARY AND CONCLUSIONS</b>	<b>104</b>
<b>7. REFERENCES</b>	<b>108</b>

## LIST OF ABBREVIATIONS

10aa	10 amino acid
[ <sup>14</sup> C]AA	Tritium labeled arachidonic acid
AA	Arachidonic acid
Akt1	Protein kinase B subtype 1
BMMNC	Bone marrow mononuclear cells
BP	Blood pressure
Ca <sup>2+</sup>	Calcium
cAMP	Cyclic adenosine monophosphate
CLI	Critical limb ischemia
COX	Cyclooxygenase
COX-1-10aa-PGIS	Triple catalytic enzyme (cyclooxygenase- 1 -10 amino acid - Prostaglandin I synthase)
cPGES	Cytosolic Prostaglandin E synthase
cDNA	Complementary deoxyribonucleic acid
EC	Endothelial cell
EPC	Endothelial progenitor cells
ER	Endoplasmic reticulum

GPCR	G protein coupled receptors
G418	Geneticin
HEK293 cells	Human embryonic kidney cells
HR	Heart rate
HPLC	High Performance Liquid Chromatography
IP	Prostacyclin receptor
LC/MS/MS	Liquid chromatography-mass spectrometry-mass
LDPI	Laser Doppler Perfusion Imager
LDFM	Laser Doppler Perfusion Monitor
mPGES-1	Microsomal Prostaglandin E synthase
MA	Mature adipocytes
miRNA	Micro RNA
mRNA	Messenger RNA
MSC	Mesenchymal stem cell
NSAIDs	Nonsteroidal anti-inflammatory drugs
nt	Nucleotide
PAH	Pulmonary arterial hypertension
PAD	Peripheral arterial disease
PBS	Phosphate buffered saline
PMA	Para-Methoxyamphetamine
PCR	Polymerase chain reaction

PGI <sub>2</sub>	Prostaglandin I <sub>2</sub>
PGE <sub>2</sub>	Prostaglandin E <sub>2</sub>
PGH <sub>2</sub>	Prostaglandin H <sub>2</sub>
PGES	Prostaglandin E synthase
6-keto-PGF <sub>1α</sub>	6-keto-prostaglandin F <sub>1α</sub>
PI3K	Phosphoinositide-3-kinase
PRP	Platelet Rich Plasma
PKA	Protein kinase A
PLA <sub>2</sub>	Phospholipase A <sub>2</sub>
PLC	Phospholipase C
PSFC	Prostanoid synthesizing fat cells
PGI <sub>2</sub> -PSFC	Prostaglandin I <sub>2</sub> -prostanoid synthesizing fat cells
PPARδ	Peroxisome proliferator activated receptor subtype delta
[ <sup>3</sup> H]PGE <sub>2</sub>	Tritium labeled PGE <sub>2</sub>
qRT-PCR	Quantitative Real Time Polymerase chain reaction
RNA	Ribonucleic acid
TXAS	Thromboxane A <sub>2</sub> synthase
TXA <sub>2</sub>	Thromboxane A <sub>2</sub>
TP	Thromboxane A <sub>2</sub> receptor
TG	Transgenic mice
TM	Transmembrane

Trip-cat-1	Triple-catalytic-enzyme-1
Tyr	Tyrosine
UTR	Untranslated region
VEGF	Vascular endothelial growth factors
VSMC	Vascular Smooth Muscle Cell
WT	Wild type

## LIST OF TABLES

1. Comparison of the biosynthesis ratio of the endogenous PGI<sub>2</sub> and PGE<sub>2</sub> in the PSFCs and PGI<sub>2</sub>-PSFCs as determined by LC/MS /MS 50
2. Up-regulated miRNAs in the PGI<sub>2</sub>-PSFCs and their predicted target genes and biological functions ([microrna.sanger.ac.uk/genetargets](http://microrna.sanger.ac.uk/genetargets)) 65
3. Down-regulated miRNAs in the PGI<sub>2</sub>-PSFCs and their predicted target genes and biological functions ([microrna.sanger.ac.uk/genetargets](http://microrna.sanger.ac.uk/genetargets)) 66

## LIST OF FIGURES

	<b>Page</b>
1 The schematic of the introduction to the statement of problem	09
2 Biosynthesis of prostanoids, comprising of prostaglandins and thromboxane	11
3 A model of the newly designed Trip-cat Enzyme-1	27
4 Time-course of the differentiation of mouse adipocytes under a conditional medium and western blot analyses for prostanoids synthesizing enzymes	49
5 Determination of the [ <sup>14</sup> C]AA metabolism using an isotope-HPLC method and endogenous AA metabolism using LC/MS analysis in PSFCs	51
6 Engineered cDNA plasmid containing COX-1 linked to PGIS cDNA , through the 10aa sequence generated by PCR approach and subcloning procedures	52
7 Western blot analysis of the COX-1-10aa-PGIS and determination of the exogenous[ <sup>14</sup> C] AA and endogenous AA metabolism in the PGI <sub>2</sub> -PSFCs by HPLC and LC/MS analysis	54
8 Effects of the PGI <sub>2</sub> -PSFCs on platelet aggregation	55
9 Effect of PGI <sub>2</sub> -PSFCs on blood perfusion of mice induced with thrombogenesis using photochemical vascular injury model	56
10 Effects of the PGI <sub>2</sub> -PSFCs on reperfusion of the mouse hindlimb-ischemic	

model as monitored by LDPI	59
11 LC/MS analysis of urine collected from mice induced with hindlimb ischemia at different time intervals and determination of running time of on treadmill	61
12 MiRNA microarray profiles of miRNA expression PSFC and PGI <sub>2</sub> -PSFC and determination of fold change in miRNA expression in the PGI <sub>2</sub> -PSFCs when compared to PSFCs.	64
13 MiRNA microarray profiles showing PGI <sub>2</sub> -PSFC miRNA expression when treated with IP antagonist and PPAR $\gamma$ antagonist	69
14 Quantification of miRNA 711 expression in PGI <sub>2</sub> -PSFCs by qRT-PCR	70
15 Simple microscopy of the PSFCs and PGI <sub>2</sub> -PSFCs when treated with adipogenic medium and comparison of integrated density values between PSFCs and PGI <sub>2</sub> -PSFCs	72
16 Illumina gene expression assay showing change in expression of mRNAs in PGI <sub>2</sub> -PSFCs compared to PSFCs	73
17 Western blots showing the expression of Akt1 in PSFCs and PGI <sub>2</sub> -PSFCs	74
18 Construction of the cDNA construct of COX-1-10aa-PGIS for generation of transgenic mice	76
19 Genotyping of the transgenic mice by PCR analysis	77

20	Image showing physical comparison between the wild type and transgenic mice	79
21	Characterization of homozygous transgenic mice by qPCR	80
22	LC/MS analysis of prostanoid in the urine of transgenic and wild type mice.	81
23	Measurement of haemodynamic parameters like bleeding time, blood pressure and heart rate in both wild type and transgenic mice	83
24	Expression of COX-1-10aa-PGIS in the different organs of the transgenic mice by PCR and western blot analysis	84
25	Determination of the number of litters born from the TG and wild type (WT) mice	86
26	Anatomical differences in the organs of the TG and WT mice	87
27	Study of resistance to thrombosis in transgenic mice by using the photochemical carotid artery thrombosis model	89
28	Schematic showing the proposed mechanism of inhibition of adipogenesis by PGI <sub>2</sub> and the proposed paracrine action as an application in obesity and atherosclerosis through up-regulating PGI <sub>2</sub> biosynthesis	98

## 1. INTRODUCTION AND STATEMENT OF PROBLEM

Prostacyclin (PGI<sub>2</sub>) is one of the most important vascular prostanoid synthesized from arachidonic acid (AA) with the help of enzymes, cyclooxygenase (COX) and prostacyclin synthase (PGIS) (Moncada *et al.* 1977, Majerus 1983). PGI<sub>2</sub> provides vascular protection through inhibition of platelet aggregation, vascular smooth muscle cell (VSMC) proliferation and leukocyte adhesion and vasodilation (Morita I. *et al.* 2002; Hinz B *et al.* 2002). These actions of PGI<sub>2</sub> oppose those of thromboxane (TXA<sub>2</sub>), which is a stimulator of platelet aggregation, VSMC proliferation and vasoconstriction (Bunting S *et al.* 1976). Thus a balance in the actions of PGI<sub>2</sub> and TXA<sub>2</sub> helps in regulating the homeostasis of the cardiovascular system (Moncada *et al.* 1979, Cheng Y *et al.* 2002). Under conditions of damaged endothelium, PGI<sub>2</sub> synthesis is decreased. Due to this, the equilibrium between the anti- and proaggregatory effects is disturbed with the former being outweighed by the vasoconstrictive and proaggregatory effects of TXA<sub>2</sub> produced primarily by the activated platelets. This forms the basis for the formation of atherosclerotic plaques (Pavel *et al.* 2000). Peripheral artery disease like critical limb ischemia is a consequence of atherosclerosis. The vascular protective effect of PGI<sub>2</sub> is well demonstrated in atherosclerosis studies in mice. In this study mice deficient in the PGI<sub>2</sub> receptor (IP<sup>-/-</sup>) were more susceptible to thrombosis (Murata *et al.* 1997), intimal hyperplasia and restenosis (Cheng *et al.* 2002) and reperfusion injury (Xiao *et al.* 2001). Whereas, IP<sup>-/-</sup> knockout mice with deletion of the TXA<sub>2</sub> receptor (TP) were rescued

from these effects (Cheng *et al.* 2002). In another study, it was demonstrated that, in female pre-menopausal low density lipoprotein receptor (LDL-R) knockout, the atheroprotective effect of estrogen was significantly reduced in the IP (-/-) mice (Egan *et al.* 2004). Recently, studies have shown that the use of COX-2 inhibitors in inflammation poses increased risk to cardiovascular diseases (Bresalier *et al.* 2005) and the most likely reason is found to be a decrease in COX-2 mediated vascular PGI<sub>2</sub> production without a concomitant change in TXA<sub>2</sub> levels thus disturbing the balance. With the knowledge of the importance of TXA<sub>2</sub>/ PGI<sub>2</sub> balance in the pathogenesis of atherosclerosis and the vascular protective actions of PGI<sub>2</sub>, PGI<sub>2</sub> and its analogues have been used to treat pulmonary arterial hypertension (Hinderliter *et al.*, 1997), atherosclerosis, peripheral vascular diseases (Pavel *et al.*, 2000, Berman *et al.*, 2006), and congestive heart failure (Kerbaul *et al.*, 2007). The administration of a PGI<sub>2</sub> analog is one of the most widely used treatments for Pulmonary Artery Hypertension (PAH) and has been associated with a reduction in PAH-associated mortality (Olschewski *et al.*, 2002, Simonneau *et al.*, 2002). Thus inspite of having cardioprotective properties, still the use of these compounds is limited due to their short half and therefore frequent administration for long term care.

During recent studies, PGIS gene transfer could significantly (although temporarily) increase the PGI<sub>2</sub> serum levels and improve hemodynamics in animal models (Geraci *et al.*, 1999; Nagaya *et al.*, 2000; Tahara *et al.*, 2004; Suhara *et al.*, 2002). Nevertheless, the effective and stable biosynthesis of PGI<sub>2</sub> requires an increase in the

expression of COX coordinated with PGIS since COX is a rate-limiting enzyme in PGI<sub>2</sub> biosynthesis. Therefore, the discovery of a system that specifically increases PGI<sub>2</sub> biosynthesis endogenously is critical for developing a preventive and therapeutic intervention against vascular and heart diseases. Recently, the specific biosynthesis of PGI<sub>2</sub> in cells has been achieved and investigated through our engineering of a novel enzyme which linked COX-2 to PGIS, and contains unique triple-catalytic (Trip-cat) functions to effectively convert arachidonic acid (AA) into PGI<sub>2</sub> (Ruan *et al.*, 2006). The engineered enzyme was termed the Trip-cat enzyme-2. Transient expression of the Trip-cat enzyme-2 in HEK293 cells could specifically direct AA metabolism into PGI<sub>2</sub> to form PGI<sub>2</sub>-producing HEK293 cells (Ruan *et al.*, 2006). Thus this indicated that we could use this triple catalytic enzyme as gene therapy to treat vascular disorders. Further our lab reengineered the triple catalytic enzyme-1 by linking COX-1 instead of COX-2 with PGIS. We selected COX-1 instead of COX-2 isoform because COX-1 is a house keeping enzyme having less pathological impacts and could be safer for gene and cell therapies compared with COX-2, which has been associated with pathological conditions, such as inflammation and cancer. Thus we hypothesized that introducing this gene (COX-1-10aa-PGIS) in vivo will lead to the specific upregulation of PGI<sub>2</sub> production, thus playing a protective role in various vascular disorders. Viral vectors are generally used for gene transfer but their disadvantages are, transient gene expression, vector induced cytotoxicity and immune response with the second dose (Thomas *et al.*, 2003). So the

question was how to transfer the fusion gene through non-viral vectors? Several endothelial progenitor cells, stem cells, stromal cells etc. have been used as cell therapy in peripheral artery disease to promote therapeutic angiogenesis and increase blood flow in the limbs (Tateishi-Yuyama *et al.*, 2002, Miyamoto *et al.*, 2006). Recently, it has been reported that adipose tissue provides with a wide array of cells, which can be easily cultured by using standard methods (Gimble *et al.*, 2003, Miranville *et al.*, 2004, Miyahara *et al.*, 2006, Planat-Benard *et al.*, 2002). It has recently been demonstrated that activation of the (COXs)/PGI<sub>2</sub>/peroxisome proliferators-activated receptor  $\delta$  (PPAR $\delta$ ) pathway is an important mechanism underlying the proangiogenic function of progenitor cells (Santhanam *et al.*, 2007, He T *et al.*, 2008). Thus isolation, culture, enzyme activity assay and LC/MS analysis of mature adipocytes (MA) from mouse adipose tissue, showed that MA had the potential to convert endogenous AA into PGE<sub>2</sub>. These observations prompted us to think that if these cells can be converted into therapeutic cells producing PGI<sub>2</sub> by overexpressing COX-1-10aa-PGIS in MA. Then we can use these cells as a medium to transfer the triple catalytic gene-1. Further we propose to study the vascular protective effect of this PGI<sub>2</sub> producing therapeutic cells in both the mouse hindlimb ischemia and thrombogenesis models. Moreover, it can be a new generation of cDNA for COX gene therapy. It is particularly interesting that COX-2 inhibitors inhibit COX-2 activity but not the COX-1 activity; thus, introduction of the

COX-1-linker-PGIS to cardiovascular systems can potentially overcome the side effects of the COX-2 inhibitors that cause damage to cardiovascular functions.

PGI<sub>2</sub> released from endothelial cells, acts in an autocrine and paracrine manner to interact with the cell surface Gs-protein coupled PGI<sub>2</sub> receptor IP, expressed on platelets and vascular smooth muscle cells (Hara *et al.*, 1995, Boie *et al.*, 1994). This leads to the activation of adenylyl cyclase, accumulation of the second messenger cAMP, and activation of its main intracellular effector, the cAMP-dependent protein kinase, PKA (Tateson *et al.*, 1977, Jaschonek *et al.*, 1988, Stitham *et al.*, 2004). IP activation inhibits platelet aggregation in response to TXA<sub>2</sub>, inhibits VSMC proliferation and migration, and promotes VSMC differentiation and vasodilation (Samuelsson *et al.*, 1978). Both COX and PGIS have shown to be localized not only at endoplasmic reticular membranes but also at nuclear membrane (Liou *et al.*, 2000, Smith *et al.*, 1983). This suggests that PGI<sub>2</sub> might have dual signaling pathways, one using cell surface IP receptor and other using nuclear receptors. Peroxisome proliferators-activated receptors (PPARs) belong to a family of nuclear receptors, which are ligand-activated transcription factors. They heterodimerize with a retinoid X receptor and bind to peroxisome proliferators response element in the promoter site of the target gene and regulate its transcription (Kliwer *et al.*, 1992, Robyr *et al.*, 2000). The PPAR family includes three isoforms,  $\alpha$ ,  $\delta$  ( $\beta$ ) and  $\gamma$  (Braissant *et al.*, 1996, Kliwer *et al.*, 1994), which are activated by a broad spectrum of ligands. These include metabolites of the COX and lipoxygenase pathway

and hypolipidemic agents eg. fibrates, which regulate inflammation, lipid metabolism and insulin sensitivity (Forman *et al.*, 1997, Becker *et al.*, 2006, Lefebvre *et al.*, 2006). PPAR $\gamma$ , which is mostly expressed in the adipose tissue, large intestine, and spleen (Fajas *et al.*, 1997), is also the only PPAR that can be activated through the IP using stable PGI $_2$  analogues (Falcetta *et al.*, 2007). Thus prostacyclin can be directly related to lipid metabolism through the IP/PPAR $\gamma$  receptor. To date there is conflicting evidence regarding a PGI $_2$ -induced increase or decrease in adipogenesis (Hodnett *et al.*, 2009, Massiera *et al.*, 2003). However, logically an early loss of endothelial PGI $_2$  could lead to adipocyte lipid deposition in the periphery and vascular smooth muscle cells (atherosclerosis). Currently atherosclerosis is characterized by inflammation that causes vascular endothelial damage (Páramo *et al.*, 2008). The first step in the development of atherosclerosis is the formation of the fatty streak. The current accepted concept is that when LDL levels increase, they accumulate in the arterial intima and get oxidized into proinflammatory particles. This provokes an innate inflammatory reaction within the intima and thus fat droplets accumulate in the cytoplasm of smooth muscle cells. The resulting hemodynamic stress causes intimal thickening of the artery. When the monocytes enter the artery, they transform into macrophages, take up lipids and become foam cells (Stary, H.C. 2003, Strong *et al.*, 1999). However, we propose that the localized loss of the autocrine and the paracrine effect of endothelial PGI $_2$  could be responsible for the sub-endothelial deposition of lipid in the smooth muscle cells of the

vascular walls. It is known that lipid deposition in the vessel wall begins as fatty streaks at a very early age (Stary, H.C. 2003, Strong *et al.*, 1999). This could represent an early loss of PGI<sub>2</sub> paracrine function. We further propose that this lipid deposition can be confirmed by identification of appropriate specific proteins involved in the lipogenesis pathway. Thus we propose that PGI<sub>2</sub> through PPAR receptors might regulate expression of genes that are involved in lipid accumulation. MicroRNAs (miRNAs) are single-stranded non-coding RNAs with 21–24 nucleotide (nt) in length, regulating target genes expression at the post-transcriptional level through translational repression or mRNA degradation (Farh *et al.*, 2005, Pasquinelli *et al.*, 2005). Thus they are endogenous, negative regulators of gene expression, which are involved in regulation of cell proliferation/growth, mobility, differentiation, and apoptosis (Ambros V. 2004, Du *et al.*, 2007, Hwang *et al.*, 2006, Jovanovic, M., and Hengartner, M.O. 2006, Rane *et al.*, 2007). This was the first verification that endogenous PGI<sub>2</sub> could inhibit lipid deposition in adipocytes possibly with the involvement of regulating miRNA expression. PGI<sub>2</sub> is a mediator of adipocyte differentiation (Georges *et al.*, 1992), a regulator of smooth muscle cell differentiation (Tsai *et al.*, 2009) and inhibitor of their proliferation. Thus miRNAs and PGI<sub>2</sub> could be linked together through their common functions as well as PGI<sub>2</sub> mediated gene regulation by signaling through PPAR receptors. However, there has been very little information on transcription factors regulating miRNA expression as their expression is controlled in a very tissue specific and development specific manner.

To date, c-Myc, cyclic AMP response element binding protein and myogenic transcription factors have been shown to regulate specific miRNAs in mammalian cells. But recently it has been demonstrated that PPAR $\alpha$  is a bonafide regulator of hepatic miRNA expression, which regulates liver proliferation (Yatrik *et al.*, 2007). Thus we propose to uncover a novel finding if miRNAs are involved in PGI<sub>2</sub> mediated regulation of gene expression. We also propose to identify any target gene regulated by PGI<sub>2</sub> through miRNA and study its function in PGI<sub>2</sub> regulated processes like adipocyte differentiation. Our PGI<sub>2</sub> producing therapeutic cells can be very good *in vitro* model to study the effect of endogenous PGI<sub>2</sub> on microRNA expression.

Adipose tissue derived fat cells overexpressing COX-1-10aa-PGIS and producing PGI<sub>2</sub> are proposed to produce vascular protective effect in mouse models of critical limb ischemia and thrombogenesis. Thus, with the objective of translating these *in vitro* results into *in vivo*, we propose to generate transgenic mice overexpressing the COX-1-10aa-PGIS and study the benefits and risks of permanently upregulating PGI<sub>2</sub> synthesis *in vivo*. The biological effects of genetically up-regulated PGI<sub>2</sub> in vivo on development, organ physiology, correction for induced stroke and heart diseases and reproductive functions will be studied.

Thus we hypothesized that 1) Mature adipocytes mediated gene transfer of triple catalytic enzyme (COX-1-10aa-PGIS) gene/protein in tissue ischemia and thrombogenesis will provide vascular protection through a sustained release of PGI<sub>2</sub> at

the site of injury, 2) MicroRNAs are involved in PGI<sub>2</sub> mediated gene expression regulation and 3) Transgenic mice overexpressing COX-1-10aa-PGIS and specifically overproducing PGI<sub>2</sub> *in vivo* can be created and used as a model to study the vascular protective effect of PGI<sub>2</sub> .

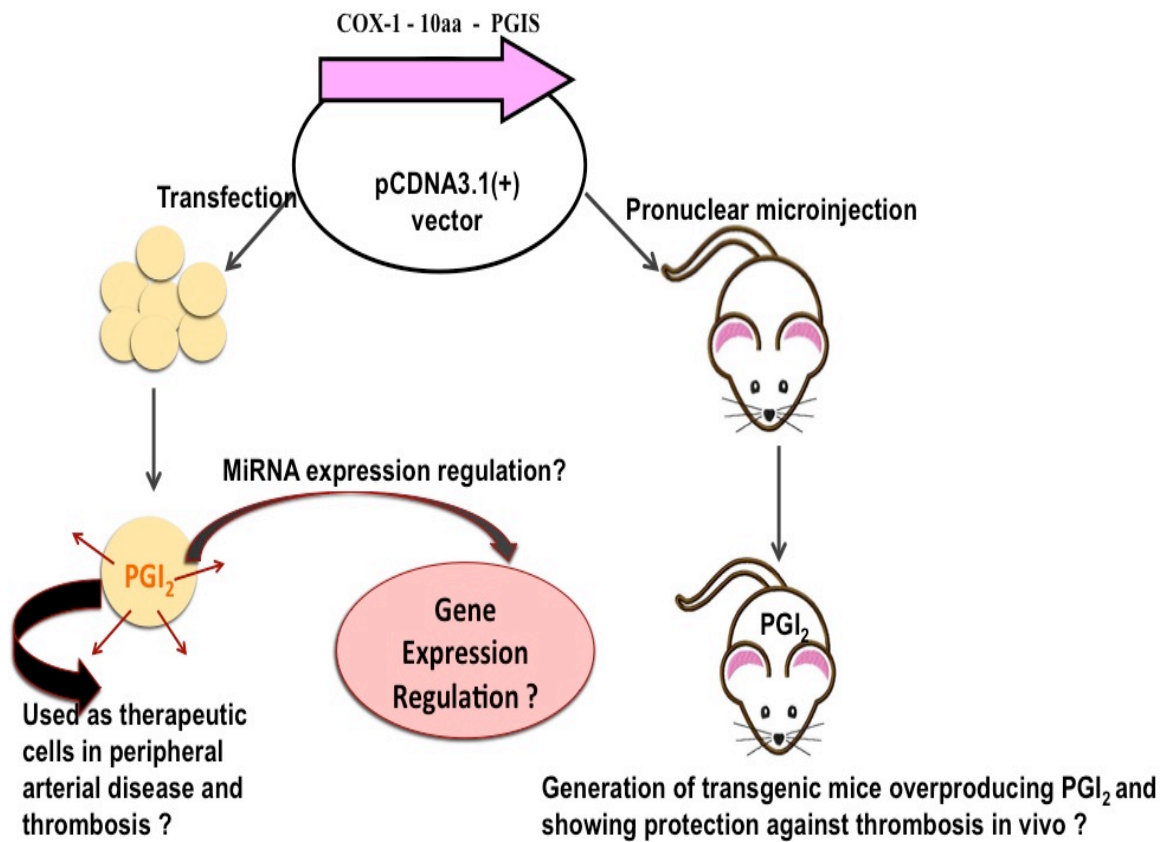


Figure 1: The schematic of the introduction to the statement of problem. Overexpression of COX-1-10aa-PGIS gene in primary culture of mature adipocytes and mice. Therefore our statement of problem is to determine whether: 1) these cells can be used therapeutically in vascular disorder through overproducing PGI<sub>2</sub> 2) cells producing PGI<sub>2</sub> regulate gene expression through miRNA expression regulation 3) transgenic mice overproducing PGI<sub>2</sub> can be generated and used as a model to study vascular protective effect of PGI<sub>2</sub>.

## 2. REVIEW OF LITERATURE

### 2.1. Biosynthesis of Prostacyclin

Prostanoids are cyclic lipid mediators belonging to the superfamily of eicosanoids (in greek stands for 20, in that case twenty carbon atoms in a molecule). Prostanoids are produced by enzymic cyclooxygenation of linear polyunsaturated fatty acids, e.g. arachidonic acid (AA or 5,8,11,14-eicosatetraenoic acid). Biologically active prostanoids that are derived from AA include stable prostaglandins (PG), e.g. PGE<sub>2</sub>, PGF<sub>2α</sub>, PGD<sub>2</sub>, PGJ<sub>2</sub> as well as labile prostanoids, i.e. PG endoperoxides (PGG<sub>2</sub>, PGH<sub>2</sub>), thromboxane A<sub>2</sub> (TXA<sub>2</sub>) and prostacyclin (PGI<sub>2</sub>). PGI<sub>2</sub> is one of the five major products of the arachidonic acid metabolism that is synthesized via the cyclooxygenase pathway. Biosynthesis of prostacyclin involves 3 steps (a) stimulus-induced mobilization of AA from membrane phosphoglycerides by cytosolic phospholipase A<sub>2</sub> (cPLA<sub>2</sub>); (b) conversion of AA to PGG<sub>2</sub> which is then electron reduced to form PGH<sub>2</sub> by the cyclooxygenase and peroxidase activities of cyclooxygenase isoform 1 or 2 (COX-1/2); and (c) conversion of PGH<sub>2</sub> to PGI<sub>2</sub> by prostacyclin synthase (PGIS) (Figure 1). PGH<sub>2</sub> is also isomerized to other biologically active prostanoid end-products, (including prostaglandin D<sub>2</sub> (PGD<sub>2</sub>), E<sub>2</sub> (PGE<sub>2</sub>), F<sub>2</sub> (PGF<sub>2</sub>), or TXA<sub>2</sub> by individual synthases in tissue specific manners (Figure 1) (Needleman *et al.*, 1986, Ruan *et al.*, 2006). Prostacyclin is the major AA metabolite of the vascular tissue and its synthesis is greatest at the intimal

surface (endothelial cells) and gradually decreases towards the adventitia (vascular smooth muscle cells) (Moncada *et al.*, 1977). PGI<sub>2</sub> has a very short half life *in vivo* (<2 min) due to its instability at physiological pH and the inactive metabolite formed is the 6-keto-prostaglandin F1α (6-keto-PGF1α; Lewis *et al.*, 1983, Smyth *et al.*, 2002).

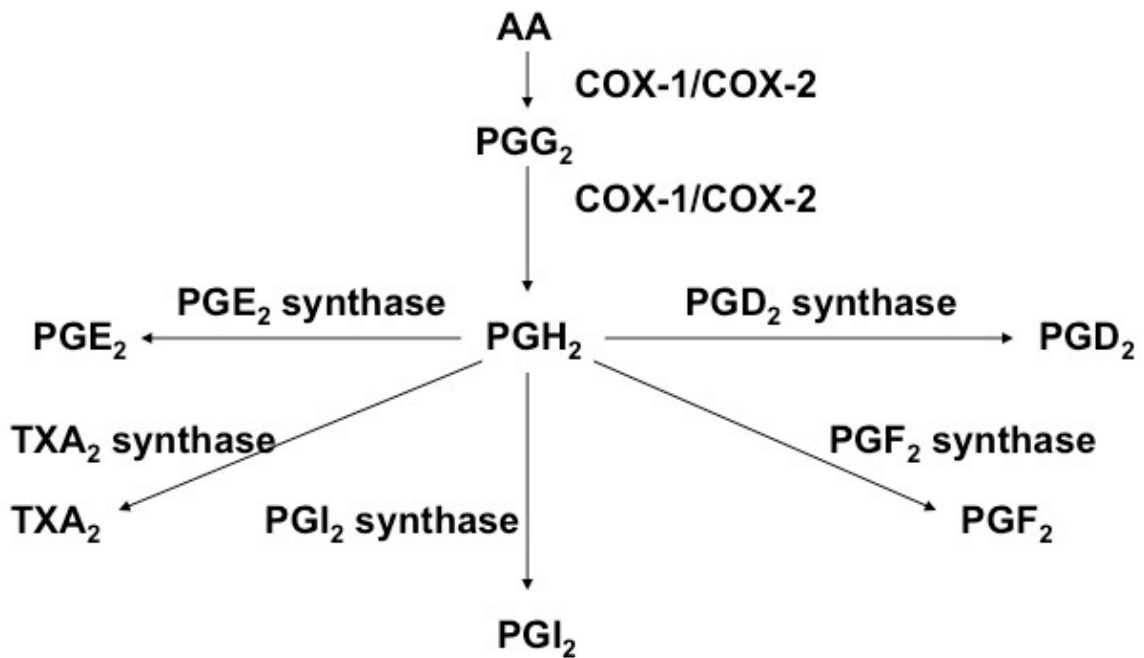


Figure 2. Biosynthesis of prostanoinds, comprising of prostaglandins and thromboxane. Arachidonic acid (AA) released from membrane phosphoglycerides by cPLA<sub>2</sub> is converted to PGG<sub>2</sub>, which is further metabolized to PGH<sub>2</sub> by COX-1/COX-2. PGH<sub>2</sub> is further isomerized to downstream PGs like PGI<sub>2</sub>, TXA<sub>2</sub>, PGE<sub>2</sub>, PGF<sub>2</sub> and PGD<sub>2</sub> by their respective cell specific downstream enzymes.

## 2.2. Cyclooxygenase 1 and 2 (COX-1 and COX-2)

The COX enzymes are bisfunctional proteins, possessing both cyclooxygenase and hydroperoxidase (HOX) activities (Smith *et al.*, 2002). The two COX enzymes are

encoded by separate genes located on different chromosomes (Ch1 for COX-2 and Ch9 for COX-1) (Funk *et al* 1991, Xie *et al* 1993), but nevertheless serve the same biosynthetic function of oxygenation of AA into PG endoperoxide intermediates PGG<sub>2</sub> and PGH<sub>2</sub> (Smith *et al.*, 1996, Smith *et al* 1997, Smith *et al.*, 2002). COX-1 is a house-keeping gene that regulates kidney and stomach function and maintains vascular homeostasis by producing prostaglandins in response to circulating hormones. COX-1 is referred to as the constitutive form (DeWitt *et al.*, 1991) as its expression remains unchanged in most tissues and pathologies during the inflammatory reaction or as a result of hormonal stimulation (Smith *et al* 1993, Brannon *et al* 1994, and Mroske *et al.*, 2000). In contrast COX-2 is the inducible form of the gene whose expression is low or undetectable in almost all of the tissues or cells but is increased dramatically upon stimulation, particularly during inflammation by inflammatory cytokines and mitogens (Herschman 1999). Both COX enzymes share a hydrophobic tunnel that affords access of the lipid substrate to the active site, deep within the proteins. However, the COX-2 tunnel is more accommodating and also has a side pocket that is not present in COX-1. This helps COX-2 to have broader substrate recognition and also is the reason for the ability of selective COX-2 inhibitors to selectively inhibit COX-2 enzyme (Kurumbail *et al.*, 1996).

### **2.3. Prostacyclin Synthase (PGIS) gene transfer studies**

Prostacyclin synthase (PGIS), a heme protein is a membrane-associated P450-like enzyme that has a molecular mass of 52 kDa (DeWitt *et al.*, 1983). It lacks the typical CYP monooxygenase activity but catalyzes the conversion of prostaglandin H<sub>2</sub> (PGH<sub>2</sub>) to prostacyclin (Ullrich *et al.*, 1981, Moncada *et al.*, 1979). PGIS catalytic activity is lost after nitration of the Tyr-430 residue by peroxynitrite (Schmidt *et al.*, 2003). PGIS is constitutively expressed in vascular endothelial cells and smooth muscle cells and non-vascular cells like neurons, oviducts, embryonic cells, and cancer cells (Wu *et al.*, 2005). PGIS is colocalized with COX-1 in resting endothelial cells (EC) and is also colocalized with COX-2 in EC stimulated by PMA (Liou *et al.*, 2000). There are several studies that have provided evidence for an important role of PGIS in vascular integrity. PGIS deficiency plays a major role in diverse diseases including arterial intimal hyperplasia (Yokoyama *et al.*, 2002), pulmonary hypertension (Tuder *et al.*, 1999), tissue infarction, atherosclerotic arterial diseases and endothelial dysfunction. A reduced expression of PGIS is associated with reduced synthesis and activity of prostacyclin thus contributing to an imbalance between prostacyclin and thromboxane actions. It is therefore logical to consider gene transfer for enhancing PGI<sub>2</sub> synthesis. Transfection of the PGIS cDNA into rat vascular smooth muscle cells resulted in an increased PGI<sub>2</sub> synthesis and inhibition of cell proliferation suggesting that in vivo gene transfer of PGIS may be useful

for gene therapy in vascular diseases (Hara *et al.*, 1995). Overexpression of PGIS in carotid arteries of experimental animals using adenoviral vector or liposome-mediated transfer of PGIS cDNA has been shown to prevent intimal hyperplasia induced by carotid injury (Todaka *et al.*, 1999). This effect was reported to be associated with increased 6-keto-PGF<sub>1α</sub> productions, the stable metabolite of PGI<sub>2</sub> (Numaguchi *et al.*, 1999). Repeated injection of PGIS cDNA into rat skeletal muscle of a pulmonary hypertension rat model is associated with an increased level of PGI<sub>2</sub> effective in controlling pulmonary hypertension and vascular remodeling (Tahara *et al.*, 2004). *In vivo* injection of adenovirus-COX-1 into carotid arteries increases PGI<sub>2</sub> levels and prevents thrombus formation in a porcine model (Zoldhelyi *et al.*, 1996). But overexpression of PGIS alone cannot contribute to an optimal PGI<sub>2</sub> production. Data from PGIS overexpression experiments have provided several important insights into PGI<sub>2</sub> biosynthesis. One of the important observations is that PGI<sub>2</sub> synthesis is not determined by the level of PGIS expression alone but by an appropriate ratio of COX-1/COX-2 to PGIS expression. It has been reported that bicistronic COX-1 and PGIS gene transfer resulted in selective augmentation in the PGI<sub>2</sub> synthesis without concurrent increase in other prostanoids (Shyue *et al.*, 2001, Heng *et al.*, 2002). Thus overexpression of PGIS with concurrent COX-1 overexpression is highly effective in controlling vascular diseases. PGI<sub>2</sub> biosynthesis is upregulated and thus associated with an increase in the expression of

PGIS coordinated with COX-2 expression during embryo implantation and decidualization (Lim *et al.*, 1999).

#### **2.4. Prostacyclin pharmacology and signaling**

PGI<sub>2</sub> released from the endothelial cells, acts in an autocrine and paracrine manner to interact with the cell surface G-protein coupled receptor (GPCR) referred to as the IP receptor (IP-International Union of Pharmacology nomenclature) on platelets and vascular smooth muscle cells (Boie *et al.*, 1994). The IP receptor couples predominantly to the G<sub>s</sub> subunit of the heterotrimeric G-protein and causes activation of adenylyl cyclase and cyclic AMP (cAMP) production (Boie *et al.*, 1994) which in turn activates the intracellular effector protein kinase A (PKA). IP activation inhibits platelet aggregation and produces vasodilation (Smyth *et al.*, 2009), inhibits vascular smooth muscle cell (VSMC) proliferation and de-differentiation (Fetalvero *et al.*, 2006, 2007). In the pulmonary vasculature, PGI<sub>2</sub> reduces pulmonary blood pressure as well as bronchial hyperresponsiveness (Idzko *et al.*, 2007). Both COX and PGIS are localized not only at endoplasmic reticular membranes but also at nuclear membrane (Liou *et al.*, 2000, Smith *et al.*, 1983). At high concentrations prostacyclin agonists can also activate the nuclear receptors such as the peroxisome proliferator activated receptor (PPAR) (Lim *et al.*, 2002). Peroxisome proliferators-activated receptors (PPARs) belong to a family of nuclear receptors, which are ligand-activated transcription factors. It has been reported

that PGI<sub>2</sub> other than binding to IP receptor, also activates PPAR $\delta$ . This activation regulates actions like embryo implanatation, vascular functions, and apoptosis (Lim *et al.*, 1999, Zhang *et al.*, 2002, Hatae *et al.*, 2001). Stable PGI<sub>2</sub> analogues like iloprost and carbacyclin, directly bind to and cause transcriptional activation of PPAR $\alpha$  and PPAR $\delta$  *in vitro* (Forman *et al.*, 1997). The anti- proliferative effects of treprostinil in lung fibroblasts may in part be due to PPAR $\delta$  activation. PGI<sub>2</sub> analogues produce IP receptor dependent PPAR $\gamma$  receptor activation (Falcettia *et al.*, 2007). PPAR $\gamma$  is an important regulator of cell differentiation and growth, particularly in the lung (Becker *et al.*, 2006), and therefore loss or dysfunctionality of the IP receptor could alter the control of these processes. Vascular inflammation is one of the primary causes of atherosclerosis. Cytokines such as tumor necrosis factor  $\alpha$  released during inflammation stimulates the biosynthesis of PGI<sub>2</sub> and upregulation of PPAR $\delta$  in vascular smooth muscle cells. Thus, it has been proposed that PGI<sub>2</sub> by acting as a ligand for PPAR $\delta$ , might release a transcriptional repressor of inflammation which in turn might inhibit the inflammatory proliferation of vascular smooth muscle (Ruan *et al.*, 2006). Thus PGI<sub>2</sub> might regulate gene expression through PPAR receptors.

## **2.5. Balance between PGI<sub>2</sub> and TXA<sub>2</sub> mediates vascular homeostasis**

Recent reports of the withdrawal of COX-2 inhibitors (e.g Vioxx) due to increased cardiovascular risks associated with their use has highlighted the cardioprotective role

of prostacyclin (Wong *et al.*, 2005). Studies of the selective COX-2 inhibitors suggest that a balance between thromboxane (TXA<sub>2</sub>) and prostacyclin is a critical factor in the regulation of cardiovascular homeostasis and disturbances of this balance might underlie some forms of vascular pathology (Moncada *et al.* 1976a). The finding that small doses of aspirin is an effective anti-thrombotic treatment came from the research originating from the concept of the balance between PGI<sub>2</sub> and TXA<sub>2</sub>. TXA<sub>2</sub> derived from the COX-1 catalyzed arachidonic acid metabolism in the platelets is a potent activator of platelets and a vasoconstrictor whereas PGI<sub>2</sub> inhibits these actions of TXA<sub>2</sub> through platelet aggregation inhibition and vasodilation (FitzGerald *et al.*, 1991, Samuelsson *et al.*, 1978). Genetic deletion of both the TXA<sub>2</sub> (TP) and IP receptor in mice provided evidence that PGI<sub>2</sub> regulates cardiovascular homeostasis by opposing the actions of TXA<sub>2</sub>. Neointimal proliferation was induced in both IP knockout (-/-) and wild type mice after catheter induced carotid artery injury but a more enhanced proliferative response was observed in IP (-/-) mice. Also this proliferative response of the carotid artery after injury was reduced after deletion of the TP receptor (Cheng *et al.*, 2002). Thus these studies indicated that the cardiovascular effects of TXA<sub>2</sub> are regulated by the actions of PGI<sub>2</sub> in the vasculature. The undesirable effects of the selective COX-2 inhibitors are explained on the basis of an imbalance theory between TXA<sub>2</sub> and PGI<sub>2</sub>. According to this theory selective inhibition of COX-2 leads to a reduction in the production of the anti-atherogenic PGI<sub>2</sub> while production of the COX-1 derived atherogenic TXA<sub>2</sub> remains

unaltered. This shifting of the balance between these two prostanoids in favor of TXA<sub>2</sub> disrupts the vascular homeostasis and increases the susceptibility to thrombosis and the onset and progression of atherosclerosis (Wong *et al.*, 2005).

## **2.6. Role of PGI<sub>2</sub> in Pulmonary Hypertension**

Pulmonary arterial hypertension (PAH) is characterized by pulmonary vasoconstriction, VSMC proliferation, endothelial loss or dysfunction and thrombosis (Faber *et al.*, 2004). The vascular changes that occur in PAH has at least in part attributed to disruption in the balance of PGI<sub>2</sub> to TXA<sub>2</sub> ratio. It has been found that in PAH patients, the expression of prostacyclin synthase within the pulmonary arteries as well as 6-keto-PGF<sub>1α</sub> (metabolite of PGI<sub>2</sub>) in the urine was decreased whereas levels of TXB<sub>2</sub> (thromboxane metabolite) were increased (Christman *et al.*, 1992). Owing to its potent vasodilatory, anti-thrombotic and antiproliferative effects, PGI<sub>2</sub> and its analogues have been effectively used in the treatment of PAH. Continuous intravenous prostacyclin-analog epoprostenol (Flolan™) has been used as a first line agent to improve overall symptoms and hemodynamics and increase exercise tolerance in PAH patients (Barst *et al.*, 2009). However, due to epoprostenol's short half-life (3-5 min) and instability at low pH, long term use requires a permanent venous catheter and a portable infusion pump which is associated with side-effects such as bleeding and catheter-related sepsis (Sitbon *et al.*, 2002). New prostacyclin analogs have been developed as alternative

therapy administered via different routes like subcutaneous treprostinil (Simonneau *et al.*, 2002), oral beraprost (Galie *et al.*, 2002), and inhaled iloprost (Olschewski *et al.*, 2002, Hoeper *et al.*, 2000). These drugs are more stable with long half-lives, but have variable safety and clinical efficacy in comparison to epoprostenol (Barst *et al.*, 1996).

Recently, endogenous lung tissue content of PGI<sub>2</sub> metabolite 6-keto PGF<sub>1α</sub> was successfully increased through gene therapy. When the human PGIS gene was intratracheally transfected into the lungs of rats with monocrotaline-induced pulmonary hypertension, high levels of PGIS expression and PGI<sub>2</sub> production were found in the bronchial epithelial cells. In these animals, the mean pulmonary arterial pressure and total pulmonary resistance was significantly attenuated (Nagaya *et al.*, 2000). Given these results, in the future gene transfer may be a potential candidate as an alternative for continuous intravenous PGI<sub>2</sub> infusion for PAH patients.

## **2.7. Role of PGI<sub>2</sub> in Atherosclerosis**

Atherosclerosis is a complex cardiovascular disease characterized by inflammation, endothelial dysfunction, lipid accumulation, cell death and fibrosis (Hanson *et al.*, 2006). Prostaglandins in atherosclerosis antagonize each others actions. TXA<sub>2</sub> and PGE<sub>2</sub> have atherogenic effects whereas PGD and PGI<sub>2</sub> are antiatherogenic. PGI<sub>2</sub> protects from atherothrombosis by inhibiting platelet activation, leukocyte adhesion, and VSMC modulation like dedifferentiation, proliferation and migration. The

imbalance theory between PGI<sub>2</sub> and TXA<sub>2</sub> also explains the pathophysiology of atherosclerosis. PGI<sub>2</sub> has been reported to induce cholesterol ester hydrolase activity that catalyzes the first step in the removal of cholesterol from the foam cells (Hajjar *et al.*, 1983). Circulating high density lipoprotein induces the expression of COX-2 and thus PGI<sub>2</sub> biosynthesis in the endothelial cells and the VSMC which further supports the anti-atherogenic role of PGI<sub>2</sub> (Pomerantz *et al.*, 1985). Iloprost (stable analogue of prostacyclin) is reported to down-regulate lymphocyte adhesion to endothelial cells, suggesting an ability to block the early events of atherosclerosis (Della Bella *et al.*, 2001). In response to vascular injury, VSMC dedifferentiate to a synthetic phenotype due to downregulation of contractile proteins and proliferate. This phenotypic plasticity contributes to the pathophysiological processes of atherosclerosis, restenosis, and hypertension (Owens *et al.*, 2004). Treatment with the stable PGI<sub>2</sub> analog Iloprost induces differentiation of VSMC including changes in morphology. Along with this it also initiates a transcriptional upregulation of contractile proteins *via* the cAMP/PKA pathway (Fetalvero *et al.* 2006). It was also demonstrated that iloprost treatment of VSMC upregulated COX-2 expression that leads to subsequent PGI<sub>2</sub> release and inhibited Akt-1 expression (Kasza *et al.*, 2009). The role of PGI<sub>2</sub> as an atheroprotective is well demonstrated in prostacyclin receptor IP knock out mice (IP<sup>-/-</sup>) studies. These mice displayed an increased proliferative response to carotid vascular injury with increased intima to media ratios, enhanced thrombosis, and increased atherosclerosis (Murata *et*

*al.*, 1997, Cheng *et al.*, 2002). Similarly, mice deficient in prostacyclin through genetic disruption of the prostacyclin synthase gene developed thickening of vascular walls, especially in the kidneys (Yokoyama *et al.*, 2002). Clinical studies on COX-2 inhibition further support the role of PGI<sub>2</sub> in inhibiting atherothrombosis. The VIGOR (Bombardier *et al.*, 2000) and APPROVe (Bresalier *et al.*, 2005) trials confirmed the hypothesis that patients with underlying cardiovascular risk factors were susceptible to coronary events due to decreased PGI<sub>2</sub> and therefore increased prothrombotic TXA<sub>2</sub> ratio when treated with COX-2 selective inhibitors. It has been shown that PGIS gene transfer in balloon injured arteries could inhibit neointimal formation and the proposed mechanism of action was that excessive PGH<sub>2</sub> derived from COX-2 after a balloon injury can be converted into PGI<sub>2</sub>, in the presence of over expressed PGIS induced by the gene transfer (Yamada *et al.*, 2002)

## **2.8. Cell mediated gene therapy in peripheral vascular disease**

### **2.8.1. Peripheral vascular disease**

Lower extremity peripheral arterial disease (PAD) is a highly prevalent atherosclerotic syndrome that is characterized by a decrease in peripheral circulation due to clogged peripheral arteries. It can lead to claudication and critical limb ischemia (CLI), a endstage lower extremity PAD occurring due to severe obstruction in blood flow which results in ischemic rest pain, ulcers, and a significant risk for limb loss. It has been

suggested that surgical or endovascular revascularization aimed at improving blood flow as a standard therapy for severe, limb-threatening ischemia. However such interventions are suitable in approximately 50% of patients with CLI and amputation is the only option left. To improve the symptoms of PAD, research has been focusing on the concept of therapeutic angiogenesis to improve vascularization of the ischemic leg by the use of cell therapy and angiogenic growth factors gene therapy. Pharmacological treatment like use of prostacyclin analogs has also been suggested to improve the symptoms and decrease the mortality rate in the CLI patients. The concept of therapeutic angiogenesis was driven by the theoretical concept that Bone-marrow (BM) derived endothelial progenitor cells (EPCs) could incorporate into damaged vessel endothelium and promote collateral vessel formation.

### **2.8.2. Cell therapy**

Cells are attractive mode of therapy due to several reasons: 1) Cells are multifunctional; 2) Cells have distinct autocrine, paracrine and endocrine effects or combination of these effects; 3) Multiple sources of donor cells exist; 4) Cells may be modified in culture or genetically to provide unique potencies for therapy. EPCs can mobilize from the BM and can promote neovascularization at sites of ischemia. The therapeutic potential of BMCs has been evaluated in various small and large animal model studies. These studies reported that BMCs and EPCs functionally contributed to

increased capillary density, improved muscle perfusion and thus wound healing in hindlimb ischemia models. In addition to EPCs and BMCs, several other candidate cell therapies have also been proposed which include including mesenchymal stem cells and adipose tissue derived stromal cells. Adipose tissue derived stromal vascular fraction cells express both hematopoietic and endothelial markers, and have the capacity to differentiate into endothelial cells, and promote post-ischemic neovascularization in murine hindlimbs. These proangiogenic effects of these cells is due to their ability to secrete proangiogenic growth factors like vascular endothelial growth factor (VEGF) and other growth peptides that prevent endothelial cell apoptosis and incorporate into the murine vasculature. Studies of these cells have reported their ability to potentially promote neovascularization and endothelial regeneration in the ischemic tissue. For cells to participate in therapeutic angiogenesis, they should have the ability to successfully home at the site of ischemia. *Ex-vivo* modification of these cells is done to improve their functional activities as disease states can impair the therapeutic efficacy of these cells. Mangi *et al* reported that MSCs overexpressing the anti-apoptotic gene Akt1 (Akt-MSCs) became more resistant to apoptosis in vitro and in vivo and secreted paracrine factors.

### **2.8.3. Gene therapy**

Gene therapy can be defined as the treatment of diseases through transfer of genes to the diseased tissues. The transferred gene can replace a defective gene, introduce a new function to the cell or can enhance the function of the cell. Wolff *et al.* demonstrated that intramuscular injection of naked plasmid deoxyribonucleic acid (DNA) is feasible, and striated muscle as suitable for heterologous transgene expression. It was thought that gene therapy with angiogenic growth factors to achieve therapeutic angiogenesis was a promising concept due to the close relation between the target (micro-vascular circulation) and the source (striated muscle fibres). It has been reported by several studies that angiogenic growth factors stimulate endothelial re-growth in denuded arteries leading to inhibition of neointimal thickening, reduction in thrombogenicity, and restoration of endothelium-dependent vasomotor reactivity. Non-viral gene delivery techniques include the use of naked plasmid DNA, electroporation, particle bombardment, and cationic liposomes and these have comparatively lower efficiency but may have demonstrable biologic effects due to secretion of high potency product. Viral vectors on the other hand are based on the introduction of new genes within genetically modified viruses and are associated with high transfection efficiencies. Adenoviruses are most often used in cardiovascular clinical gene therapy. Gene transfer through viral vectors is associated with inflammatory reactions. Besides this, a major disadvantage is that it's not possible to

treat repeatedly using viral vectors because transduction efficiency is limited by prior viral exposure. This is a very critical issue as the induction of a robust neovascularization is dependent on an angiogenic stimulus over a particular period of time. Also since the angiogenic proteins have a very short half- life, repeated treatment is necessary for a significant therapeutic effect.

#### **2.8.4. Cell Mediated Gene therapy**

Cell-based gene therapy involves the harvesting of cells from patients, *ex vivo* modification of the cells to express therapeutic genes, and subsequent reimplantation of genetically-modified autologous cells. There are very few studies in this area. The maximum benefit from cell therapy depends on their survival at the ischemic site and their function. However cases of graft failure is a major issue. There are several findings that have shown that progenitor function and mobilization could be impaired in certain disease states. Genetic modification of EPCs to overexpress angiogenic growth factors not only enhances the angiogenic response but also extends the lifespan of EPCs. More importantly, it has been shown in experiment that the number of EPCs needed to achieve limb salvage was comparatively less than that required in the previous experiments involving unmodified EPCs. Other than improving the function of cells through gene transfection, these cells can be used as vectors to transfer gene for therapeutic angiogenesis. Ishii *et al* has shown that mesenchymal stem cell (MSC) based

gene therapy with prostacyclin synthase enhanced neovascularization in hindlimb ischemia through sustained release of PGI<sub>2</sub>

### **2.9. Triple catalytic enzyme 1**

As discussed earlier, the prostanoids are biosynthesized through the arachidonate-COX pathway through 3 catalytic steps. The first catalytic step is in which arachidonic acid (AA) is first converted into prostaglandin G<sub>2</sub> (PGG<sub>2</sub>) and in the second catalytic step PGG<sub>2</sub> further converted to prostaglandin endoperoxide (PGH<sub>2</sub>) by COX isoform-1 (COX-1) or COX-2 in cells. In the third catalytic step PGH<sub>2</sub> serves as a common substrate for downstream synthases and is isomerized to prostaglandin D<sub>2</sub> (PGD<sub>2</sub>), E<sub>2</sub> (PGE<sub>2</sub>), F<sub>2</sub> (PGF<sub>2</sub>), and I<sub>2</sub> (PGI<sub>2</sub>) or thromboxane A<sub>2</sub> (TXA<sub>2</sub>) by individual synthases. Considering the vascular protective functions of PGI<sub>2</sub>, increasing its biosynthesis was thought to be a very useful way of protecting the vascular system. Specifically increasing PGI<sub>2</sub> biosynthesis requires a highly efficient chain reaction between COX and PGIS, which consists of the triple catalytic (Trip-cat) functions mentioned above. With this view in mind, a hybrid enzymatic protein was engineered with the ability to perform the Trip-cat functions by linking the constitutive human COX-1 to PGIS through a transmembrane domain of 10 amino acids (His-Ala-Ile-Met-Gly-Val-Ala-Phe-Thr-Trp (10aa)). Thus this enzyme was referred as the Triple-catalytic Enzyme-1 (Trip-cat Enzyme-1) (Figure 3). (Ruan et al., 2006, 2008).

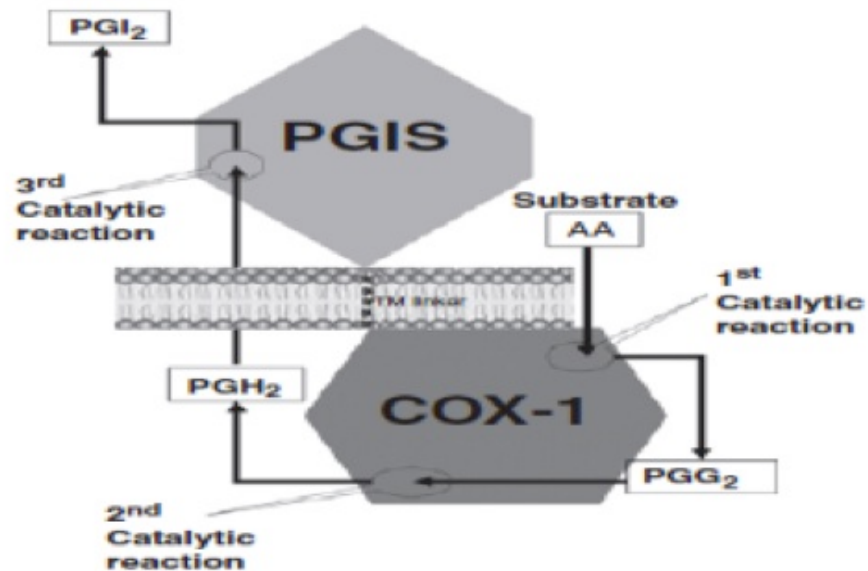


Figure 3. A model of the newly designed Trip-cat Enzyme-1. The Trip-cat Enzyme-1 was created by linking COX-1 to PGIS through an optimized TM linker (10 amino acid residues) without alteration of the protein topologies in the ER membrane. The three catalytic sites and reaction products in COX-1 and PGIS enzymes are shown.

Studies with this enzyme demonstrated that the Trip-cat Enzyme-1 could be stably expressed in HEK293 cells. These cells when treated with exogenous AA were able to convert most of the AA into PGI<sub>2</sub>. In addition, the stable HEK293 cell line, with a capacity to biosynthesize PGI<sub>2</sub>, revealed strong antiplatelet aggregation properties through its unique dual functions (increasing PGI<sub>2</sub> production while decreasing TXA<sub>2</sub> production) in the TXA<sub>2</sub> synthase (TXAS) platelet rich plasma (PRP). The engineering of the triple catalytic enzyme-1 and its capacity to stably express in a human cell line and upregulate PGI<sub>2</sub> biosynthesis provided a basis for developing a PGI<sub>2</sub>- producing therapeutic cell line against vascular diseases.

## **2.10. MicroRNA**

MicroRNAs (miRNAs) are short single-stranded non-coding RNAs with 21–24 nucleotide in length, which play an important role in several regulatory pathways. MiRNAs negatively regulate gene expression at the post transcriptional level by two ways: 1) miRNAs cause translational repression/ gene silencing by binding to the sequences on the target gene; 2) miRNAs cause mRNA degradation by forming complementary base pairing with the target gene sequences. The human encodes at least more than over 1000 miRNAs, which may target about 60% of mammalian genes. MiRNAs show very different characteristics between plants and animals. In animals, miRNAs bind to target sequences in the 3'-UTR of the target gene through imperfect base pairing and resulting in the arrest of translation. Whereas in plants, miRNAs bind with the target sequences through perfect or near perfect complementarity, causing direct cleavage and degradation of the mRNA. It is reported that one miRNA can target many different sites on the same mRNA or on many different mRNAs. By regulating gene expression, miRNAs are proposed to be involved in several biologic processes like proliferation, differentiation, apoptosis, embryogenesis and oncogenesis.

Furthermore, miRNAs genes have been shown to be transcribed by both RNA polymerase II and III and are termed as pri-miRNAs, that contain Cap structures and poly(A)-tails and are hundreds or thousands of nucleotides in length. The maturation of

small RNAs occurs with the help of two RNA type-III endonucleases, named Drosha and Dicer. Drosha along with DGCR8 (RNA binding protein), processes the pri-miRNA transcript in the nucleus by cleaving it at the bottom of its stem loop. The resulting double-stranded RNA precursor molecule called as pre- miRNA is then exported into the cytoplasm, with the help of exportin, a nuclear transport receptor. Once in the cytoplasm, pre-miRNAs are further processed by Dicer to form the short 21-24 nt mature miRNA duplexes. These duplexes are then incorporated into the RNA-induced silencing complex (RISC), and based on the thermodynamic properties; one strand is eliminated whereas the other one remains in the complex. Of the several proteins of the argonaute family that are associated with the RISC complex, argonaute-2 was shown to be responsible for mRNA cleavage. MiRNAs expression can be studied using microarray technique in which miRNAs are hybridized with chips that contain probes to hundreds or thousands of miRNAs targets and thus the relative level of different miRNA expression can be compared. The miRNA expression can be further quantified by quantitative real time PCR. The first miRNA to be discovered was lin-4 in *Caenorhabditis elegans* (Lim *et al.*, 2003).

### **3. METHODS AND MATERIALS**

#### **3.1. Engineering of the cDNA plasmid encoding the hybrid enzyme COX-1-10aa-PGIS sequences.**

The pcDNA 3.1 vector containing a cytomegalovirus early promoter was cloned with cDNAs of the COX-1 and PGIS using a PCR (polymerase chain reaction) cloning approach. The sequences were confirmed by DNA sequencing and endonuclease digestion analyses. The sequence of COX-1 was linked with the PGIS sequence through a 10 amino acid (10aa) (His-Ala-Ile-Met-Gly-Val-Ala-Phe-Thr-Trp) linker to form COX-1-10aa-PGIS (Triple catalytic enzyme-1) on the pcDNA 3.1(+) vector (Ruan *et al.*, 2008).

#### **3.2. Establishing a primary cultured cell line derived from adipose tissue.**

Inguinal adipose tissue, excised from a C57BL/6 mouse, was washed thoroughly with phosphate buffered saline (PBS), pH 7.5, and then digested by collagenase (2mg/mL) at 37° C for 1hr. The digested adipose tissue was then filtered through glass wool and subjected to low speed centrifugation for further separation. The mature adipocytes collected from the upper-layer of the collagenase-digested mouse adipose tissue were placed between two cover slides in a 10-cm cell culture dish with DMEM-F12 containing 10% newborn calf serum (NCS) and 1% antibiotic and antimycotic, and

then were grown at 37° C in a humidified 5% CO<sub>2</sub> incubator. After 15 days, the lipid droplets within the cells completely disappeared. Furthermore, the cells had converted into attached “Fat Cells” with the capacity to synthesize endogenous prostanoids, and were referred to as prostanoid-synthesizing fat cells (PSFCs). The protocol was approved by the Animal Safety Committee of the University of Houston.

### **3.3. Stable expression of the Trip-cat enzyme-1 in the cultured fat cells.**

The PSFCs were grown and transfected with the cDNA of pcDNA3.1-COX-1-10aa-PGIS by the Lipofectamine 2000 method following the manufacturer's instructions (Invitrogen). The stable cell line was created after 4 weeks of using Geneticin (G418) as the selection antibiotic. The cells stably expressing the Trip-cat enzyme-1 were further identified by enzyme assays, western blot analysis and LC/MS analysis and were termed “PGI<sub>2</sub>-PSFCs.”

### **3.4. Enzyme Activity Determination for the Trip-cat Enzyme-1 Using the HPLC Method.**

To determine the activities of the COX-1-10aa-PGIS enzyme, [<sup>14</sup>C] AA (10μM) was added to the PGI<sub>2</sub>-PSFCs in a total reaction volume of 0.1mL. After incubation, the reactions were stopped with 0.2mL of the solvent (solvent A) containing 0.1% acetic acid and 35% acetonitrile. After centrifugation (12,000 rpm for 5min), the supernatant was injected into a C18 column (Varian Microsorb-MV 100-5, 4.6 × 250 mm) using the

solvent A with a gradient from 35 to 100% of acetonitrile for 45min at a flow-rate of 1.0mL/min. The [<sup>14</sup>C]-labeled AA metabolites, including 6-keto-PGF<sub>1α</sub> (degraded PGI<sub>2</sub>), were monitored directly by a flow scintillation analyzer (Packard 150TR).

### **3.5. Determination of the endogenous AA metabolisms in the cultured cells using LC/MS.**

Simultaneous quantification of AA metabolites in the cultured PSFCs (with and without transfection of the Trip-cat Enzyme-1 cDNA) was detected by LC/MS following the reported methods (Ruan et al., 2006, Ruan et al., 2008). Briefly, the cell culture media was collected and applied to a C18 cartridge (Honeywell Burdick & Jackson - Model BJ9575). After washing with water, the AA metabolites bound to the cartridge were eluted with acetone, dried by nitrogen gas, and then dissolved in solvent A (0.1% acetic acid and 35% acetonitrile). The sample was injected into the Waters Micromass LC/MS/MS system by an auto-sampler. The metabolites are first separated by the RP-HPLC C18 column and then automatically injected into the mass detector equipped with an ESI source in a negative mode. Synthetic AA and 6-keto-PGF<sub>1α</sub>, obtained from Cayman Chemical Company (Ann Arbor, MI), were used as standards to calibrate the LC/MS system, identify the corresponding prostanoids, and normalize the detection limits and sensitivities.

### **3.6. Immunoblot analysis.**

The stable transfected cells (PGI<sub>2</sub>-PSFCs) expressing the Trip-cat Enzyme-1 or those PSFCs transfected with vector (pcDNA 3.1) alone were collected and washed with PBS. Membrane proteins were separated by 10% (w/v) SDS-PAGE under denaturing conditions and then transferred to a nitrocellulose membrane. Bands recognized by specific primary antibodies (PGIS, COX-1, or cPGES) were visualized with horseradish peroxidase-conjugated secondary antibody.

### **3.7. Anti-Platelet Aggregation Assays.**

Fresh blood was collected from healthy adult rabbits (in University of Texas) in a 3.2% sodium citrate tube and then centrifuged to separate the platelet-rich plasma (PRP). A total of 0.45mL PRP was placed inside the 37° C incubator of an aggregometer (Chrono-Log) for a total of 3 min. Fifty microliters of sodium arachidonate (5mg/mL) was added to the PRP in the absence and presence of the PSFCs and PGI<sub>2</sub>-PSFCs. The platelet aggregation was then monitored and the readings by the anticoagulant analyzer were obtained indicating the percentage of platelet aggregation inhibited by each of the treated samples.

### **3.8. Mouse Hindlimb Ischemia Model.**

The male C57BL/6J mice (8-10 wk) were anesthetized using isoflurane anesthesia. Excess hair was removed by depilatory cream from both hindlimbs, and the proximal portion of the femoral artery (right side) was ligated with a silk suture. The overlying skin was closed with three surgical staples. The mice were then randomized to three groups (n=6) for: (i) PBS injection; (ii) PGI<sub>2</sub>-PSFC injection and (iii) PSFC injection (empty vector transfected). 24h post-femoral artery ligation, PBS, PSFCs, or PGI<sub>2</sub>-PSFCs (1.5 x 10<sup>6</sup> cells) were injected intramuscularly at 3-different sites around the ischemic region. Blood flow recovery was assessed by the Laser Doppler Perfusion Imager (LDPI) technique. Specifically, blood flow reperfusion was evaluated at 0hr (before ligation), 24hr, 3 day, 7 day, 14 day and 21 day post ligation using LDPI. The results were expressed as the ratio of perfusion in the ischemic and the non-ischemic limb.

### **3.9. Determination of the endogenous AA metabolisms in the mice urine using LC/MS analysis.**

Urine samples were collected from mice induced with ischemia (PBS, PGI<sub>2</sub>-PSFC and PSFC groups, n=6) at time points 0 (before femoral artery ligation), 3, 7, 14 and 21 days (post femoral artery ligation). These urine samples were further processed for injection into the Waters Micromass LC/MS/MS as discussed in method 3.5.

### **3.10. Mouse Running Time model.**

To further confirm, if the mice with limb ischemia after treatment showed recovery in perfusion, a functional mobility assay was performed. Mice were familiarized with treadmill running each day from the beginning for one week before hindlimb unilateral femoral artery ligation. Only those mice that were able to run on a treadmill for 1hr underwent the complete process of running time testing. After 1 week, the mice were ligated and each of the three treated groups (PBS, PGI<sub>2</sub>-PSFC and PSFC groups, n=6) were placed on a treadmill at a 7-degree angle for 5 minutes at 5 m/min to acclimate, and then speed was increased to 10 m/min (t = 0). Speed was increased every 2 minutes until fatigue (when animals spent more than 5 seconds on the stimulator grid at the rear of the treadmill). The mice were tested for running time on days 3, 7, 14 and 21 days postligation.

### **3.11. Thrombotic occlusion model. (Photochemical vascular injury)**

A photochemical thrombotic occlusion model was used to produce injury in the mouse carotid artery. Briefly the male mice were anesthetized with sodium pentobarbital (80mg/kg, i.p.) and placed in a supine position. After a midline cervical incision, a cannula was inserted into the left jugular vein for administration of Rose Bengal (Sigma Aldrich). The left common carotid artery was exposed and a laser doppler

flow probe 407 connected to Laser Doppler Perfusion Monitor (LDPM) Unit-Periflux System (PF) 5010 was placed on the artery for recording the blood flow. After recording a constant baseline blood flow, approximately  $1.5 \times 10^6$  PGI<sub>2</sub>-PSFCs (overexpressing COX-1-10aa-PGIS) or empty vector transfected PSFCs were added locally over the carotid artery. Next, the carotid artery was exposed to 1.5mW green laser beam 540nm (Melles Griot, CA, USA) from a distance of 5cm and rose bengal (50mg/kg) was injected through the jugular vein. At this point blood flow was constantly recorded using the accompanying software. The formation of an occlusive thrombus was indicated by the cessation of blood flow.

### **3.12. MiRNA Microarray Analysis.**

PSFCs and PGI<sub>2</sub>-PSFCs were cultured as described above and after 24hrs the total RNA was isolated using TRIZOL reagent. In another experiment, PGI<sub>2</sub>- PSFCs were serum starved for 5-6 hrs and then one plate was treated with IP antagonist CAY10441 (1 $\mu$ M) and the other with PPAR $\gamma$  antagonist GW9662 (5 $\mu$ M). After 24hrs, total RNA was isolated. Total RNA samples were analyzed by LC Sciences (Houston, TX, USA), which provided microarray analyses. Briefly, detection was done by fluorescence labelling using tag-specific Cy3 (for PSFCs) and Cys 5 dyes (for PGI<sub>2</sub>-PSFC). Hybridization images were collected using a laser scanner. The ratio of the two sets of detected signals (log<sub>2</sub> transformed, balanced) and P- values of the t- test were calculated. Differentially

detected signals were those with less than 0.05 P- values. Upon receiving their results, a search was performed on the target genes of the individual miRNAs using the website, [microrna.sanger.ac.uk](http://microrna.sanger.ac.uk).

### **3.13. Quantitative Real Time PCR (qRT-PCR).**

The miRNA-711 expression upregulation observed in the microarray was further confirmed and quantified by qRT-PCR approach using three kits obtained from SA Biosciences (Frederick, MD) following the detailed instructions in the kits. Firstly, the miRNAs were isolated from the cultured PGI<sub>2</sub>-PSFCs or control PSFCs using RT<sup>2</sup> qPCR-Grade miRNA Isolation Kit. Secondly, the isolated miRNAs were converted into cDNAs using RT<sup>2</sup> miRNA First Strand Kit; and finally, the cDNAs were mixed with another kit, RT<sup>2</sup> SYBR<sup>®</sup> Green qPCR Master Mix, the primer for miRNA711 and sno RNA-142 (control), and then analyzed by qPCR using Applied Biosystems 7300 Real Time PCR System. Differential expression of miRNA-711 in the cells was analyzed by the  $\Delta\Delta\text{CT}$  method using the mouse housekeeping sno RNA-142 (small nucleolar RNA) as the endogenous control. The levels of miRNA711 in the cells were calculated using the formula  $2^{-\Delta\Delta\text{Ct}}$  (n=3).

### **3.14. Illumina gene expression assay**

Two hundred nanograms of total RNA from PSFCs and PGI<sub>2</sub>-PSFCs were amplified and purified using Illumina TotalPrep RNA Amplification Kit (Ambion, Inc.) following the manufacturer's instructions. Briefly, the first strand cDNA was synthesized by incubating RNA with T7 oligo(dT) primer and reverse transcriptase mix at 42 °C for 2 hours. RNase H and DNA polymerase master mix were immediately added into the reaction mix following reverse transcription and were incubated for 2 hours at 16 °C to synthesize second strand cDNA. RNA, primers, enzymes and salts that would inhibit in vitro transcription were removed through cDNA filter cartridges (part of the amplification kit). In vitro transcription was performed and biotinylated cRNA was synthesized by 14-hour amplification with dNTP mix containing biotin-dUTP and T7 RNA polymerase. Amplified cRNA was subsequently purified and the concentration was measured by a NanoDrop ND-1000 Spectrophotometer (NanoDrop Technologies, DE). An aliquot of 1.5 micrograms of amplified products were loaded onto Illumina Sentrix Beadchip Array Mouse-6 arrays, hybridized at 58 °C in an Illumina Hybridization Oven (Illumina, Inc.) for 17 hours, washed and incubated with streptavidin-Cy3 to detect biotin-labeled cRNA on the arrays. Arrays were dried and scanned with BeadArray Reader (Illumina, Inc.). Data were analyzed using BeadStudio software (Illumina, Inc.). Clustering and pathway analysis were performed with BeadStudio and Ingenuity Pathway Analysis (Ingenuity Systems, Inc.) software respectively.

### **3.15. Akt1 immunoblot.**

Cells were harvested and lysed in lysis buffer [50mM Tris-HCl (pH 7.4), 1% Triton X-100, 150mM NaCl, 1mM EDTA, 1mM phenylmethanesulphonylfluoride, 1% aprotinin, 10mg/mL leupeptin, 1mM sodium orthovanadate, and 1mM sodium fluoride. Cell lysates were centrifuged at 12,000 g for 10 min at 4°C. Protein concentration of the cell lysate was determined by performing BCA protein assay. SDS-PAGE sample buffer was added to the lysates, which were then heated to 100°C for 5 min. 25µg of protein was loaded in each well of 10% acrylamide gel and separated by electrophoresis. Proteins were transferred onto a nitrocellulose membrane, which was incubated with primary antibody against Akt1 and a horseradish peroxidase conjugated secondary antibody. Chemiluminescence was detected using ECL Kit (Amersham).

### **3.16. Lipid accumulation study in PSFCs and PGI<sub>2</sub>-PSFCs.**

PSFCs and PGI<sub>2</sub>-PSFCs were grown to 50% confluency in DMEM-F12 medium containing 10% newborn calf serum. This medium was then replaced by adipogenic medium: DMEM containing 10% fetal bovine serum (FBS), 1µM dexamethasone (Sigma-Aldrich), 0.5mM Isobutyl methyl xanthine (IBMX) and insulin (10µg/mL), and the cells were allowed to grow in this medium for 4 days. After 4 days the cells were re-fed with DMEM-F12 media containing 10% FBS and 10µg/mL insulin, and were grown for an

additional 3 days. Images were taken everyday to observe cells accumulating lipid droplets.

### **3.17. Oil Red-O staining.**

After treating the cells with differentiation media for 7 days, accumulation of intracellular lipid was identified by Oil Red-O (Sigma-Aldrich) staining. A 0.36% (w/v) solution of Oil Red-O was prepared in 60% isopropanol. The cells were washed twice with PBS and fixed with 4% paraformaldehyde for 5 min and then washed with PBS and isopropanol. The cells were then stained with Oil Red-O solution for 30 min and rinsed with isopropanol. Cells were observed via light microscope with 100X magnification and then photographed using a Kodak DC 290 Zoom Digital Camera (NY, USA).

### **3.18. Construction of the cDNA plasmid for generating the transgenic mice overexpressing COX-1-10aa-PGIS.**

The sequence of COX-1 linked to PGIS through a 10 amino acid linker (COX-1-10aa-PGIS, Trip-cat enzyme-1) was generated by a PCR approach and subcloning procedures provided by the vector company (Invitrogen). The resulting cDNA of the engineered COX-1-10aa-PGIS was successfully subcloned into the pcDNA 3.1 vector at KpnI and BamHI sites containing a cytomegalovirus early promoter using a polymerase chain reaction (PCR) cloning approach. The procedures have been previously described

[Ruan, 2006, Ruan, 2008]. The correct cDNA sequences were confirmed by DNA sequencing and restriction enzyme digestion analyses. A 3.2 Kb cDNA plasmid construct (COX-1-10aa-PGIS) containing CMV promoter and PGH polyadenylation site (pA) was cut at the NruI and SphI sites. The identity of the construct was confirmed by restriction enzyme mapping and DNA sequence analysis.

### **3.19. Generation of Transgenic Mice overexpressing COX-1-10aa-PGIS.**

The transgene construct fragment was gel purified with QIAGEN Kit. All live animal procedures were conducted with the approval of institutional animal care and use committee. The transgenic mice were generated using pronuclear microinjection technique (Nature Protocols 2, 2007) in the M.D. Anderson Institute. Mice used for the generation of transgenic mice were maintained on a 14hr light/10hr dark cycle. FVB/NJ (Jackson Lab) female mice were superovulated with 5 IU of pregnant mare serum-gonadotropin and after 48hrs with 5 IU of human-chorionic gonadotropin. These females were placed with intact FVB males for mating. Fertilized oocytes were collected from the isolated oviducts of the superovulated females the following morning and treated briefly with bovine hyaluronidase in M2 medium to remove the associated debris. The purified cDNA construct was diluted just before microinjection to a concentration of 3ng/uL. The cDNA (COX-1-10aa-PGIS) was microinjected into the pronuclei of fertilized oocytes using standard techniques, and the manipulated oocytes

were transferred surgically into the oviducts of surrogate (pseudo-pregnant) recipient female mice and allowed to develop to full term.

### **3.20. Identification of the Transgenic Mice by PCR Analysis.**

The initial screening of founder mice for COX-1-10aa-PGIS transgene was carried out by PCR analysis on mouse tail DNA. This protocol was developed by Jon Neumann (<http://cmn.osu.edu/1894.cfm>). Briefly, tail samples (1.5-2 mm) were digested in 100  $\mu$ l of 1xPCR buffer with added detergents (0.45% NP40, 0.45% TWEEN 20) and 10  $\mu$ l Proteinase K (10 mg/ml) @ 60°C overnight. The sample was further denatured for the Proteinase K by boiling for 15 min, and then cooled on ice for 5 minutes. The isolated genetic DNA (2uL tail DNA was added into a final 20uL volume reaction) was subjected to PCR analysis using PCR Reaction Buffer (1x PCR buffer, 2.5 mM MgCl<sub>2</sub>, 200  $\mu$ M dNTPs, 1  $\mu$ M each designed primer and 1 unit Taq Polymerase with conditions (hold @ 94°C for 4.5 min, 30x step cycles of 94°C for 30 sec (requires annealing temperature for 20 sec - varies according to G/C content of primers), 72°C for 1 min and holding @ 4°C until ready to analyze. PCR was performed. The primer sets for the COX-1-10aa-PGIS gene are: sense 5'-CCTCAAGGGTCTCCTAGGGA-3' and antisense 5'-GTGCTTCTCCTTCATCCTCGT-3'. The amplified product length is 445 bp. The PCR product was analyzed by agarose gel. The RNA isolated from tail clips of the mice was used as template for qPCR using the designed primers.

### **3.21. Breeding of the transgenic mice to get a colony of homozygous mice.**

The hemizygous FVB/N founder mice expressing COX-1-10aa-PGIS were further bred with wild type FVB/N mice to get a colony of F1 heterozygous mice. After achieving enough number of heterozygous mice and identifying them by tail clip PCR, these heterozygous mice were bred (male and female mating) to further get a colony of homozygous mice expressing COX-1-10aa-PGIS.

### **3.22. Identification of homozygous transgenic mice by qPCR.**

The tail clips collected from a set of heterozygous, homozygous and wild type mice was cut into small pieces with the help of sterile razor blade. About 100mg of the tissue was crushed with the help of pestle in a porcelain mortar containing 1mL of TRIzol reagent from Invitrogen. The ground tissue was transferred to eppendorff tubes and allowed to stand for 5 minutes and then the tubes were centrifuged at 10,000g for 15 minutes at 4°C. The supernatant was isolated and the procedure was followed as given in the Invitrogen protocol to isolate the RNA. The concentration of RNA was measured using Nanodrop Bioanalyzer. First strand cDNA was synthesized using the Superscript III First-Strand Synthesis System for RT-PCR from Invitrogen. 5µg of total RNA was used as the starting material. The first strand cDNA obtained in the synthesis reaction was further amplified using PCR and Qiagens QuantiTect SYBR Green PCR kit and platinum

Pfx DNA polymerase. The cDNA used was diluted in a 1:10 ratio and 8 $\mu$ L of this cDNA was used in a final reaction volume of 20 $\mu$ L. Real time quantitative PCR was run using the ABI7500 Fast Real Time PCR system. The PCR conditions were 95°C for 15mins. Subsequent PCR amplification consisted of 35 cycles with 95°C for 15s, annealing at 60°C for 30s and 72°C for 30s. GAPDH was used as the internal control. Each sample was run as duplicate. Ct values were obtained and compared.

### **3. 23. Bleeding time measurement.**

A 2mm tip of the tail was cut with scissor and time was noted as 0 seconds and blood was blot on the filter paper. Then every 30 seconds the tip of tail drop was blot on a filter paper. This was continued until there was no stain of blood and this was considered as the bleeding time. The bleeding time was compared between the wild type and transgenic mice.

### **3.24. Determination of endogenous PGI<sub>2</sub> production in transgenic mice by LC/MS analysis.**

Each of the wild type mice and transgenic mice were placed in metabolic cages and the urine was collected until a final volume of 1mL. Then the urine samples were processed for LC/MS injection as above in method section 3.5. The data was analyzed to detect 6-keto-PGF<sub>1 $\alpha$</sub> , TXB<sub>2</sub> and PGE<sub>2</sub> in both wild type (WT) and transgenic (TG) mice. The

values of the corresponding prostanoids were normalized with background and then the ratio of 6-keto-  $\text{PGF}_{1\alpha}$  to other prostanoids was calculated and plotted.

### **3.25. Determination of COX-1-10aa-PGIS expression in the different organs in transgenic mice by PCR analysis.**

The mice were euthanized and organs and tissues (brain, heart, adipose tissue, liver, lung, kidney, uterus, pancreas, intestine) were isolated from the mice (both wild type and transgenic mice). Photographs were taken to identify any phenotype difference between the WT and TG mice. Then about 50mg of the tissue was taken in eppendorff tubes and digested overnight using the same procedure as described above. Then on the next day, DNA was isolated using Qiagen's DNAeasy mini kit. 400ng of DNA was used as the starting material for running the PCR. PCR was run using the same procedure as described above in method section 3.20.

### **3.26. Immunoblot analysis of COX-1-10aa-PGIS in the different organs of transgenic mice.**

The organs were isolated from mice and 100mg tissue were homogenized on ice in lysis buffer (protease inhibitor, 1mM PMSF, 1M Tris (pH 7.4), 0.5 M EDTA) for 2-3 mins. The lysate was centrifuged at 10,000 rpm for 10 mins at 4°C. Protein concentration was determined by BCA protein assay method. A concentration of 25 $\mu\text{g}$

protein was loaded in each well and bands were visualized using specific antibodies of COX-1 and PGIS.

### **3.27. Blood pressure and heart rate measurement.**

The blood pressure (BP) and heart rate (HR) was measured using the tail cuff method using the CODA system from Kent Scientific Corporation, Torrington, CT. Blood pressure of every individual mouse was measured for three consecutive days to allow for acclimatization and thereby obtain a more accurate measure. Systolic, Diastolic BP, and HR were measured and plotted to compare any change in these parameters between WT and TG mice.

### **3.28. Thrombotic occlusion model. (Photochemical vascular injury) in transgenic mice.**

A photochemical thrombotic occlusion model was used to produce injury in the mouse carotid artery of both the wild type and transgenic mice. Briefly the male mice were anesthetized with isoflurane and placed in a supine position. After a midline cervical incision, the left common carotid artery was exposed and a laser doppler flow probe 407 connected to Laser Doppler Perfusion Monitor (LDPM) Unit-Periflux System (PF) 5010 was placed on the artery for recording the blood flow. After recording a constant baseline blood flow, the carotid artery was exposed to 1.5mW green laser beam 540nm (Melles Griot, CA, USA) from a distance of 5cm and rose bengal (50mg/kg)

was injected through the tail vein. At this point blood flow was constantly recorded using the accompanying software. The formation of an occlusive thrombus was indicated by the cessation of blood flow. The blood perfusion was measured for 120 mins and perfusion values were plotted in both the WT and TG groups of mice at different time intervals.

## 4. RESULTS

### 4.1. Isolation, culture, and conversion of the adipocytes into prostanoid-synthesizing fat cells (PSFCs).

It has been reported that adipocytes could be reversely differentiated into bipotent cells with a characteristic loss of lipid synthesis and increased adherence tendency. Figure 4. A shows the time course display of the differentiation of adipocytes with the conditional medium. The lipid droplets within the adipocytes gradually disappeared and formed attached cells (Figure 4A). The cells were able to metabolize endogenous AA and synthesize a large amount of PGE<sub>2</sub> (3ng/10-cm dish cells) and a very small amount of 6-keto-PGF<sub>1α</sub> (0.1ng/10-cm dish cells), as identified by LC/MS analysis (Table 1, Figure.5. B). To further confirm the AA metabolism in the cells, an exogenous AA-metabolized profile was investigated by an assay using [<sup>14</sup>C] AA as a starting substrate (Figure 5A). The assay clearly showed that both [<sup>14</sup>C] PGE<sub>2</sub> and [<sup>14</sup>C] 6-keto-PGF<sub>1α</sub> were produced when [<sup>14</sup>C] AA was added (Figure.5A). This indicated that these cells, similar to the endothelial cells, contain the enzymes necessary to synthesize PGE<sub>2</sub> and PGI<sub>2</sub>. Using Western blot analysis, the cell's expression of COX-1, PGIS, and cPGES were confirmed and the inducible COX-2 and mPGES-1 were not detectable (Figure 4B, panel i). The cells expressing the TXA<sub>2</sub> receptor (TP), PGI<sub>2</sub> receptor (IP), and the four PGE<sub>2</sub> subtype receptors (EP1- EP4) were also detected (Figure 4B, panel ii). In addition,

the ability to be reproduced for many passages (a stromal cell property) was also confirmed in the cells.

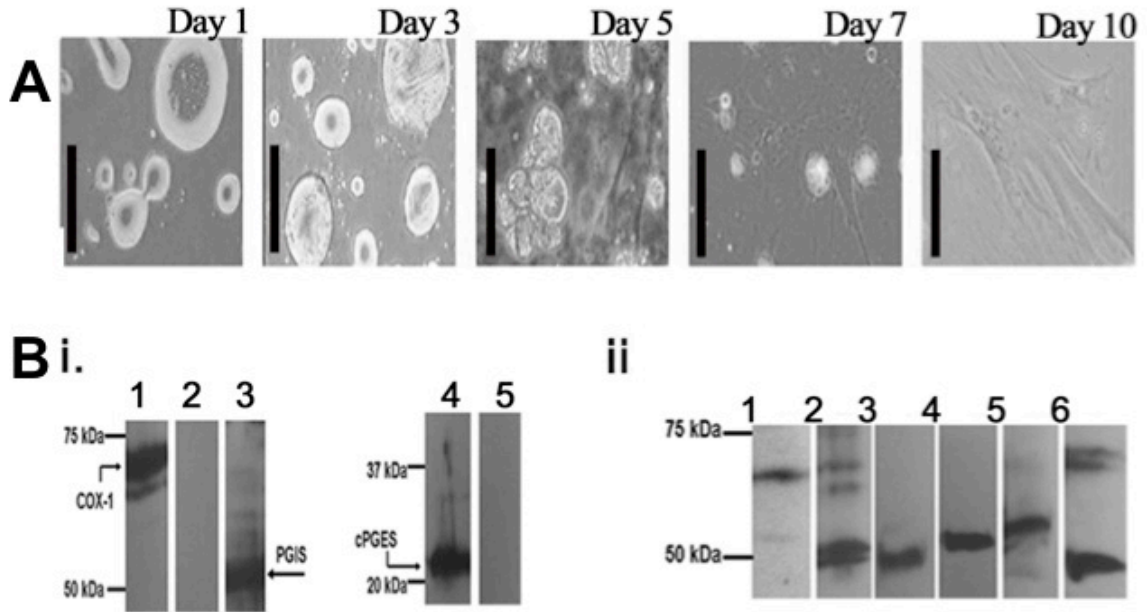


Figure. 4. A.) Time-course of the differentiation of mouse adipocytes under a conditional medium. The days of the culture are indicated as labeled. Black bar, 50μm. Briefly, mature adipocytes from the supernatant of the digested adipose tissue was placed between two coverslips and then allowed to differentiate in the DMEM F-12 medium. B.) Profiles of the Western blot analyses for prostanoids synthesizing enzymes (i) and receptors (ii) for the prostanoid-synthesizing cells. The COX-1, PGIS, and cPGES were identified in panel i, and the IP, TP, EP1, EP2, EP3 and EP4 receptors were identified in panel ii in lanes 1, 2, 3, 4, 5 and 6 respectively. The inducible COX-2 (lane 2) and mPGES-1 (lane 5) were not present (i).

Thus, these cells were referred to as prostanoid-synthesizing fat cells (PSFCs).

The generated cells also demonstrated some endothelial cell properties, such as the expression of endogenous PGI<sub>2</sub> synthase and its receptor, which are part of the endothelial cell markers.

Table 1. Comparison of the biosynthesis ratio of the endogenous PGI<sub>2</sub> and PGE<sub>2</sub> in the PSCs and PGI<sub>2</sub>-PSCs as determined by LC/MS

Cell Types	PGI <sub>2</sub> (ng/10-cm dish of cells) (n=3)	PGE <sub>2</sub> (ng/10-cm dish of cells) (n=3)	PGI <sub>2</sub> /PGE <sub>2</sub>
PSCs	0.1 ± 0.01	3 ± 0.1	0.03
PGI <sub>2</sub> -PSCs	5 ± 0.3	0.2 ± 0.02	25
Change in Vascular Protection Factors	50-fold PGI <sub>2</sub> Increase	15-fold PGE <sub>2</sub> Decrease	N/A

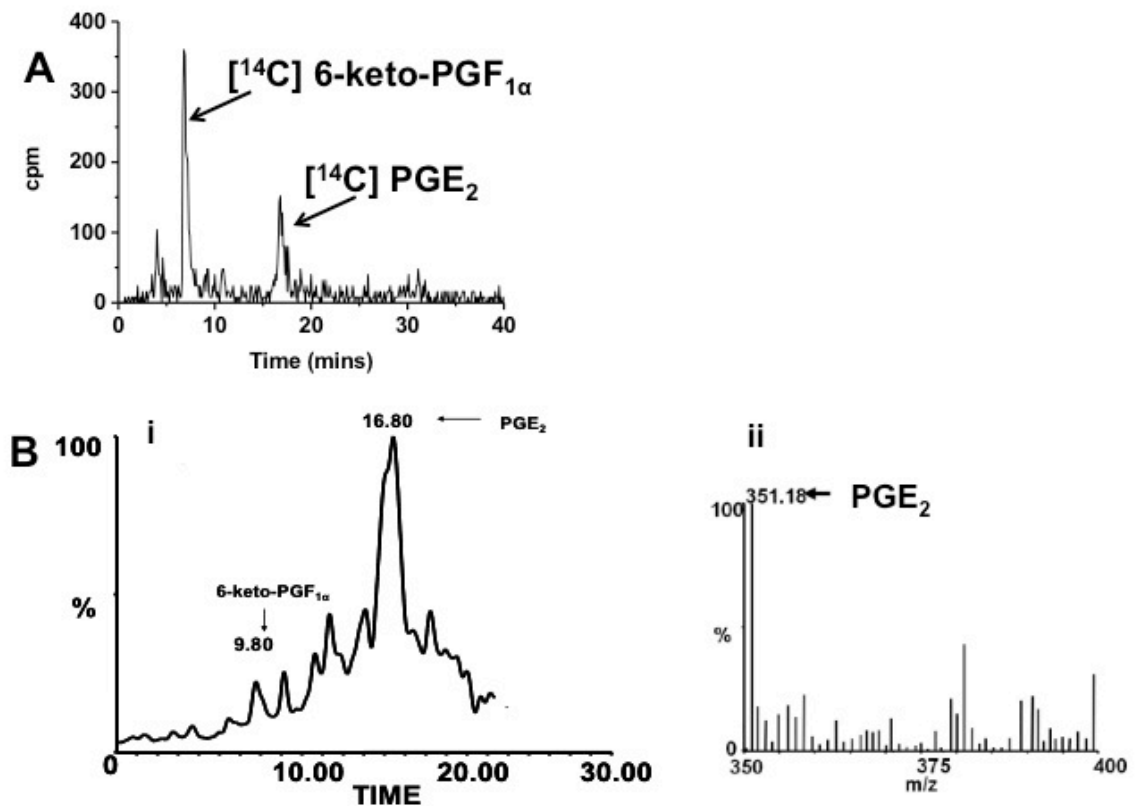


Figure 5. A.) Determination of the [ $^{14}\text{C}$ ]AA metabolism in the PSFC using an isotope-HPLC method. The cells ( $\sim 0.1 \times 10^6$ ) transfected with the empty vector pcDNA 3.1 were washed three times, suspended in 0.01 M phosphate buffer, pH 7.4 containing 0.15% NaCl (PBS) and then incubated with [ $^{14}\text{C}$ ]-AA (10  $\mu\text{M}$ ) in a total volume of 100  $\mu\text{L}$ . After 5 min, the reaction was terminated by the addition of 200  $\mu\text{L}$  of 0.1% acetic acid containing 35% acetonitrile (buffer A), and centrifuged at 12 000 rpm for 5 min. The supernatant was separated by HPLC on a C18 column (4.5  $\times$  250 mm) using buffer A with a gradient of 35-100% acetonitrile. The [ $^{14}\text{C}$ ]-AA metabolites were determined by a liquid scintillation analyzer built in the HPLC system. The retention times of [ $^{14}\text{C}$ ]-6-keto-PGF $_{1\alpha}$  and [ $^{14}\text{C}$ ]-AA were calibrated by standards under the same conditions. The amounts of produced 6-keto-PGF $_{1\alpha}$  represented the amounts of the produced PGI $_2$ .

B.) LC/MS analysis of PSFCs showing endogenous metabolism of AA to PGE $_2$ . (i) chromatogram of PGE $_2$  at 16.8 mins, (ii) Mass spectrum of PGE $_2$  (molecular weight 351 in negative mode). Cells were cultured in a 10cm plate. The supernatant was passed through C18 column and eluted with acetone. It was dried and dissolved in 150 $\mu\text{L}$  buffer A with 100  $\mu\text{L}$  used for LC/MS/MS analysis

#### 4.2. Engineering and cloning of the triple catalytic enzyme -1 (COX-1-10aa-PGIS)

A cDNA sequence encoding a novel Trip-cat Enzyme-1 (COX-1-10aa-PGIS), linking the C-terminus of human COX-1 to the N-terminus of human PGIS by a helical linker with 10 amino acid residues (His-Ala-Ile-Met-Gly-Val-Ala-Phe-Thr-Trp (10aa)) derived from human rhodopsin, was created by a PCR approach and then subcloned into pcDNA3.1, with a CMV promoter (Figure 6) using a similar approach, as described by Ruan *et al*, 2006.

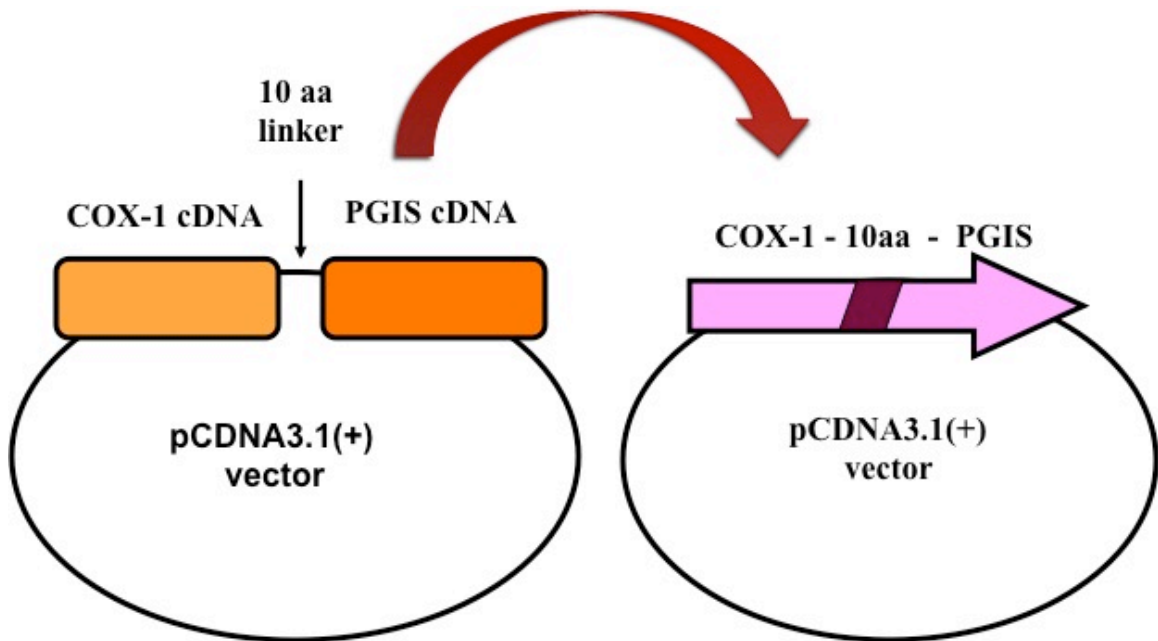


Figure.6. Engineered cDNA plasmid containing COX-1 linked to PGIS cDNA , through the 10aa sequence generated by PCR approach and subcloning procedures . The pcDNA 3.1 vector containing a cytomegalovirus early promoter was cloned with cDNAs of the COX-1 and PGIS using a PCR (polymerase chain reaction) cloning approach. The sequences were confirmed by DNA sequencing and endonuclease digestion analyses. The sequence of COX-1 was linked with the PGIS sequence through a 10 amino acid (10aa) (His-Ala-Ile-Met-Gly-Val-Ala-Phe-Thr-Trp) linker to form COX-1-10aa-PGIS (Triple catalytic enzyme-1) on the pcDNA 3.1(+) vector.

### **4.3. Redirecting the PSFC line to specifically and constantly convert AA into PGI<sub>2</sub>, thereby forming the PGI<sub>2</sub>-PSFC line.**

The PSFCs are suitable to be engineered into PGI<sub>2</sub>-producing cells because these cells contain endogenous AA, which can be metabolized to PGI<sub>2</sub> by overexpressing COX-1-10aa-PGIS. The PSFCs were transfected with the pcDNA3.1-COX-1-10aa-PGIS plasmid. Using G418 screening approach, which was followed for more than three weeks, generated the stable cell line. Subsequently, the successful overexpression of the recombinant COX-1-10aa-PGIS protein in the PSFCs was confirmed by a Western blot analysis that showed the correct molecular mass of the PGI<sub>2</sub>-producing enzyme, approximately 130 kDa (Figure 7A, panel i). The stable transfection of COX-1-10aa-PGIS in PSFCs cells and its enzymic activity was further confirmed by the metabolism of the [<sup>14</sup>C] AA into [<sup>14</sup>C] 6-keto-PGF<sub>1α</sub> (degraded [<sup>14</sup>C] PGI<sub>2</sub>, Figure 7B, panel i) as analyzed by HPLC assay. The endogenous AA that was metabolized into PGE<sub>2</sub> (by the endogenous cPGES, Figure. 5B) in the PSFC line was redirected to produce PGI<sub>2</sub> in the PSFC line overexpressing the Trip-cat Enzyme-1 (PGI<sub>2</sub>-PSFC line) as analyzed by the LC/MS analysis (Figure. 7A and B, panel ii). Thus, this cell line was termed the “PGI<sub>2</sub>-PSFC” line, an exceptional model for studying the biological functions of continuously produced, unstable PGI<sub>2</sub> from the endogenous AA. By transfecting the COX-1-10aa-PGIS cDNA into the PSFCs, the vascular protector (PGI<sub>2</sub>) production was increased by 50-fold and the inflammatory PGE<sub>2</sub> synthesis was decreased by 15-fold (Table 1). Thus, the cells

resulting from this cell line were termed, PGI<sub>2</sub>-PSFCs in respect to their specific biosynthesis of PGI<sub>2</sub>.

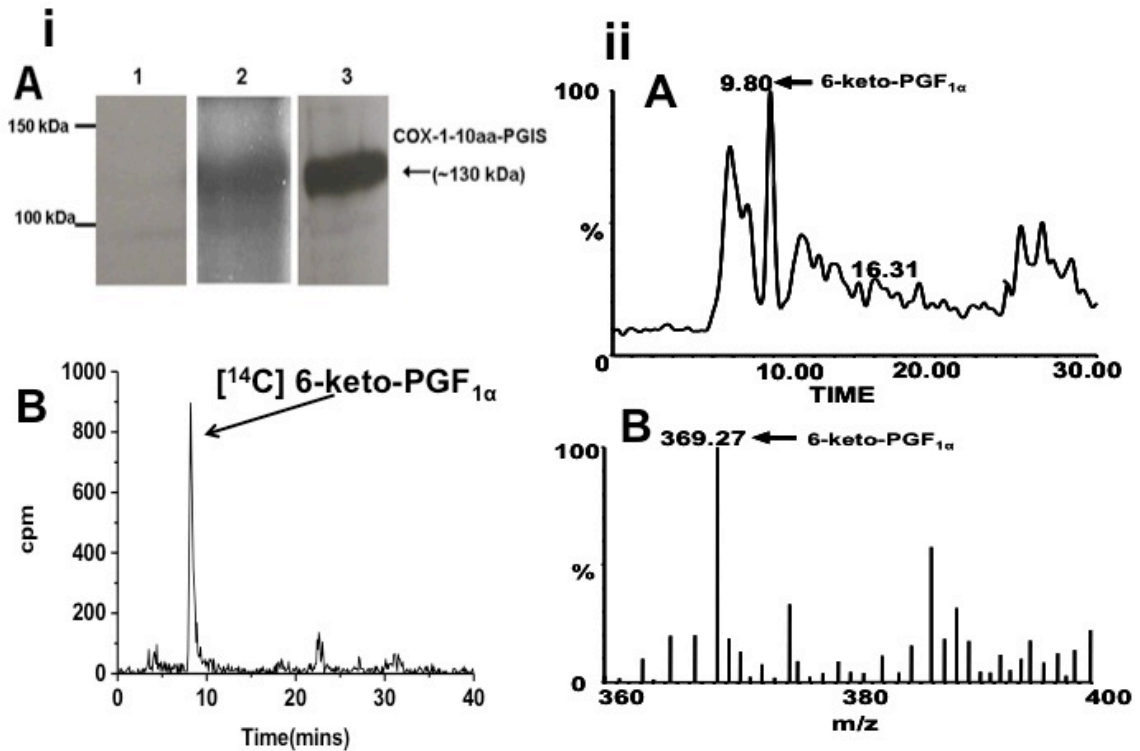


Figure.7.i. (A) Western blot analysis of the PGI<sub>2</sub>- prostanoid-synthesizing cells using 7% SDS-PAGE. Untransfected prostanoid-synthesizing cells (Lane 1), HEK293 cells positively expressing COX-1-10aa-PGIS (Lane 2) the PGI<sub>2</sub>-PSFCs stably expressing COX-1-10aa-PGIS (Lane 3). The Trip-cat enzyme-1 is indicated with an arrow at 130kDa. B). Determination of the [<sup>14</sup>C] AA metabolism in the PGI<sub>2</sub>-PSFCs to 6-keto-PGF<sub>1α</sub>. The same method as described in figure 5 was followed. 6ii. LC/MS analysis of PGI<sub>2</sub>-PSFCs. A) chromatogram of 6-keto-PGF<sub>1α</sub> at 9.8 mins with B) spectrum showing molecular weight 369.

#### 4.4. PGI<sub>2</sub>-PSFCs inhibiting platelet aggregation in vitro

It is known that platelets primarily convert AA into TXA<sub>2</sub> through the coupling actions of COX-1 and TXAS. In the platelet rich plasma (PRP), the majority of the added

AA was metabolized into TXA<sub>2</sub>, which triggered platelet aggregation in minutes (Figure 8A). However, in the presence of PGI<sub>2</sub>-PSFCs, the platelet aggregation was completely blocked (Figure 8C), which indicated that the cells were able to shift the AA metabolisms from TXA<sub>2</sub> to PGI<sub>2</sub> and thereby mediate anti-platelet aggregation in the PRP. On the other hand, the empty vector transfected PSFCs, which produce PGE<sub>2</sub>, could only delay and not completely block platelet aggregation (Figure 8B). This indicates that the engineered COX-1-10aa-PGIS, expressed in the PSFCs, was able to effectively compete in the AA metabolism with the endogenous TXAS. Furthermore, the results imply that the PGI<sub>2</sub>-PSFCs should be able to increase PGI<sub>2</sub> levels and decrease TXA<sub>2</sub> production in the circulation for vascular protection if the cells are delivered into the circulation system.

#### **4.5. Effect of the PGI<sub>2</sub>-PSFCs on mouse thrombotic occlusion model.**

PGI<sub>2</sub>-PSFCs' effect producing PGI<sub>2</sub> upon thrombogenesis in mice was investigated. Blood flow was recorded before and after thrombotic occlusion in the mouse carotid artery in the presence of PGI<sub>2</sub>-PSFCs and the empty vector transfected PSFCs - the control. Photochemical injury induced by rose bengal and laser light produced a cessation of blood flow. Although eventually restored in the presence of PGI<sub>2</sub>-PSFCs (Figure 9A), the blood flow continuously decreased in the presence of PSFCs, the negative control (Figure 9B). This suggested that PGI<sub>2</sub>-PSFCs, which produce PGI<sub>2</sub>,

help to abolish the formation of a thrombus in the carotid artery almost completely when applied locally.

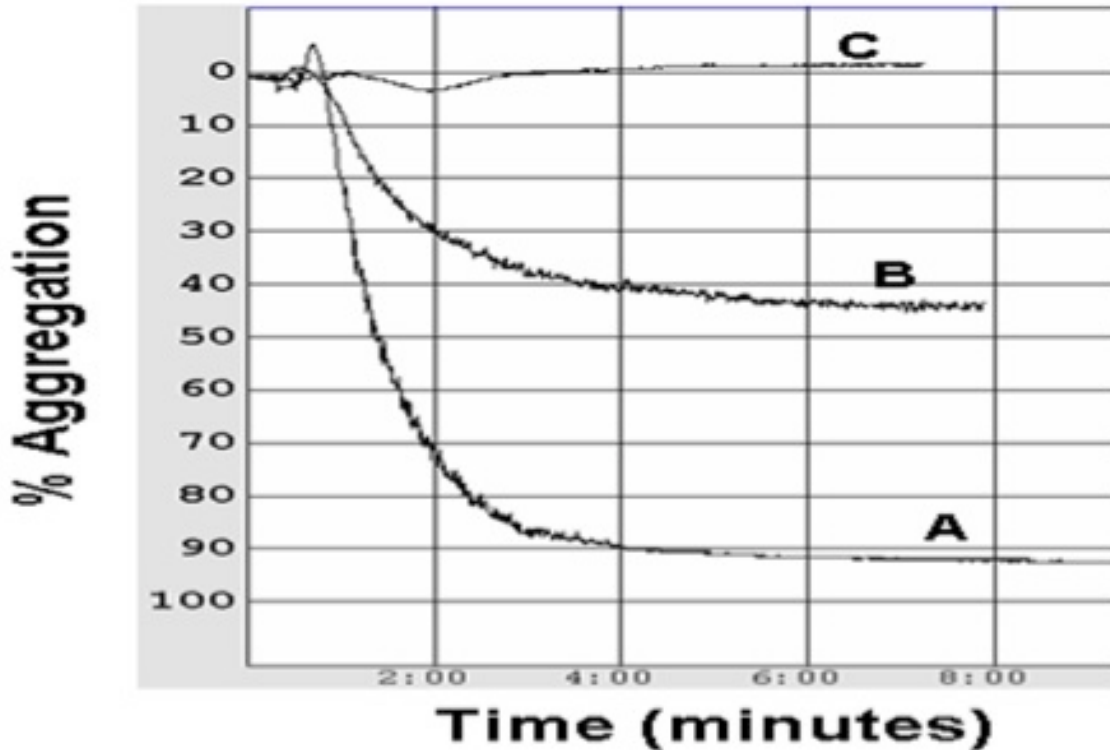


Figure 8. Effects of the PGI<sub>2</sub>-PSFCs on platelet aggregation. The platelet-rich plasma was incubated with 100 μM AA at 37°C in the presence of 50μL PBS (A), PSFCs empty vector transfected (B) and the PGI<sub>2</sub>-PSFCs expressing Trip-cat Enzyme-1 (C). The amount of cells used for the experiments were approximately  $0.2 \times 10^6$  per assay.

#### 4.6. Effect of the PGI<sub>2</sub>-PSFCs on mouse ischemic hindlimb model.

To test the vascular protection of the PGI<sub>2</sub>-PSFCs *in vivo*, a mouse ischemic hindlimb model was generated by placing a ligature on the right femoral artery of the C57BL/6J mice, following the procedures described previously. The reduction in blood

flow in the right hindlimb, following the ligation, was clearly detected (Figure 10A, panel i – ‘2’) using a Laser Doppler Perfusion Imager (LDPI) System, in comparison to that of the

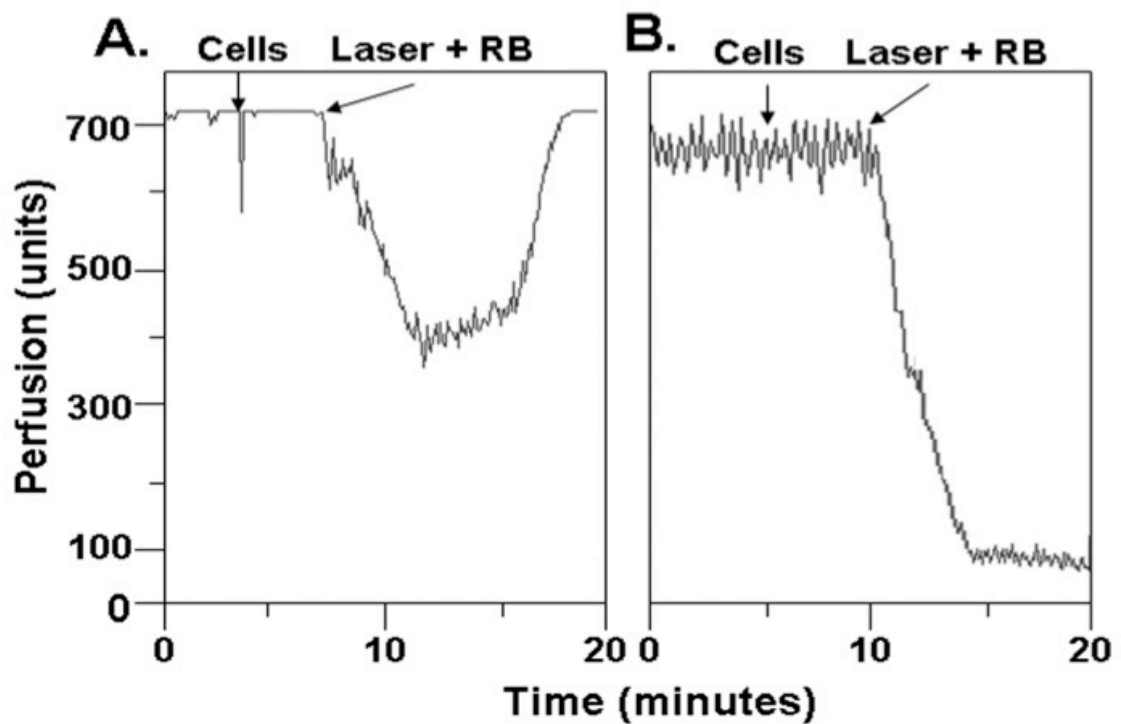


Figure.9. Effect of the cell treatment on blood perfusion induced with thrombogenesis using photochemical vascular thrombotic occlusion model. The cessation of blood flow in the presence of  $1.5 \times 10^6$  locally applied PGI<sub>2</sub>-PSFCs (A) or PSFCs (B) is shown. Thrombus formation was induced with rose bengal and laser beam. Blood flow was measured with a laser Doppler flow probe monitor. Blood flow was recorded for a period of 120 mins to see obstruction in blood flow.

the unligated left hindlimb (Figure 10A, panel i – ‘1’). A single injection of the PGI<sub>2</sub>-PSFCs at the ischemic hindlimb resulted in a significantly greater enhancement of limb

perfusion recovery (Figure 10C, panel i). In contrast, the injection of empty vector transfected PSFCs did not significantly improve the ischemic condition (Figure 10B, panel i). On days 3, 7, 14, and 21 post ligation, the ischemic/ non-ischemic hindlimb blood perfusion ratio as evaluated by LDPI were significantly increased in the PGI<sub>2</sub>-PSFC treated group (Figure 10, panel ii, triangles) when compared with PSFCs (Figure 10, panel ii, •) and control group (Figure 10, panel ii, ■) (P<0.01, n=6 per group). No autoamputation occurred in the PGI<sub>2</sub>-PSFC treated group whereas autoamputations were significantly more in the control group and PSFC group by day 21. These studies further validated the therapeutic potential of the PGI<sub>2</sub>-PSFCs used for ischemic protection and treatment.

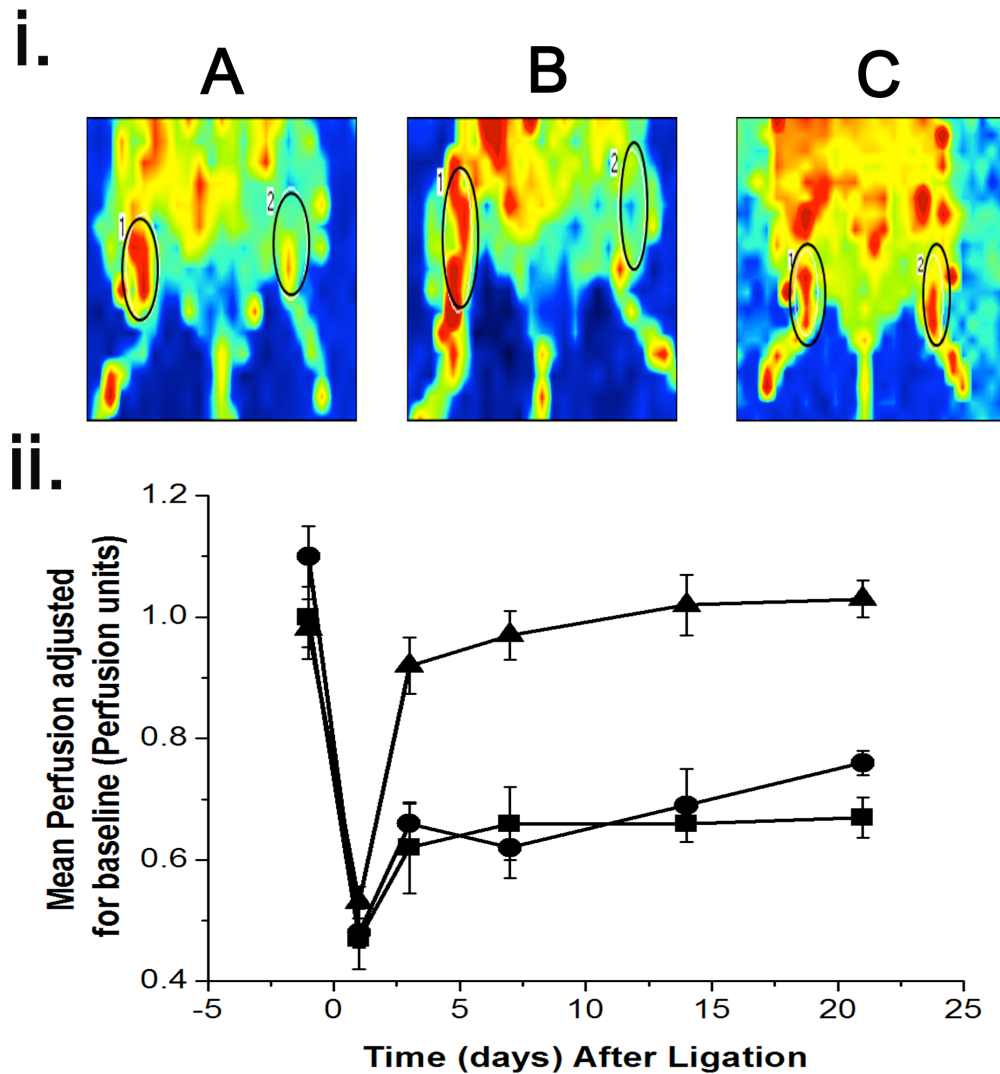


Figure 10. Effects of the PGI<sub>2</sub>-PSFCs on reperfusion of the mouse hindlimb-ischemic model as monitored by LDPI. The blood flow images (Panel i) and perfusion intensity (Panel ii) of the mouse hindlimbs with (Panel i – “2”) and without (Panel i – “1”) femoral artery ligation are displayed. The red color within the circled areas (Panel i, A-C) in both hindlimbs represents the blood flow intensity (perfusion), which was integrated and plotted, as shown in Panel ii. The perfusion after injection of PBS (■), PGI<sub>2</sub>-PSFCs (triangles), or empty vector transfected PSFCs (●) in the femoral artery-ligated hindlimb are shown (n=7). All values were expressed as mean ± SEM. A student t-test was used to analyze statistical significance (P<0.001).

#### **4.7. Determination of the endogenous AA metabolisms in the mouse urine using LC/MS.**

LC/MS analysis of urine from mice group treated with PGI<sub>2</sub>-PSFCs showed a significant increase in 6-keto-PGF<sub>1α</sub> (stable metabolite of PGI<sub>2</sub>)/PGE<sub>2</sub> ratio on days 3 and 7 when compared to the control group and PSFCs-treated group (Figure 11A;  $P < 0.001$ ;  $n=6$ ). This was followed by a subsequent decrease on days 14 and 21. This indicated that PGI<sub>2</sub>-PSFCs when injected in mice induced with ischemia in the hindlimb were able to significantly produce PGI<sub>2</sub> during the 21 day study period.

#### **4.8. Determination of Mouse Running Time in hindlimb ischemia model.**

In order to illustrate that the enhanced recovery of ischemic hind limb perfusion is indeed improved, a unilateral ligation of the femoral artery in ischemic mice dramatically inhibited mouse performance in a treadmill stress test ( $P < 0.05$ ). Treatment with PGI<sub>2</sub>-PSFCs producing PGI<sub>2</sub> ( $P < 0.05$ ) significantly increased performance in the treadmill test, with improved performance lasting over 21 days (Figure 11B). After 3, 7, 14 and 21 days treatment with PGI<sub>2</sub>-PSFCs post ligation, mice ran significantly longer than mice in the PBS ischemia group and ischemia group treated only with PSFCs. Results represent mean $\pm$ SD treadmill run time.

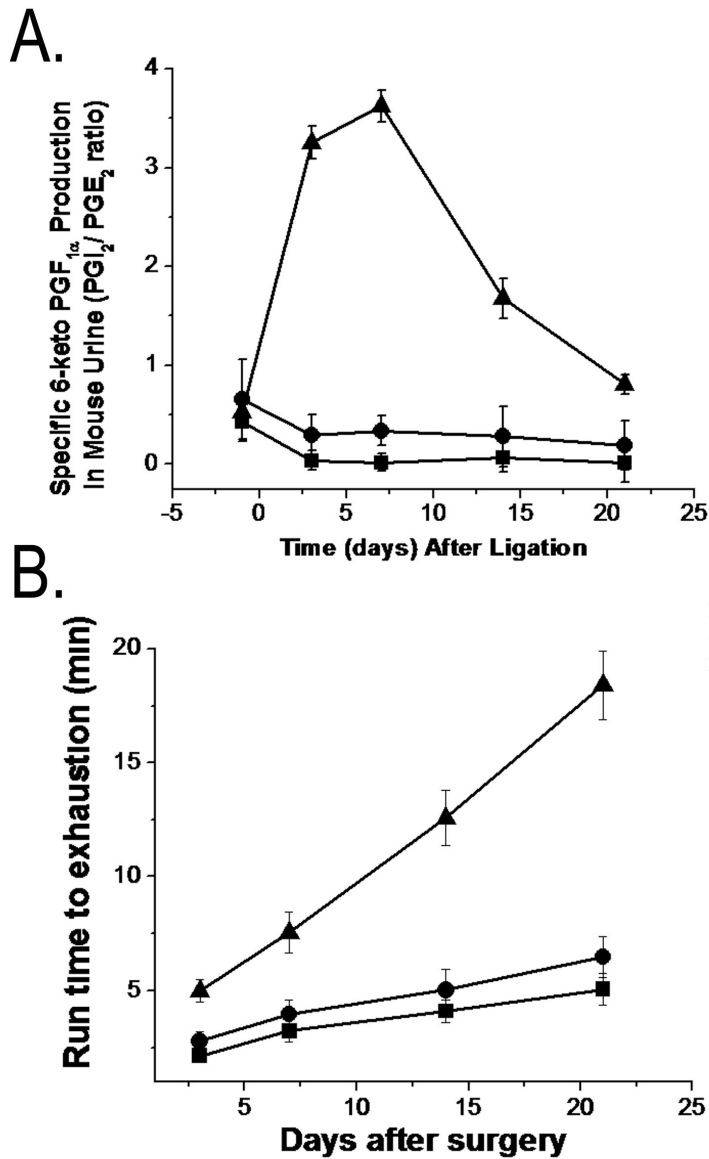


Figure 11 A.) LC/MS analysis showing the specific PGI<sub>2</sub> production expressed as the ratio of 6-keto PGF<sub>1α</sub> (stable metabolite of PGI<sub>2</sub>) and PGE<sub>2</sub>. Shown here is the PGI<sub>2</sub> production in the urine of ischemia induced mice treated with PGI<sub>2</sub>-PSFCs (triangles), non-transfected PSFCs (•) or PBS (■), where n=6 for each group, P<0.001. B.) Treadmill running time. Mouse performance on a treadmill was recorded following a unilateral ligation of the femoral artery and treatment with PGI<sub>2</sub>-PSFCs (triangles), non-transfected PSFCs (•) or PBS (■), (n=6, for each group, P<0.05).

#### **4.9. Detection of miRNA expression in the PGI<sub>2</sub>-PSFCs**

The miRNA microarray analysis of the total RNA in the cultured PGI<sub>2</sub>-PSFCs (Figure. 12a, panel ii) showed a significant change in the expression levels of 114 miRNAs in the cells. The expression level of these miRNAs in the empty vector transfected PSFCs (derived from the same source of adipocytes), were used as a control (Figure. 12a, panel i). High quality signals for the miRNAs in both cells were obtained. From these analyses it was determined that after comparison with the control (Figure. 12a, panel i), several miRNAs in the PGI<sub>2</sub>-PSFCs (Figure. 12a, panel ii) were either up-regulated (circles) or down-regulated (squares).

#### **4.10. Profile of the miRNAs that are up-regulated by the endogenous PGI<sub>2</sub> in PGI<sub>2</sub>-PSFCs.**

After comparing the miRNAs' expression levels in the PGI<sub>2</sub>-PSFCs and the PSFC control cells, we observed that 64 out of 114 miRNAs showed different folds of increase. Of these 64 miRNAs, 5 showed an increase of more than 2-folds (Figure. 12b). There was an approximate 15-, 4-, and 3-fold increase in the miRNAs 711, 31\* and 720 respectively (Figure.12b). Interestingly, these miRNAs have predicted target genes (microRNA.sangers.ac.uk) that are associated with adipocyte differentiation, atherosclerosis, tumors, and brain angiogenesis as listed in Table 2. Therefore we postulate that up-regulated miRNAs in PGI<sub>2</sub>-PSFCs will inhibit the expression of these

target genes and thus have a protective role in atherosclerosis and tumors. In particular, the expression level of the miRNA711 increased by almost 15-folds (Figure 12b), making this a very significant observation because endogenous PGI<sub>2</sub> could be a powerful up-regulator for the miRNA711 expression in mammalian cells.

#### **4.11. Profile of the miRNAs that are down-regulated by the endogenous PGI<sub>2</sub> in PGI<sub>2</sub>-PSFCs.**

There were 54 miRNAs down-regulated by PGI<sub>2</sub> in the PGI<sub>2</sub>-PSFCs when compared with the control PSFCs. The top five miRNAs with more than a 5-fold decrease in their expression levels are shown in Figure 12b, and the target genes for these miRNAs are listed in Table 3. The most significantly down-regulated miRNA is the 466f-3p (13.5-fold decrease), which might regulate the expression of target genes whose biological function is associated with lipid clearance, tumors, and apoptosis (Table 3). There was also an approximate 10-fold decrease in miRNAs 148a and 467b\*, which have similar functions to that of the 466f-3p. It was also worth noting that a 4-fold decrease in miRNAs 206 and 574-5p (data not shown), whose predicted target genes are embryonic ectoderm development, could suggest that PGI<sub>2</sub> plays a role in embryonic development.

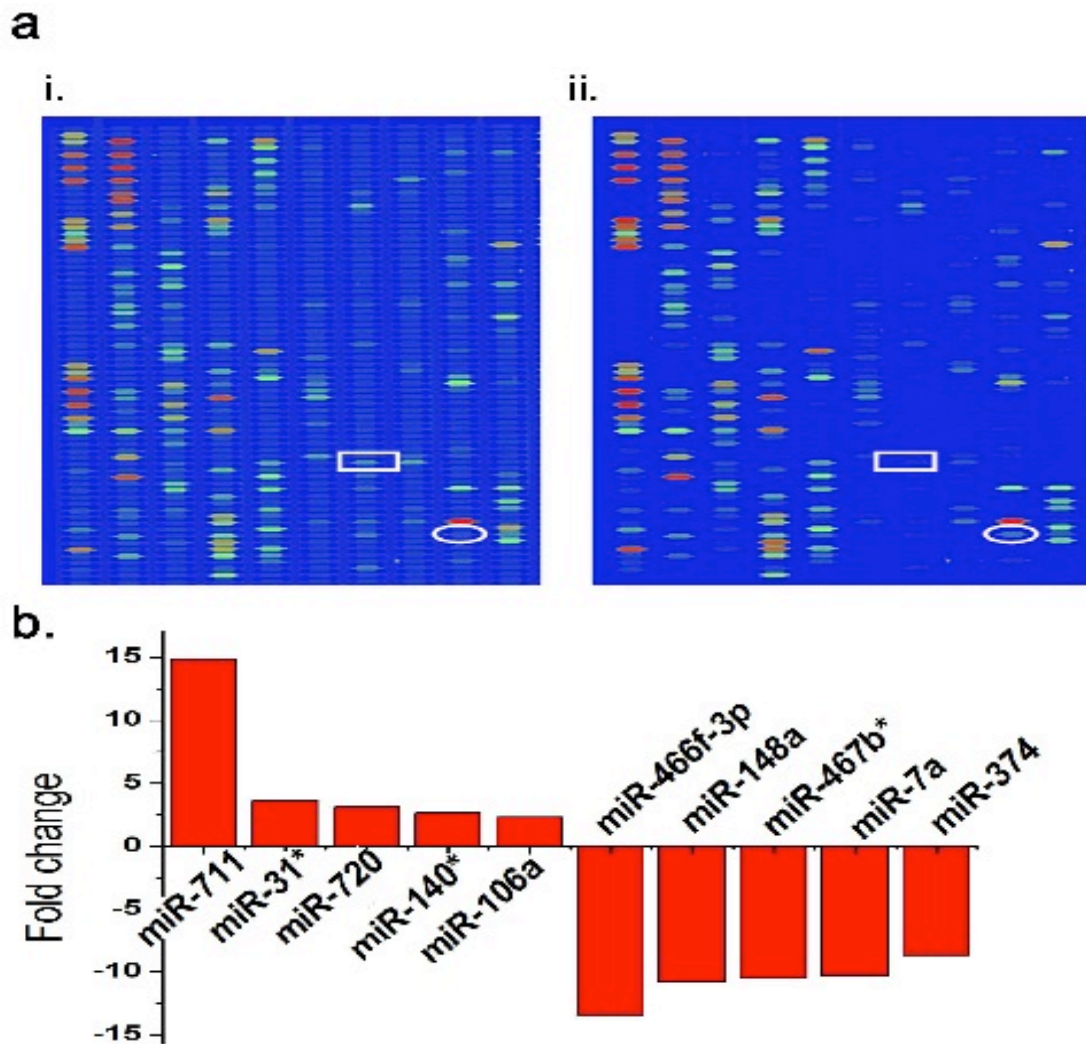


Figure 12: (a.) MiRNA microarray profiles showing PSFC miRNA expression (panel i) and PGI<sub>2</sub>-PSFC miRNA expression (panel ii). Circle indicates the expression profile of the up-regulated miRNA-711 and the square indicates the expression profile of the down-regulated miRNA-466f-3p. RNA was isolated from both the PGI<sub>2</sub>-PSFCs and PSFCs and send to LC sciences for microarray analysis. The miRNAs were detected by fluorescence labeling using tag-specific Cyc3 (PSFCs) and Cyc5 dyes (PGI<sub>2</sub>-PSFCs). Hybridization images were collected as shown above in 11a by laser scanner. The values obtained from the ratio of detected signals of Cyc5 to Cyc3 was used to calculate the p values and student t -test was performed. Differentially detected signals were those with less than 0.05 p-values. (b.) The top 5 miRNAs' fold increase and decrease in PGI<sub>2</sub>-PSFCs when compared to PSFCs. MiRNAs that showed a significant change in signals in PGI<sub>2</sub>-PSFCs when comapred with PSFCs were selected and fold change was calculated and plotted.

**Table 2. Up-regulated miRNAs in the PGI<sub>2</sub>-PSFCs and their predicted target genes and biological functions (microrna.sangers.ac.uk/genetargets)**

Up-regulated microRNAs	Predicted target genes	Predicted biological function
miR-711	CCAAT/C/EBP beta	↓ Adipocyte differentiation ↓ Tumorigenesis
	CD160	↓ Pathologic neovascularization
	Akt1	↓ Adipogenesis, VSMC differentiation/proliferation, proliferation/invasion of malignant tumors, and vascular dysfunction in obesity
	Lipase	↓ Atherogenesis
miR-31*	PPARα	↓ Adipocyte differentiation
	Brain specific angiogenesis inhibitor	↓ Angiogenesis
miR-720	Lipase endothelial	↓ Atherogenesis
miR-140*	Amyloid beta (A4) precursor protein-binding, family A	↓ Alzheimer's disease
	3-hydroxy-3-methylglutaryl-coenzyme A synthase 2	↓ Ketogenesis
miR-106a	Tumor susceptibility gene	↓ Tumors

**Table 3. Down-regulated miRNAs in the PGI<sub>2</sub>-PSFCs and their predicted target genes and biological functions (microrna.sangers.ac.uk/genetargets)**

Down-regulated microRNAs	Predicted target genes	Predicted biological function
miR-466f-3p	ABC1	↑ Lipid clearance
	Large tumor suppressor	↓ Tumors
	Lipase	↓ Atherogenesis
miR-148a	ABC7	↑ Lipid clearance
miR-467b*	CASP8 and FADD-like apoptosis regulator	↑ Apoptosis regulation
miR-7a	Insulin induced gene 2, insulin receptor substrate 1 and 2	↑ Insulin sensitivity
	Block of proliferation 1	↓ Proliferation
miR-374	Suppression of tumorigenicity gene	↓ Tumors

**4.12. Inhibition of up-regulated miRNA expression in PGI<sub>2</sub>-PSFCs using PPAR<sub>γ</sub> antagonist.**

PGI<sub>2</sub>-PSFCs were treated with the PPAR<sub>γ</sub> antagonist, GW 9662 (5μM), for 24hrs and the total RNA was isolated using TRIZOL reagent and analyzed by microarray (Figure. 13a, panel i). Interestingly, the effects of the endogenous PGI<sub>2</sub>-upregulated and

downregulated miRNAs' expression in the PGI<sub>2</sub>-PSFCs were inhibited (Figure 13b, panel i). It was particularly interesting to note that the miRNAs 711 and 466f-3p, whose expression levels were up/down-regulated more than 12-folds by PGI<sub>2</sub> signaling (Figure. 12b) returned to or below their basal level (Figure 13b, panel i). This result indicated that 1) PPAR $\gamma$  signaling is involved in regulating miRNA expression in mammalian cells; 2) PGI<sub>2</sub>-mediated up-regulation and down-regulation of miRNA expression could be through PPAR $\gamma$ ; and 3) at least miRNA711 and 466f-3p are targets for the endogenous PGI<sub>2</sub> signaling through PPAR $\gamma$ .

#### **4.13. Inhibition of up-regulated miRNA expression in PGI<sub>2</sub>-PSFCs using IP antagonist**

The effects of the IP antagonist (CAY 10441, 1 $\mu$ M) on the changes in the miRNAs' expression in PGI<sub>2</sub>-PSFCs were compared with that of the control PSFCs (Figure. 13a, panel ii). Interestingly, the top-five up-regulated and down-regulated miRNAs in the PGI<sub>2</sub>-PSFCs were inhibited (Figure. 13b, panel ii) similar to the PPAR $\gamma$  antagonist (Figure. 13b, panel i). Again, the expression of the dramatically up-regulated miRNA711 and down-regulated 466f-3p (by the PGI<sub>2</sub> signaling) was blocked by the IP antagonist (Figure. 13b, panel ii). These results demonstrated that: 1) up-regulated and down-regulated miRNAs' expression in PGI<sub>2</sub>-cells indeed results from the PGI<sub>2</sub> produced by the cells; 2) both IP and PPAR $\gamma$  are involved in PGI<sub>2</sub> signaling - affecting miRNA expression; 3) there is likely a signaling molecule linking IP with PPAR $\gamma$  during the PGI<sub>2</sub> signaling affecting

miRNA expression; and 4) Since the nuclear receptor, PPAR $\gamma$ , is directly involved in the regulation of gene expression, it can be deduced that PPAR $\gamma$  is a downstream target and IP is an upstream target mediating the PGI $_2$  signaling for miRNA expression.

#### **4.14. Quantitative determination of miRNA711 up-regulated in PGI $_2$ -PSFCs by qRT-PCR approach.**

We further validated the observation of the miRNAs regulated by PGI $_2$  in the PGI $_2$ -PSFCs. The miRNA711 which has the highest level up-regulated in the cells was selected as a target for *qRT-PCR* analysis. As a result, the level of miRNA711 in PGI $_2$ -PSFCs was up to 6-fold higher than that of the control PSFCs (Figure 14). This information is similar to that of the miRNA microarrays' results shown in Figure. 12a and b, in which the miRNA711 was increased by more than 10-folds, compared to that of the control cells. This quantitative data has further confirmed that miRNA711 could be used as one of the miRNA targets to reveal the relationship between PGI $_2$  and miRNA's.

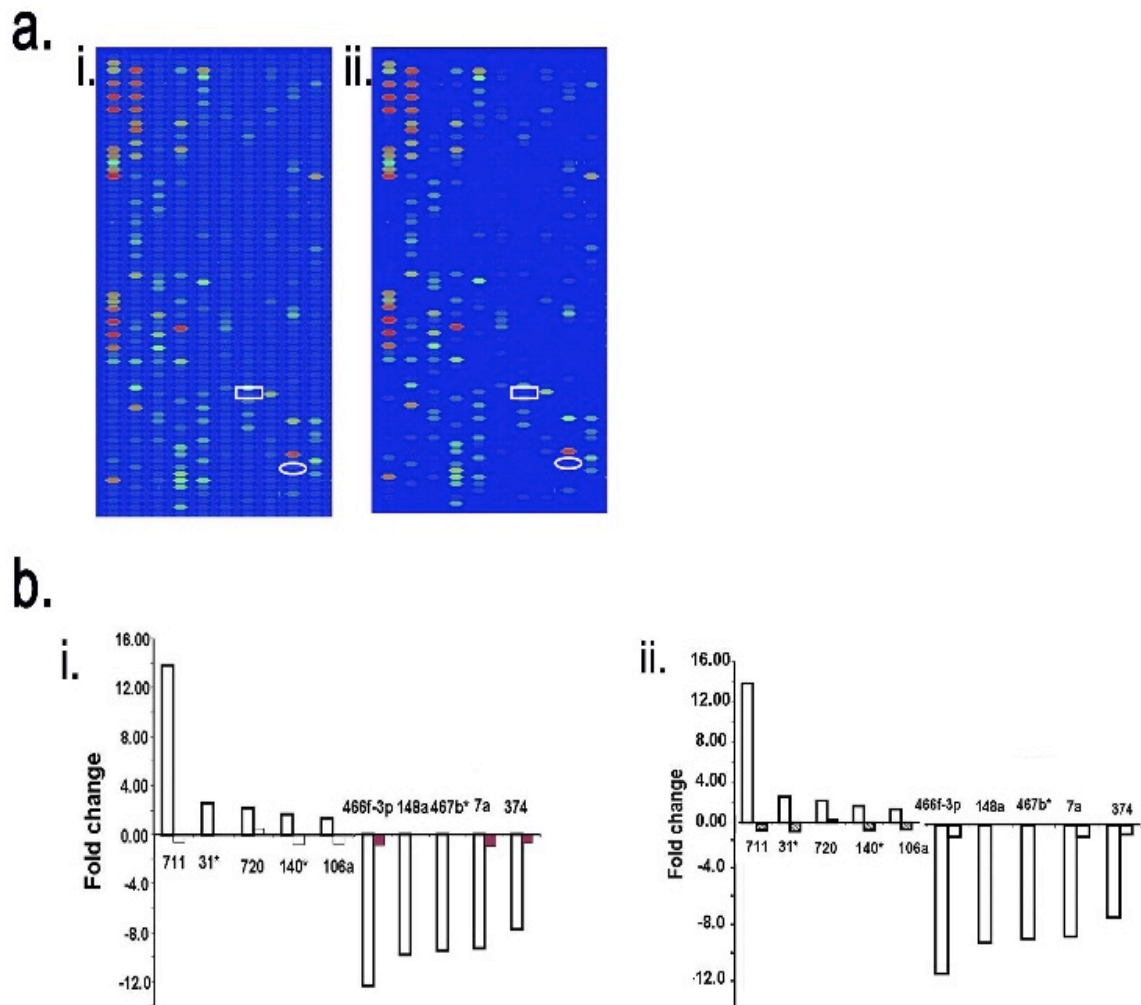


Figure .13. (a.) MiRNA microarray profiles showing PGI<sub>2</sub>-PSFC miRNA expression when treated with IP antagonist (panel i) and PPAR $\gamma$  antagonist (panel ii). Circle indicates the expression profile of miRNA711 and the square indicates the expression profile of miRNA-466f-3p. PGI<sub>2</sub>-PSFCs were serum starved for 5-6 hrs and then one plate was treated with IP anatanogist (CAY10441, 1 $\mu$ M) and the other was treated with PPAR $\gamma$  antagonist GW9662 (5 $\mu$ M). After 24hrs, total RNA was isolated using TRIZOL reagent. Total RNA was send to LC Sciences for performing miRNA microarray. Detection was performed by fluorescence labeling. Hybridization images were collected using laser scanner. (b.) The return to baseline of the up-regulated and down-regulated miRNA with PPAR $\gamma$  antagonist (panel i) or IP antagonist (panel ii) in PGI<sub>2</sub>-PSFCs is shown. The detected signal values obtained from miRNA microarray analysis from both the IP and PPAR $\gamma$  antagonists treated PGI<sub>2</sub>-PSFCs was compared with the values of PGI<sub>2</sub>-PSFCs and the values were plotted to see the inhibition. The signals returned to baseline level after treatment with antagonists as seen in panel i and ii.

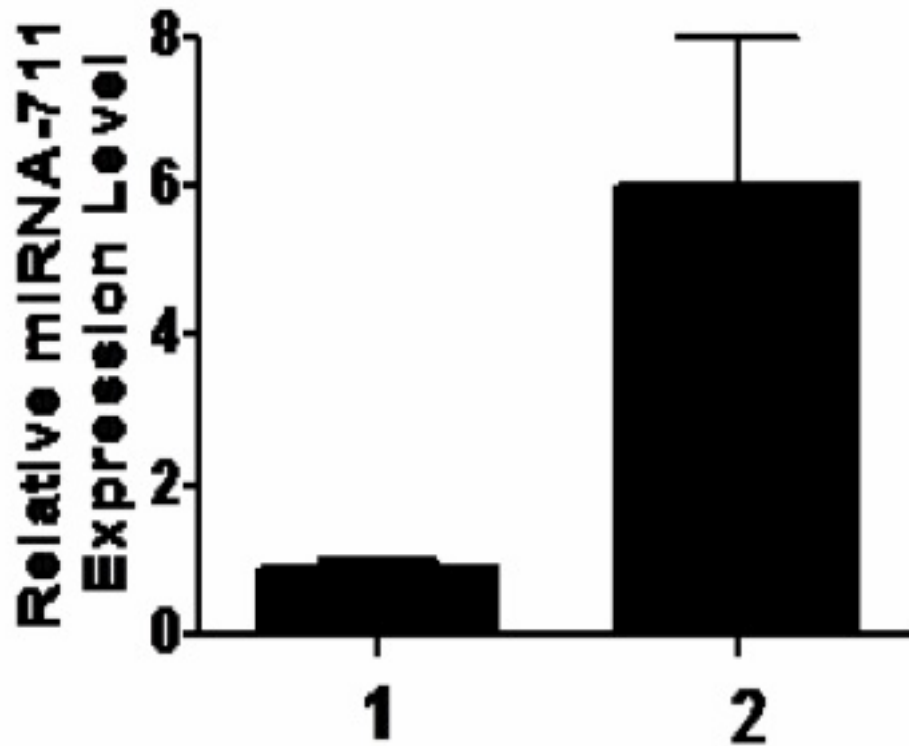


Figure. 14. Quantification of miRNA 711 expression in PGI<sub>2</sub>-PSFC by qRT-PCR. The miRNA711 was measured by qRT-PCR approach using RT<sup>2</sup> SYBR<sup>®</sup> Green qPCR Master Mix, the primer for miRNA711 and sno RNA-142 (housekeeping endogenous control), and then analyzed by qPCR using Applied Biosystems 7300 Real Time PCR System. Differential expression of miRNA711 in the cells was analyzed by the  $\Delta\Delta CT$  method. The levels of miRNA711 in the cells were calculated using the formula  $2^{-\Delta\Delta Ct}$  (n=3). Firstly, the miRNAs were isolated from the cultured PGI<sub>2</sub>-PSFCs or control PSFCs using RT<sup>2</sup> qPCR-Grade miRNA Isolation Kit. Secondly, the isolated miRNAs were converted into cDNAs using [RT<sup>2</sup> miRNA First Strand Kit](#); and finally, the cDNAs were mixed with another kit, RT<sup>2</sup> SYBR<sup>®</sup> Green qPCR Master Mix, the primer for miRNA711 and sno RNA-142 (control).

#### **4.15. Inhibition of lipid accumulation in PGI<sub>2</sub>-PSFCs.**

There was reduced accumulation of lipid droplets in PGI<sub>2</sub>-PSFCs as compared to the control PSFCs detected by Oil Red O staining after 7 days (Figure. 15). PGI<sub>2</sub>-PSFCs did not accumulate lipid droplets when treated with adipogenic media containing dexamethasone, IBMX, and insulin. This indicates that PGI<sub>2</sub>, through the up-regulation of miRNAs 711, 744 and 148b, could inhibit lipid accumulation (Figure. 15).

#### **4.16. Detection of down-regulated mRNAs using illumina gene expression assay.**

This assay showed a more than a 2-fold increase in 354 mRNAs (Figure 16i) and more than a 2-fold decrease in 471 mRNAs in PGI<sub>2</sub>-PSFCs in comparison to PSFCs (Figure. 16ii). In addition, the mRNA Akt1 was identified to be down-regulated by 4-folds. The up-regulated miRNA 711 (Table 2), 744, and 148b, identified by microarray analysis also have Akt1 as one of their gene target ([microrna.sanger.ac.uk/genetargets](http://microrna.sanger.ac.uk/genetargets)). Upon comparison, it can be deduced that these miRNAs were possibly down-regulating Akt1 gene expression.

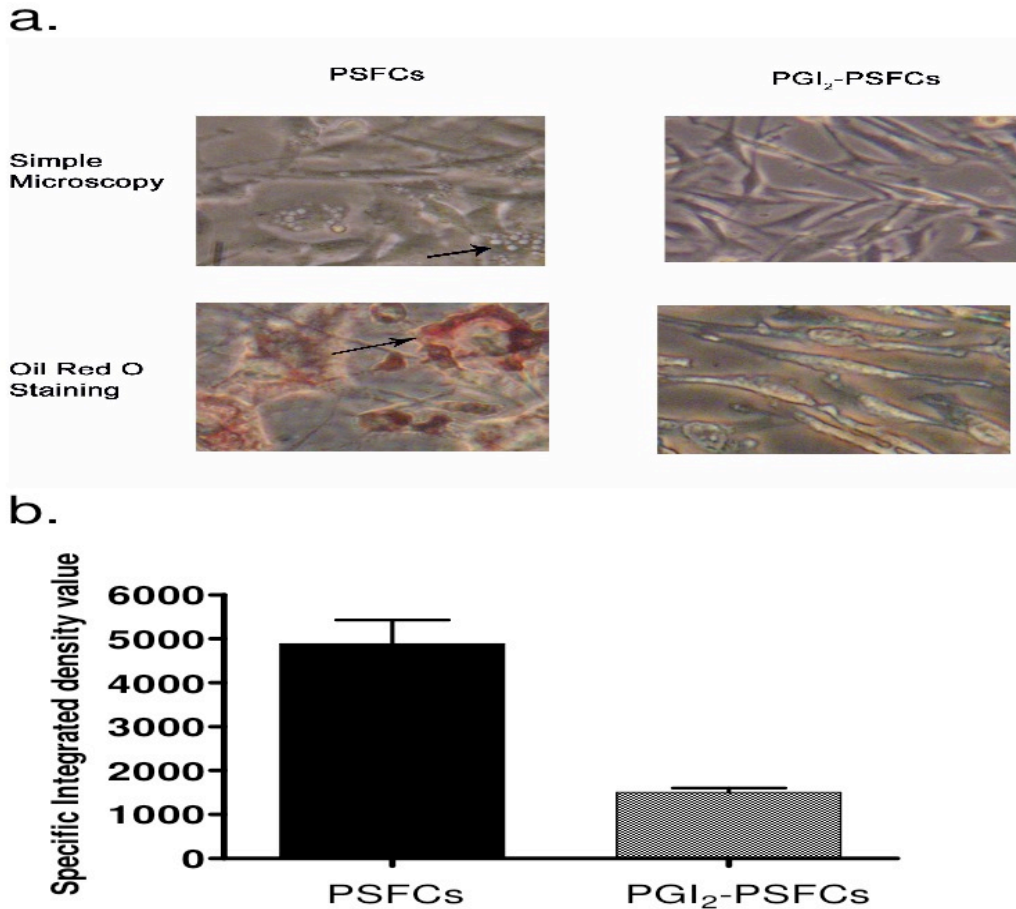


Figure .15. (a.) Simple microscopy (Row 1) of the PSFCs (arrow indicates lipid droplets) and PGI<sub>2</sub>-PSFCs. Oil Red O staining (Row 2) of PSFCs (arrow indicates red color of lipid droplets) and PGI<sub>2</sub>-PSFCs showing lipid accumulation. PSFCs and PGI<sub>2</sub>-PSFCs were treated with adipogenic medium: DMEM containing 10% fetal bovine serum (FBS), 1 $\mu$ M dexamethasone (Sigma-Aldrich), 0.5mM Isobutyl methyl xanthine (IBMX) and insulin (10 $\mu$ g/mL), and the cells were allowed to grow in this medium for 4 days. After 4 days the cells were re-fed with DMEM-F12 media containing 10% FBS and 10 $\mu$ g/mL insulin, and were grown for an additional 3 days. Images were taken everyday to observe cells accumulating lipid droplets. After treating the cells with the differentiation medium for 7 days, accumulation of lipid was identified by Oil Red O staining. The cells were then observed via light microscope with 100X magnification and then photographed using Kodak DC 290 Zoom Digital camera (NY, USA). (b.) Comparison of integrated density values between PSFCs and PGI<sub>2</sub>-PSFCs. Intensities were determined using AlphaEase FC software from Cell Biosciences (Santa Clara, California USA) and taking values of 5 images, n=5.

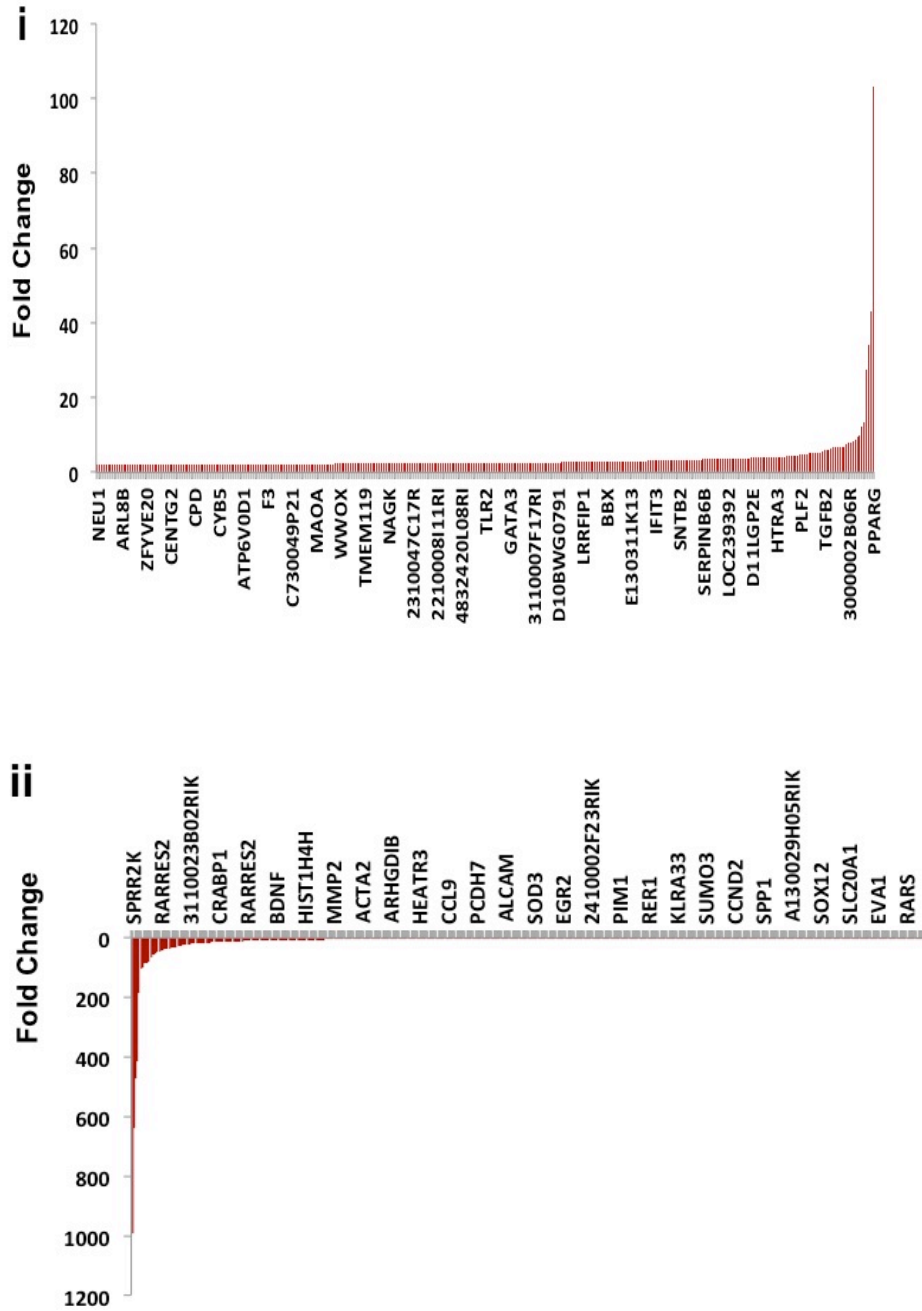


Figure. 16. Illumina gene expression assay showing change in expression of mRNAs in PGI<sub>2</sub>-PSFCs compared to PSFCs. i) Upregulation of 354 mRNAs, ii) Downregulation of 471 mRNAs. Total RNA was amplified and the first and second cDNA strands were synthesized with the help of T7 oligo (dT) primers and reverse transcriptase and DNA polymerase. *In vitro* transcription was performed and biotinylated cRNA was amplified and illumina hybridization array was run and scanned with Bead array reader.

#### 4.17. Down-regulation of Akt1 expression in PGI<sub>2</sub>-PSFCs using Immunoblot analysis.

Using a monoclonal Akt1 primary antibody, we detected the down-regulation of Akt1 expression in PGI<sub>2</sub>-PSFCs (Figure. 17, Lane 2) as compared to PSFCs (Fig. 17, Lane 1). The experiment was normalized using GAPDH primary antibody. This finding suggested that the up-regulated microRNAs 711, 744, 148b may be down-regulating the Akt1 gene expression.

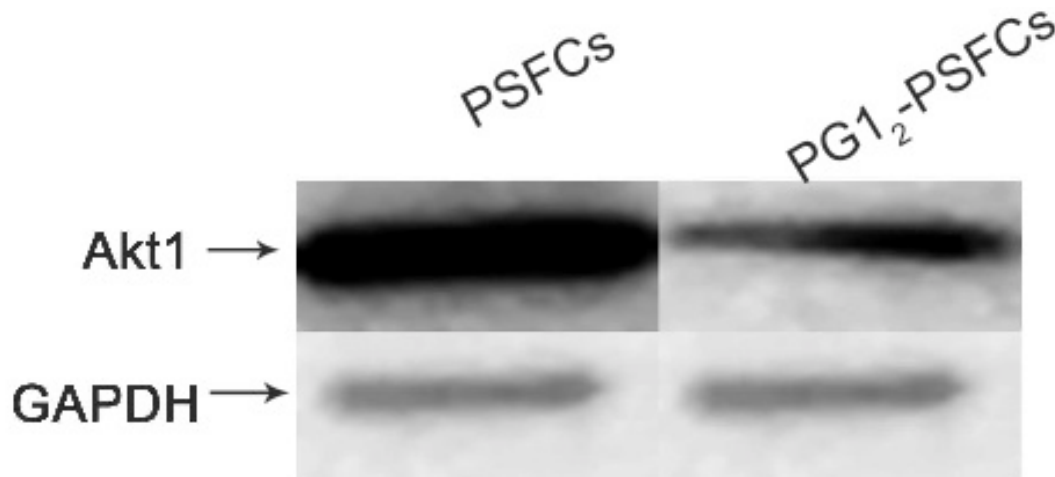


Figure. 17. Western blots showing the expression of Akt1 (Lane 1) in PSFCs and PGI<sub>2</sub>-PSFCs (Lane 2). GAPDH was used to normalize the expression level of the Akt1. Cells were harvested and lysed in lysis buffer [50mM Tris-HCl (pH 7.4), 1% Triton X-100, 150mM NaCl, 1mM EDTA, 1mM phenylmethanesulphonylfluoride, 1% aprotinin, 10mg/mL leupeptin, 1mM sodium orthovanadate, and 1mM sodium fluoride. Cell lysates were centrifuged at 12,000 g for 10 min at 4°C. Protein concentration of the cell lysate was determined by performing BCA protein assay. SDS-PAGE sample buffer was added to the lysates, which were then heated to 100°C for 5 min. 25µg of protein was loaded in each well of 10% acrylamide gel and separated by electrophoresis. Proteins were transferred onto a nitrocellulose membrane, which was incubated with primary antibody against Akt1 and a horseradish peroxidase conjugated secondary antibody. Chemiluminescence was detected using ECL Kit (Amersham).

#### **4.18. Generation of transgenic mice (TG) over expressing COX-1-10aa-PGIS to increase endogenous PGI<sub>2</sub> level**

First, the cDNA fragment of human COX-1-10aa-PGIS from pcDNA3.1 vector, with a general expression promoter, PCMV (Figure. 18), was successfully created by the lab and used for expressing the active COX-1-10aa-PGIS in mice. Using pronuclear microinjection transgenic mice technology, from the 30 founders generated, two transgenic founders were identified by PCR (Figure 19i and ii) at 445bp. These 2 founders were bred with wild-type FVB/N mice and were found to pass the transgene, following Mendelian rules. To test for expression of the transgene, tail PCR was performed (Figure 19iii). The resulting heterozygous mice were bred to get the homozygous mice colony that was identified by performing qPCR.

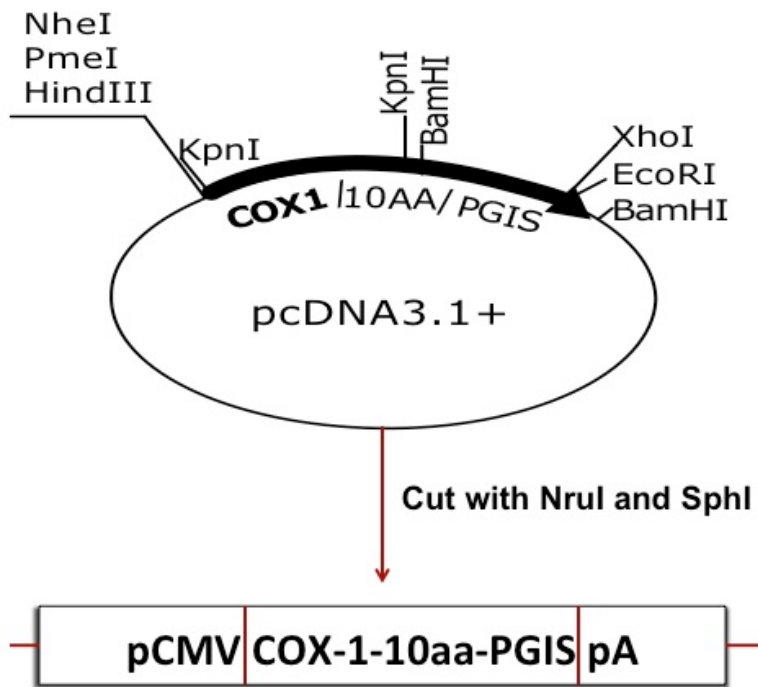


Figure 18: Construction of the cDNA construct of COX-1-10aa-PGIS. The sequence of COX-1 linked to PGIS through a 10 amino acid linker (COX-1-10aa-PGIS) was generated by PCR approach and subcloning procedures provided by the vector company (Invitrogen). The resulting cDNA was successfully subcloned into the pcDNA 3.1 vector at KpnI and BamHI sites containing a cytomegalovirus early promoter using PCR cloning approach. The pcDNA3.1 vector containing COX-1-10aa-PGIS was cut at the NruI and SphI sites to obtain a 3.2Kb of cDNA of COX-1-10aa-PGIS with a pCMV promoter and PGH polyadenylation site (pA).

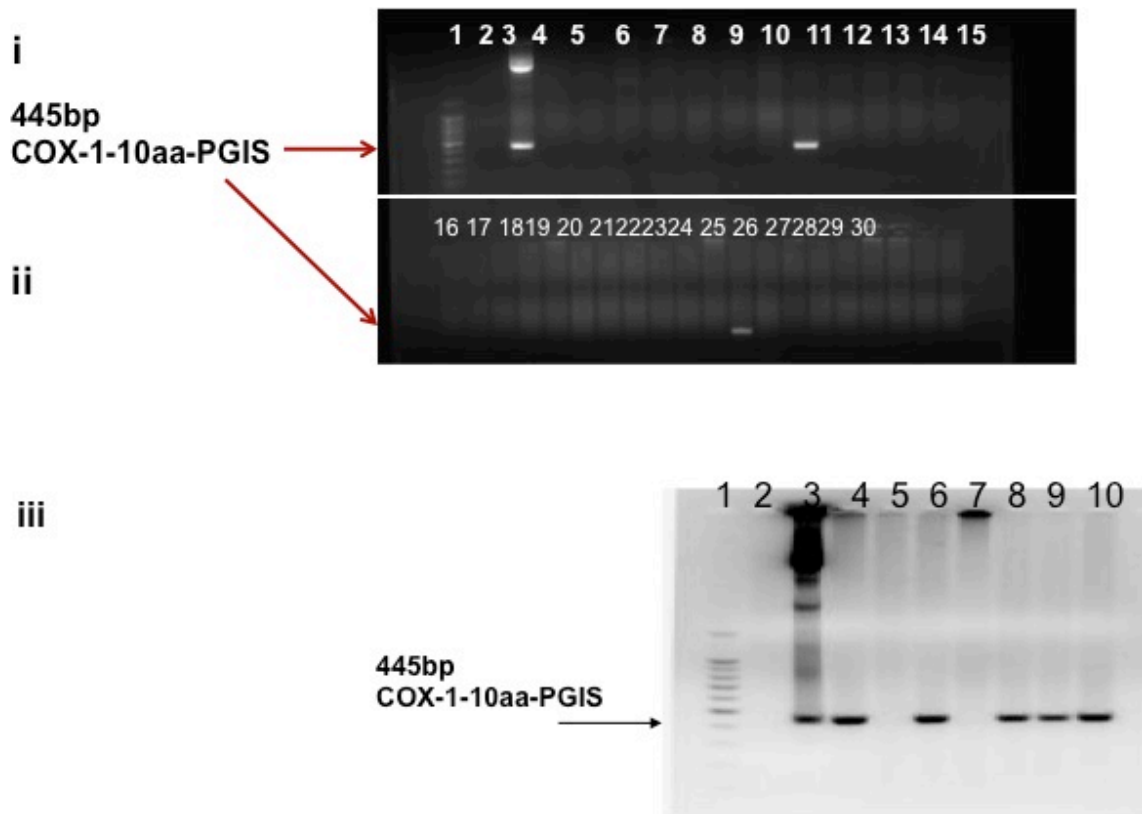


Figure. 19. Genotyping of the transgenic mice by PCR analysis. The expression of COX-1-10aa-PGIS was determined by performing PCR showing band at 445bp, i) in founder transgenic mice lane 11 and lane 26, lane 3 is the COX-1-10aa-PGIS cDNA. ii) F1 transgenic mice in lanes 4, 6, 8, 9 and 10 whereas lane 3 is the positive standard COX-1-10aa-PGIS. Briefly, tails (1.5-2 mm) were digested in 100  $\mu$ l of 1xPCR buffer with added detergents (0.45% NP40, 0.45% TWEEN 20) and 10  $\mu$ l Proteinase K (10 mg/ml) @ 60°C overnight. The sample was further denatured for the Proteinase K by boiling for 15 min, and then cooled on ice for 5 minutes. The isolated genetic DNA (2uL tail DNA was added into a final 20uL volume reaction) was subjected to PCR analysis using PCR Reaction Buffer (1x PCR buffer, 2.5 mM MgCl<sub>2</sub>, 200  $\mu$ M dNTPs, 1  $\mu$ M each designed primer and 1 unit Taq Polymerase with conditions (hold @ 94°C for 4.5 min, 30x step cycles of 94°C for 30 sec, 72°C for 1 min and holding @ 4°C until ready to analyze. The primer sets for the COX-1-10aa-PGIS gene are: sense 5'-CCTCAAGGGTCTCCTAGGGA-3' and antisense 5'-GTGCTTCTCCTCATCCTCGT-3'. The amplified product length is 445 bp. The PCR product was analyzed by agarose gel.

#### **4.19. Generation and Characterization of homozygous transgenic mice**

The transgenic mice carrying the gene of COX-1-10aa-PGIS was identified by PCR approach. First, two males (out of 30 new birth) permanently carrying COX-1-10aa-PGIS gene (Figure.19.i and ii) were identified by PCR using a set of designed and specific primers covering the C-terminal COX-1, 10aa linker and N-terminal PGIS , and named as COX-1-10aa-PGIS-transgenic mice. Homozygous mice were obtained by breeding the heterozygous transgenic mice and these mice did not show any physical phenotype change when compared with the wild type mice (Figure 20). The homozygous mice were further bred and identified by qPCR approach. It was found that Ct values for heterozygous, homozygous and wildtype individuals were 24.57, 23.61 and 34.82 respectively. Thus mice were characterized as heterozygous, homozygous and wildtype by comparison of the Ct values with the respective standard Ct values (Figure. 21).

#### **4.20. Endogenous production of PGI<sub>2</sub> is increased in COX-1-10aa-PGIS transgenic mice**

The catalytic activity of the over expressed COX-1-10aa-PGIS in the TG mice was investigated by determination of the PGI<sub>2</sub> metabolite in the urine of the TG mice using LC/MS analysis. It was observed that the ratio of the metabolite of PGI<sub>2</sub>, 6-keto-PGF<sub>1α</sub> to PGE<sub>2</sub> and TXB<sub>2</sub> was 7 in TG mice and 1 in the wild type mice (Figure 22A and B). This demonstrates more than 5 fold increase in PGI<sub>2</sub> biosynthesis in the TG mice. These observations have clearly confirmed that the induced COX-1-10aa-PGIS gene in the TG

mice had been successfully expressed in the tissues and functionally active to produce PGI<sub>2</sub>.



Figure. 20. Image showing physical comparison between the WT and the TG mice. Images were taken of the homozygous transgenic mice and wild type mice with the camera to see if there was any phenotype physical change observed in the TG mice.

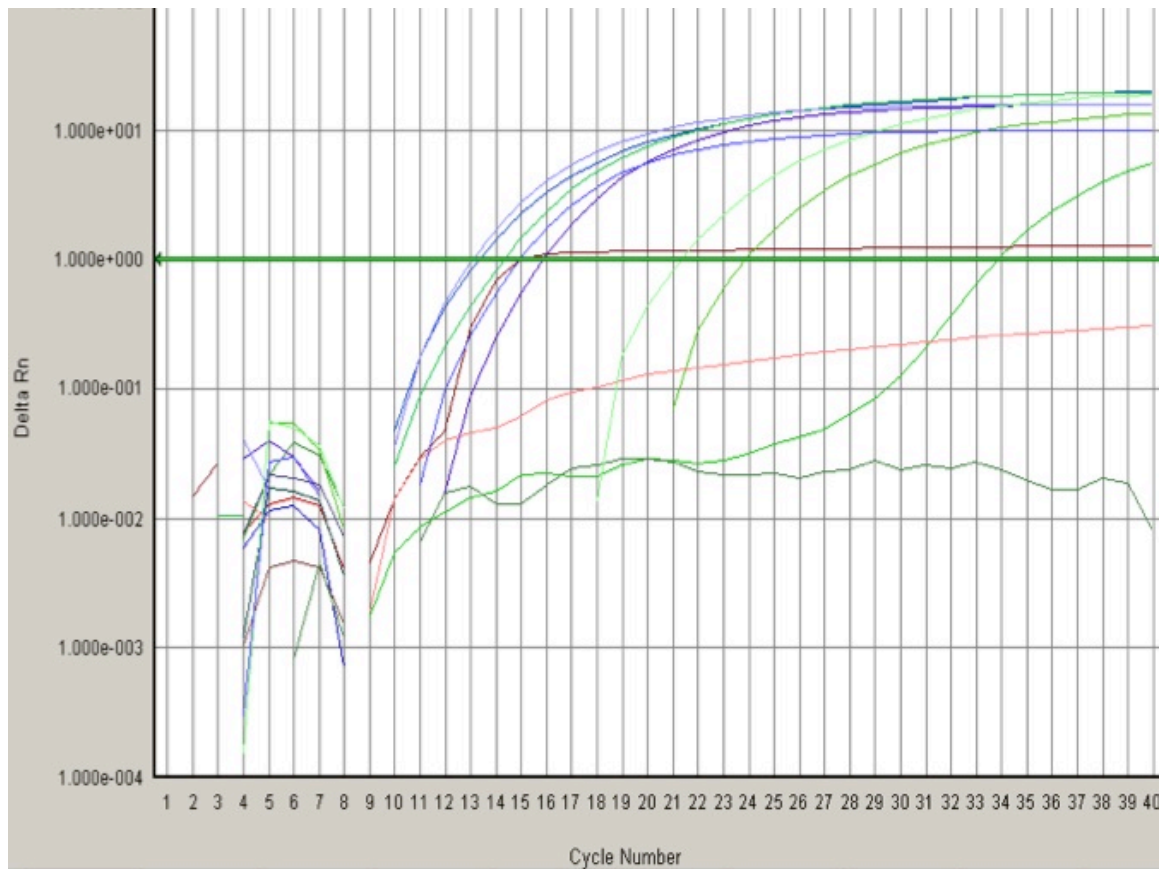


Figure. 21. Characterization of homozygous transgenic mice by qPCR. Shown here is the amplification plot obtained after running the qPCR. Briefly, RNA was isolated from the tail tissue (100mg) collected from a set of heterozygous, homozygous and wild type mice with TRIZOL reagent. The concentration of RNA was measured using Nanodrop Bioanalyzer. First strand cDNA was synthesized using the Superscript III First-Strand Synthesis System. The first strand cDNA obtained in the synthesis reaction was further amplified by PCR and Qiagen's QuantiTect SYBR Green PCR kit and platinum Pfx DNA polymerase. Real time quantitative PCR was run using the ABI7500 Fast Real Time PCR system. PCR amplification consisted of 35 cycles with 95°C for 15s, annealing at 60°C for 30s and 72°C for 30s. GAPDH was used as the internal control. Each sample was run as duplicate. Ct values were obtained and compared.

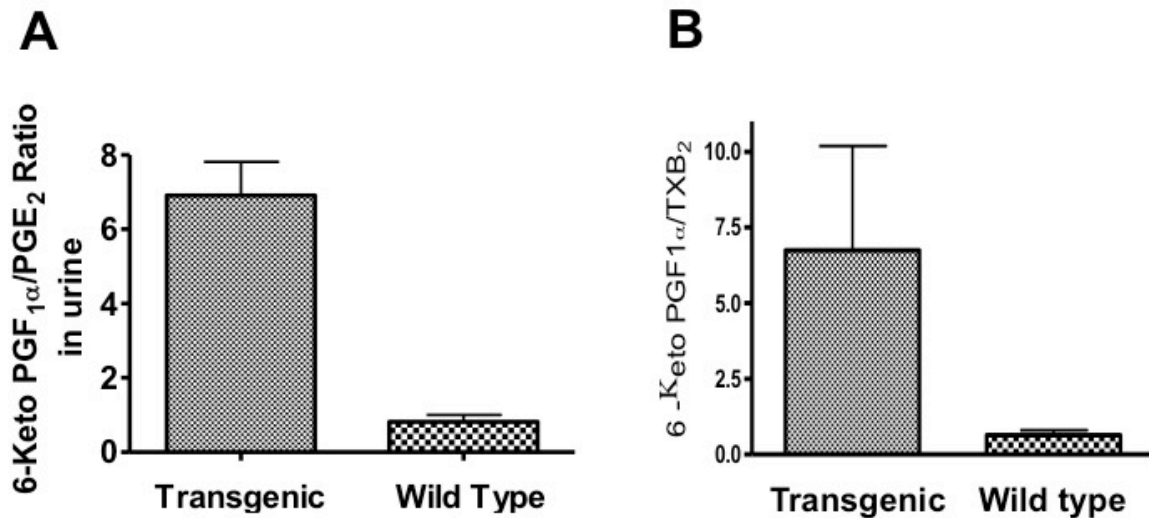


Figure 22: LC/MS analysis of prostanoid in the urine of transgenic (TG) and wild type (WT) mice. A) Ratio of 6-keto-PGF<sub>1α</sub> to PGE<sub>2</sub> in both the TG and WT mice, B) Ratio of 6-keto-PGF<sub>1α</sub> to TXB<sub>2</sub> in both the TG and WT mice. Each of the WT and TG mice were placed in metabolic cages and urine was collected (n=6). Then the urine samples were passed through C18 cartridges and then eluted with acetone. The eluent was dried with nitrogen gas. The dried substrate was then diluted in buffer A and injected for detection by LC/MS/MS analysis. The spectrum (molecular weight) and chromatogram (retention time) was obtained and compared with the standards for 6-keto-PGF<sub>1α</sub>, TXB<sub>2</sub> and PGE<sub>2</sub> for the respective prostanoids. The signal values obtained from the injected urine samples were normalized with the background and then ratio of 6-keto-PGF<sub>1α</sub> to PGE<sub>2</sub> and TXB<sub>2</sub> was found to be 7 for the transgenic mice and 1 for the wild type mice. The above graph represents mean±SD (p<0.001).

#### 4.21. Effect of increased endogenous PGI<sub>2</sub> production on haemodynamic parameters in COX-1-10aa-PGIs transgenic mice.

Prostacyclin is a potent inhibitor of platelet function and a vasodilator. Thus the bleeding time of the transgenic mice was increased to 55 mins (n=6) as compared to the wild type mice which showed a mean bleeding time of 15 mins (Figure 23i). One of the most important risk factors for up-regulated prostacyclin production is it may cause lowering of blood pressure. However, blood pressure, both systolic and diastolic

(Figure.23ii) along with heart rate measurement (Figure 23iii) of both the TG(+/+) and WT mice showed no significant difference .

#### **4.22. The gene profile of the COX-1-10aa-PGIS expression in different organs**

Unlike COX-1, PGIS is tissue specific . In general, it is largely localized in vascular endothelial cells to produce PGI<sub>2</sub> for vascular protection through the biological functions of vasodilatation and anti-platelet aggregation. It becomes very interesting in finding the tissue specificity of the gene and proteins in different tissues after combining the COX-1 and PGIS in one molecule. The general level of distribution of the COX-1-10aa-PGIS in different tissues of the transgenic mice was identified by PCR using the specific primers as described above. Figure. 24i shows the different organs expressing COX-1-10aa-PGIS gene permanently. It is particularly valuable to find the gene expressed in heart, kidneys and brain which suggests that the gene could provide protection from ischemic heart disease, kidney failure and stroke due to thrombosis and vasoconstriction. The protein level expression of the COX-1-10aa-PGIS enzyme in the major organs was further identified by Western blot analysis (Figure. 24 ii). COX-1-10aa-PGIs have a unique molecular weight at 130 kDa, which could be easily distinguished from endogenous COX-1 and PGIS using specific anti-COX-1 and PGIS antibodies. COX-1-10aa-PGIS protein was overexpressed in the important organs, heart, lungs, brain and kidneys.

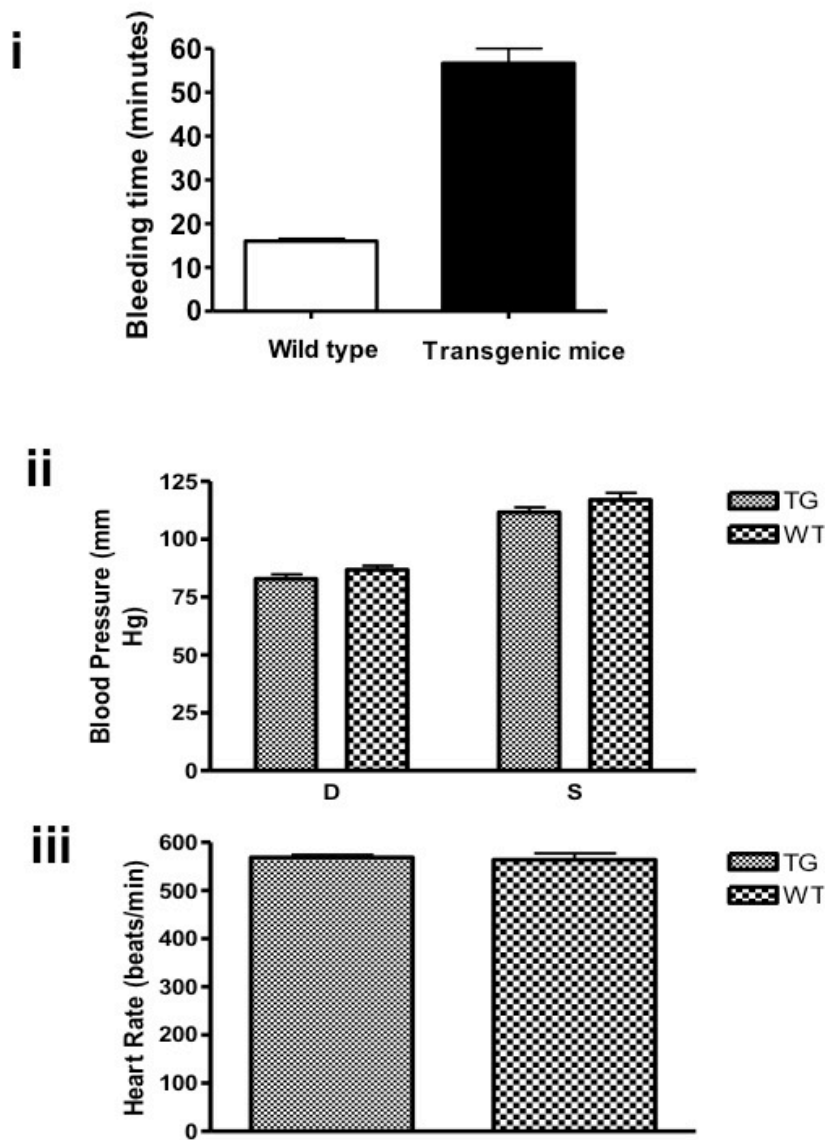


Figure 23: Measurement of haemodynamic parameters in mice. i) Bleeding time measurement in TG and WT mice. After clipping the tail, blood was blot on filter paper every 30s until bleeding stopped. Bleeding time was 55 mins in TG and 15 mins in WT mice. ii) Blood pressure measurement by tail cuff method. Both systolic and diastolic blood pressure was measured in both TG and WT mice. iii) Heart rate measurement by tail cuff method. Heart rate was measured along with blood pressure in both the TG and wild type mice. The values shown here are mean $\pm$ SD (n=7)

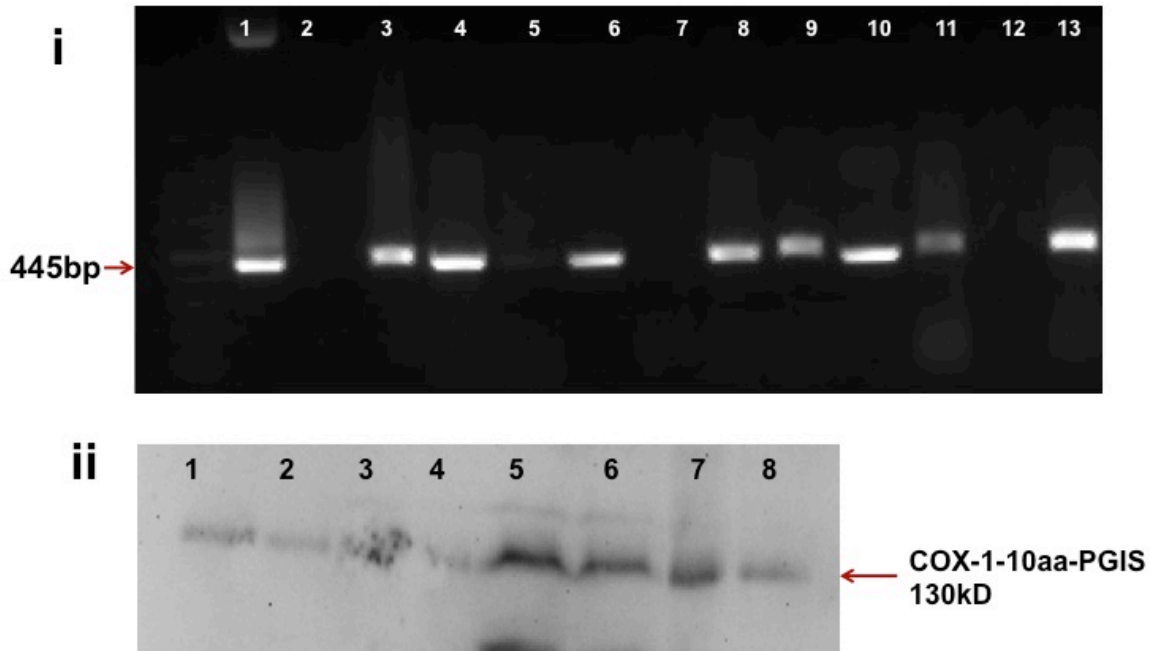


Figure 24.i. PCR analysis of the different organs of the transgenic mice. An arrow indicates 445bp length COX-1-10aa-PGIS. Lanes 1) Positive control, 2) Negative control, 3) Lung, 4) Adipose tissue, 5) Intestine, 6) Brain, 7) Wild type tail, 8) Heart, 9) Liver, 10) TG tail, 11) pancreas, 12) prostrate and 13) uterus. ii) Western blot analysis of the different organs of the transgenic mice. The arrow indicates COX-1-10aa-PGIS protein expression at 130kDa. Lanes 1) Lung, 2) Heart, 3) Intestine, 4) pancreas, 5) Adipose tissue, 6) Brain, 7) Uterus and 8) Liver

#### 4.23. Effects of overproduction of PGI<sub>2</sub> on live birth

PGI<sub>2</sub> is reported to help in embryonic development. It was observed that the reproductive activity of the TG mice were significantly increased which was indicated by higher numbers of live birth, compared to that of the bred wild type mice (Figure.

25). It provided direct evidence to settle a conclusion that PGI<sub>2</sub> could increase female reproductive activity to increase the live birth in mice, and put forward the idea that that any drugs and approaches reducing PGI<sub>2</sub>-biosynthesis, such as, NSAIDs might reduce the fertility in women. The existing clinical protocol using aspirin to improve success rate of fertility procedures, such as IVF may be needed to be reevaluated if this observation is further clarified by indepth studies.

#### **4.24. Anatomical study of the different organs of the transgenic mice**

Since a transgene was overexpressed in the mice, we wanted to study if its overexpression in the different organs changed the anatomy of the organs. Therefore heart, lung, kidney, brain, liver were isolated from both the TG and WT mice (n=3) and pictures were taken with camera and compared to observe any difference . None of the organs showed any anatomical difference as observed from the Figure 26. Thus the transgene COX-1-10aa-PGIS did not change the anatomy of the organs in the transgenic mice.

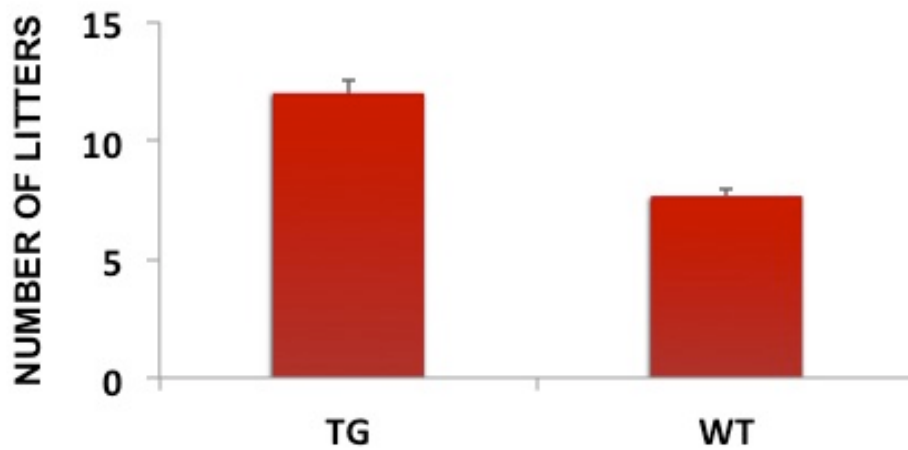


Figure 25: Determination of the number of litters born from the TG and wild type (WT) mice. Transgenic mice when bred were able to give birth to higher number of pups (~12) compared to wild type mice (~7). Observations were done in 5 different breeding pairs of mice. The photograph here shows the number of litters born from TG mice.

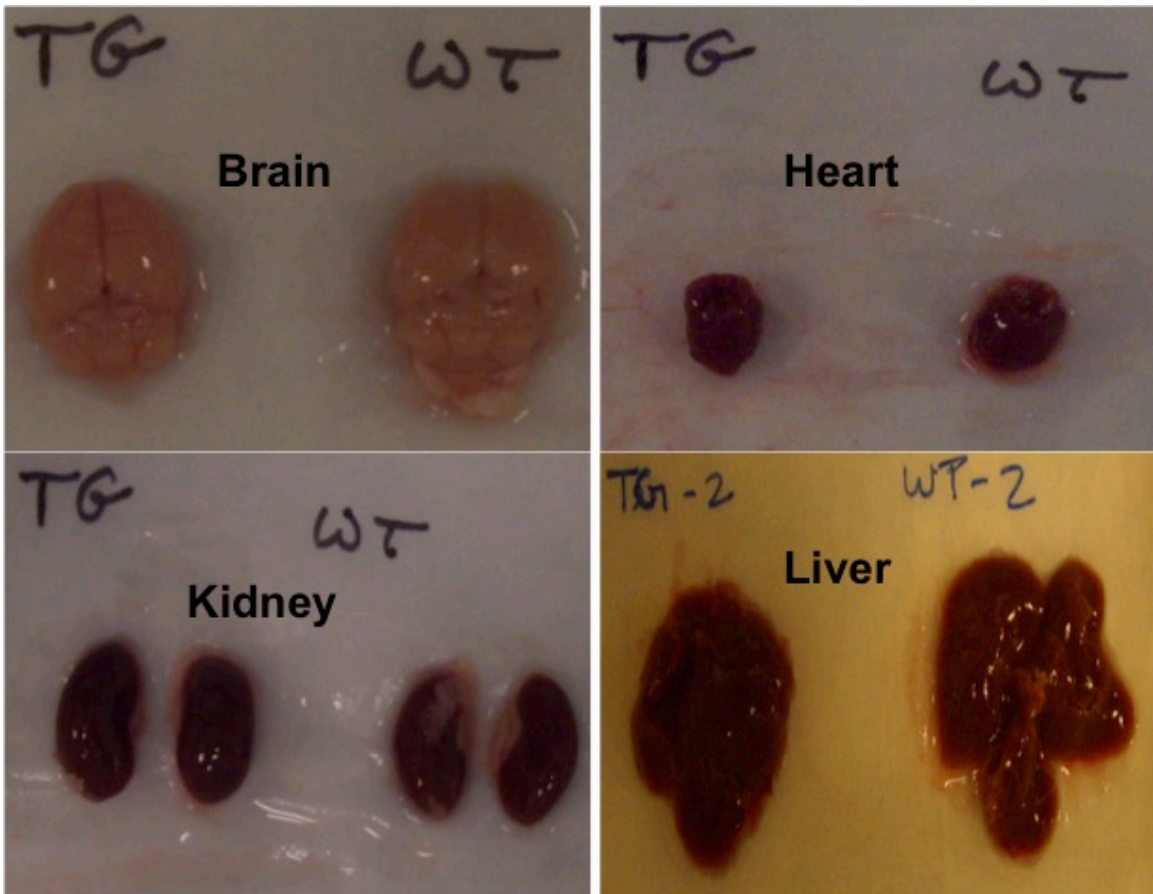


Figure. 26. Anatomical differences in the organs of the TG and WT mice. Organs like heart, brain, kidney and liver were isolated from both the TG and WT mice (n=3) and images were taken with the help of camera. The organs of both WT and TG as shown in the picture above did not show any anatomical difference.

#### **4.25. Resistance to thrombosis in the transgenic mice using carotid artery thrombosis model**

The effect on vascular protection in cases of vascular disease by the permanent COX-1-10aa-PGIS gene expression was demonstrated in a carotid artery thrombosis model. In this the both the TG and WT mice were tested for their resistance to

thrombosis which is one of the major causes of stroke and heart diseases. The combination of laser beam and rose bengal induced thrombosis in the carotid artery which was associated with a reduction in blood flow within 10 mins after injection of rose bengal leading to death in the wild type mice within 2 hrs (Figure 27B and C(red squares), n=10). Whereas, in the transgenic mice the decreased blood flow was reversed after rose bengal injection and thus they survived from the thrombosis. (Figure 27A and C(black squares), n=10).

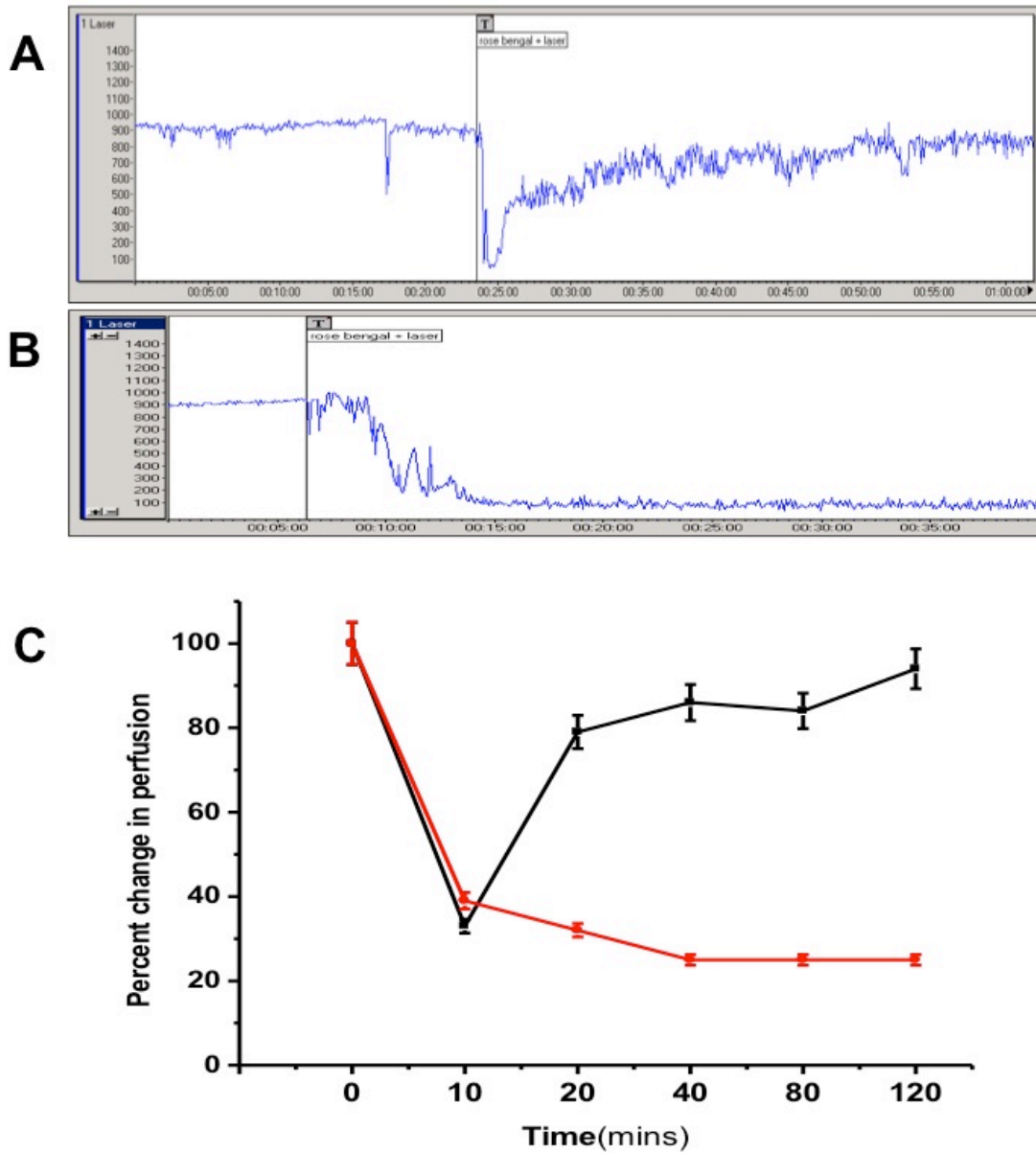


Figure 27: Study of resistance to thrombosis in TG mice by using the photochemical carotid artery thrombosis model. Representative graphs recorded on the Laser doppler perfusion imaging system, showing the change in blood perfusion in response to photochemical vascular injury in A) TG mice and B) WT mice. C) Percentage change in perfusion was calculated at different time intervals and plotted against time. Red squares and black squares indicate perfusion change in WT and TG mice respectively. Rose bengal (50mg/kg) was injected through the tail vein and this time of injection was considered as zero mins. The blood perfusion was recorded for a period of 120 mins. (n=10, p<0.01).

## 5. DISCUSSION

### 5.1. Stable expression of COX-1-10aa-PGIS in adipose tissue derived primary culture of mature adipocytes

PGI<sub>2</sub> is a potent endogenous inhibitor of platelet aggregation and vascular smooth muscle cell proliferation and a vasodilator. Therefore, since decades there have been ongoing attempts to use PGI<sub>2</sub> and its analogues to treat vascular diseases. Many studies have been reported, in which PGI<sub>2</sub> and its mimics have been used to treat pulmonary arterial hypertension (Gomberg et al., 2008), atherosclerosis (Arehart et al., 2007), peripheral vascular diseases (Berman et al., 2006) and congestive heart failure (Kerbaul et al., 2007). In spite of having such benefits in several vascular disorders, use of PGI<sub>2</sub> and its analogues is challenged with a major limitation of short half-life. Therefore they have to be administered as continuous intravenous infusion for a beneficial effect, which results in bleeding and injury at the site of injection. Our study was aimed at providing new insights for developing a novel approach for using endogenous PGI<sub>2</sub> to protect the vascular system.

Cell therapy is widely used to promote therapeutic angiogenesis in several vascular disorders. Adipose tissue serves, as a rich source of wide array of cells and it's easy to obtain and culture them. The fact that mature adipocytes could be differentiated into cells that had the capacity to metabolize endogenous AA to prostanoids (Figure 4a and 5) provided the evidence that these prostanoid synthesizing

fat cells (PSFCs) could be further modified to therapeutic cells. Initially, adipose tissue-derived stem cells were compared against the differentiated adipocytes to determine which cell type produced more PGI<sub>2</sub>. Although many similarities exist between the two types of cells, it was determined that the differentiated adipocytes had a higher PGI<sub>2</sub> production.

It was particularly interesting to see that the PSFCs showed a capacity to metabolize endogenous AA predominantly into PGI<sub>2</sub> and PGE<sub>2</sub>, one of the characteristics of stem, stromal, and endothelial cells (Kleiveland et al., 2008, Denizot et al., 1998, Taylor et al., 1987). Another stromal cell characteristic also seen in the PSFCs was their ability to reproduce over a long period of time. This implied that the cells might have the capacity to survive *in vivo* for a long period as well, and further differentiate into functional tissue. Recombinant protein cDNA-based gene transfer for primary culture cells is often unpredictable and unstable. It is particularly challenging when using pcDNA3.1. vector. Our current study has shown that the COX-1-10aa-PGIS cDNA could be transferred into the PSFCs using Lipofectamine 2000 (Figure 6 and 7). This has provided a general approach for transferring other enzymes' cDNA into the cell line derived from the primary cultured fat cells, which have potential to be developed into therapeutic intervention.

The COX-1-10aa-PGIS gene transfer was not only able to produce PGI<sub>2</sub> in the PSFCs, but also shifted the metabolized production of endogenous AA into a more

favorable PGI<sub>2</sub> production and a reduced PGE<sub>2</sub> production in the cells (Figure 7). This demonstrated a dual effect on potential vascular protection by increasing PGI<sub>2</sub> production and reducing PGE<sub>2</sub> production. Such specific vascular protection is not available through existing treatments with drugs like Aspirin, COX-2 inhibitors and PGI<sub>2</sub> analogs. Additionally, we would like to further investigate the effect of overexpression on VEGF, HGF, and IGF1 secretion by the PGI<sub>2</sub>-PSFCs to confirm any paracrine effects. The effect of PGI<sub>2</sub> indirectly and/or directly enhancing VEGF/HGF activities through an autocrine action of adipose derived cells needs to be further investigated, and is currently part of our future work. It has been reported that the overproduction of PGI<sub>2</sub> in HEK293 cells transiently expressing PGIS promoted cell apoptosis and led to cell death (Hatae et al., 2001). However, our established stable PGI<sub>2</sub>-PSFC line, which constantly synthesizes high levels of PGI<sub>2</sub>, showed no signs of apoptosis after over 30 passages. Additionally, we have determined that intramuscular injection of the PGI<sub>2</sub>-PSFCs into the mice did not result in tumor formations - after three weeks. However, the primary culture PSFCs may adopt different properties in comparison to the HEK293 cells, which were used for previous studies (Hatae et al., 2001). Therefore, it becomes very interesting to differentiate between primary cultured cells and the HEK293 cell line for PGI<sub>2</sub> signaling. For example, HEK293 cells contain a very low level of PGI<sub>2</sub> receptor (IP) protein; however, a significant amount of IP is present in the PSFCs (Figure 4Bii). This raises the possibility that PGI<sub>2</sub>-mediated apoptosis in HEK293 cells could be through its

binding to other receptors, such as nuclear receptor PPAR. This remains to be investigated. This study will provide a model for the future engineering of PGI<sub>2</sub>-producing cells derived from other cell types, such as stem cells and stromal cells.

## **5.2. Effect on hindlimb ischemia and thrombogenesis after treatment with PGI<sub>2</sub>-PSFCs in mice.**

In the present study, the efficiency of a new strategy involving treatment of limb ischemia and thrombogenesis with therapeutic cells producing PGI<sub>2</sub> was examined. The adipose tissue derived cells could not only be converted to PGI<sub>2</sub> producing cells by overexpressing COX-1-10aa-PGIS but these cells could also be used as a medium to transfer COX-1-10aa-PGIS *in vivo*. This strategy minimizes the adverse effects of using adenoviral vectors, which pose immune reactions as well as tissue toxicity. To achieve the benefits of cell therapy, it is necessary for the cells to home and survive in the tissue. But majority of the cells don't survive for a long time. Here our study showed that the PGI<sub>2</sub>-PSFCs could survive and produce PGI<sub>2</sub> for a longer time. Urine prostanoid profile analysis was used to monitor the survival time of the PGI<sub>2</sub>-PSFCs *in vivo* because the increased 6-keto-PGF<sub>1α</sub> level in the urine is directly related to the PGI<sub>2</sub> produced by the PGI<sub>2</sub>-cells *in vivo* (Figure 11). From a therapeutic point of view, monitoring the cell functions *in vivo* through the detection of the urine 6-keto PGF<sub>1α</sub> level does not contain the risk of triggering immuno-rejection and damaging the cells like GFP, a foreign

protein. Figure 11A showed the up-regulated 6-keto-PGF<sub>1a</sub> peak in urine at 7 days, which then decreased after another two weeks following injection of the PGI<sub>2</sub>-cells in mice. This suggested that the cells were active *in vivo* for up to 3 weeks. In addition, using a PSFC line could minimize immune rejection issues, since these cells could be generated from the same subject. Critical limb ischemia, a consequence of atherosclerosis is characterized by vascular endothelial injury and therefore a decrease in the production of PGI<sub>2</sub>. We tried to mimic this vascular disorder by ligating the femoral artery of mice and thus the mice developed ischemia in the hindlimb of the mice. It was observed that treatment of these mice with PGI<sub>2</sub>-PSFCs increased perfusion and decreased the rate of amputation (Figure 10). PGI<sub>2</sub> acts in a paracrine and autocrine manner. So it could be that PGI<sub>2</sub> released by the PGI<sub>2</sub>-PSFCs may cause the neighboring endothelial cells to promote the production of PGI<sub>2</sub> through induced expression of COX-2 and PGIS. This needs to be investigated. Critical limb ischemia patients suffer from pain at rest. Thus treadmill run of the mice was used to assess the functional mobility of mice after ischemia and treatment with PGI<sub>2</sub>-PSFCs (Figure 11B). Many recombinant human membrane proteins mediate important pathophysiological functions in cells and are great candidates for correcting cell disorders in many diseases. However, membrane proteins are only dissolved in detergent solvents, which are not suitable for general use *in vivo*. In the current studies we were able to deliver the overexpressed membrane-

bound COX-1-10aa-PGIS into mice using the stable cell line strategy, and have provided a model for developing membrane proteins into potential therapeutic reagents.

Anti-platelet aggregation assays provide an important method that confirms the benefits of the newly engineered Trip-cat Enzyme-1 in anti-thrombosis function. Human platelet cells are rich in COX-1 and TXAS. Following the AA released from the cell membrane (via stimuli on the platelets), the majority of the AA is converted to TXA<sub>2</sub> by the coordinated action of COX-1 and TXAS. The resultant TXA<sub>2</sub> binds to its receptor on the surface of the platelet and causes platelet aggregation. The inhibition of the platelet aggregation by the PSFC cells stably expressing the Trip-cat Enzyme-1 (Figure 8) has strongly indicated that: 1) The expressed Trip-cat Enzyme-1 was able to compete with the endogenous COX-1 and use AA as a substrate; 2) The PGH<sub>2</sub> produced by the Trip-cat Enzyme-1 was readily available to the PGIS active site, even in the presence of TXAS, which competitively binds to the PGH<sub>2</sub>; and 3) The immediate increase in PGI<sub>2</sub> production by the Trip-cat Enzyme-1 reduced the amount of PGH<sub>2</sub> available for TXAS to produce TXA<sub>2</sub>, which further prevented platelet aggregation. These factors have led the Trip-cat Enzyme-1 to possess dual functions: increasing PGI<sub>2</sub> and reducing TXA<sub>2</sub> biosynthesis, which is a unique and novel anti-thrombosis and anti-ischemic approach that has not yet been available thus far. Thus to translate this *in vitro* study into *in vivo* results, the effect of PGI<sub>2</sub>-PSFCs on thrombogenesis in carotid artery induced by photochemical vascular injury was studied. Injury to the endothelium causes activation

of the circulating platelets in the blood vessel. These activated platelets release TXA<sub>2</sub> and thus are responsible to form aggregates as well as cause vasoconstriction. This is one of the first steps in atherosclerosis. Thus treatment with PGI<sub>2</sub>-PSFCs inhibited this platelet activity of thromboxane through overproduction of PGI<sub>2</sub> at the site of injury and therefore protected from thrombogenesis (Figure 9).

Engineering of therapeutic cells producing PGI<sub>2</sub> by overexpression of fusion enzyme (COX-1-10aa-PGIS) is a novel model in PGI<sub>2</sub> therapy. This cell therapy will have advantages like: 1) The enzyme will be expressed for a longer time thus producing PGI<sub>2</sub> continuously; 2) Long term care is possible.

### **5.3. Study of microRNA expression regulation in PGI<sub>2</sub>-PSFCs**

The recombinant hybrid enzyme (COX-1-10aa-PGIS) overexpressed in a primary culture of mouse adipose tissue was able to integrate its triple catalytic functions of COX-1 and PGIS to effectively and continuously convert endogenous AA into PGI<sub>2</sub>. We were able to detect the stable production of PGI<sub>2</sub> through the presence of 6-keto-PGF<sub>1α</sub> (the stable byproduct) using LC/MS (Figure 7ii). The miRNA microarray analysis of the PGI<sub>2</sub>-PSFCs (expressing COX-1-10aa-PGIS) versus the vector-transfected primary culture adipocytes (PSFCs) showed that overproduction of PGI<sub>2</sub> causes an up-regulation in miRNAs 711, 148b and 744, and a down-regulation in miRNAs 466f-3p, 148a, 7a and 374 etc (Figure 12). This PGI<sub>2</sub>-induced miRNA regulation was IP- and PPAR $\gamma$  receptor-

mediated because the effect was reversed by using CAY10441 (IP antagonist) and GW9662 (PPAR $\gamma$  antagonist) (Figure. 13a). Our experimental data showing the analyzed correlation between the miRNA expression and IP/PPAR $\gamma$  blockade (Figure 13a) has provided evidence that the effects of the miRNA expression were possibly related to the PGI $_2$  receptor mediation, as there was no difference between the IP and PPAR receptors. This raises the possibility that the two receptors may coordinate together for the miRNA expression. Upregulation of miRNA-711 was further confirmed by quantification using quantitative real time PCR.

MiRNAs regulate gene expression either by inhibiting mRNA translation or by causing degradation of mRNAs (Farh et al., 2005, Pasquinelli et al., 2005). MiRNA have been reported to play a role in adipogenesis of preadipocytes (Kajimoto et al., 2006). By referring to a list of targets ([microRNA.sangers.ac.uk](http://microRNA.sangers.ac.uk)) we identified that C/EBP beta is one of the predicted gene targets of miRNA 711 and the Akt1 gene is the predicted target of miRNA 711 (Table 2), 148b and 744. The transcription factor C/EBP beta/delta is known to mediate the transcriptional activation of PPAR $\gamma$  and C/EBP $\alpha$  which in turn cause differentiation of adipocytes and induce maturation of pre-adipocytes into lipid-containing fat cells (Tang et al., 2004). Similarly, the phosphatidylinositol-3-kinase (PI3K)/Akt1 pathway regulates the process of adipocyte differentiation. It has been reported that absence of Akt1/PKB $\alpha$  in primary mouse fibroblasts cells does not promote adipocyte differentiation (Yun et al., 2008). Akt1 in association with ProF has

been suggested to produce phosphorylation of FoxO1 and thereby cause its nuclear export. This, in turn, results in the inactivation of FoxO1 which is a repressor of adipogenesis and a negative regulator of insulin actions (Nakae et al., 2003, Fritzius et al., 2008). It is also reported that PGI<sub>2</sub>, through its paracrine effect of inhibiting the Akt1

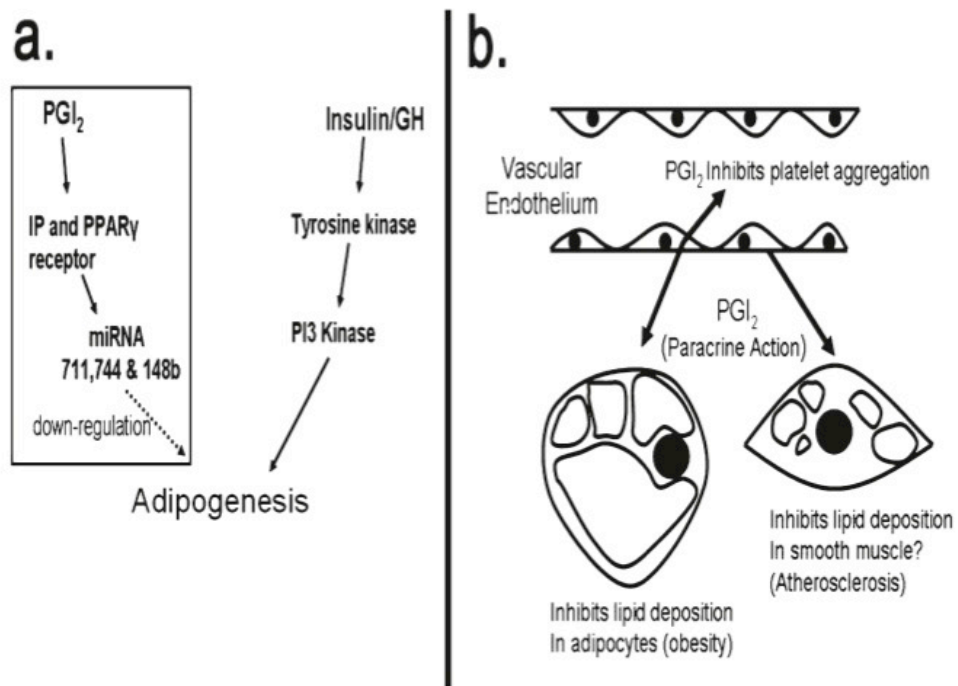


Figure 28. (a.) Schematic showing the proposed mechanism of inhibition of adipogenesis by PGI<sub>2</sub>. The box indicates the proposed pathway. PGI<sub>2</sub> by signaling through the IP and PPAR $\gamma$  receptors produces a change in the expression level of miRNA 711, 744 and 148. These three miRNAs have Akt1 as their gene target. Therefore an increase in the expression of miRNAs 711, 744 and 148 produces a decrease in the expression of Akt1 which is possible the reason behind inhibition of adipogenesis (lipid accumulation) in PGI<sub>2</sub>-PSFCs. Akt1 is a target of insulin signaling. (b.) The proposed paracrine action as an application in obesity and atherosclerosis through up-regulating PGI<sub>2</sub> biosynthesis. PGI<sub>2</sub> released from the endothelial cells acts in a paracrine manner on the smooth muscle cells to inhibit lipid deposition.

pathway, induces inhibition of vascular smooth muscle cell proliferation and prevents de-differentiation thus indicating its role as atheroprotective (Kasza et al., 2009). This is a very complex system that has not been settled yet. Thus, we have initiated a very preliminary study for the regulation of gene expression through miRNA and performed an RNA illumina assay. The results showed many of the mRNA were up-regulated /down-regulated in the PGI<sub>2</sub>-PSFCs when compared to the vector-transfected PSFCs (Figure 16). From the assay we were able to show that there was a down-regulation of the mRNA Akt1 in PGI<sub>2</sub>-PSFCs in comparison to the control PSFCs. Therefore Akt1 may be a gene target of microRNA 711, 148b and 744. We were able to confirm the observed RNA illumina assay's down-regulation of mRNA Akt1 by performing an immunoblot of total Akt1 in both primary culture cell lines (Figure 17). However, to confirm the relationship between Akt1 and PGI<sub>2</sub>, many more and intensive studies are required. Such studies would exceed our current experimental designs, however they could be included in our future work.

Thus, identification of the signaling molecule, microRNA 711 indicated that PGI<sub>2</sub> plays a role in inhibiting lipid deposition and facilitating clearance (Table 2 and 3). We further incubated our PGI<sub>2</sub>-PSFCs and PSFCs (control) cells in adipogenic medium with insulin and found that there was decreased lipid deposition in PGI<sub>2</sub>-PSFCs when

compared with the control PSFCs (Figure 15). This shows that PGI<sub>2</sub> reduced the sensitivity of insulin-mediated lipid deposition in cells.

Our findings also predict that the loss of paracrine and autocrine effect of endothelial PGI<sub>2</sub> could be responsible for early atherosclerosis as fatty streaks. These fatty streaks are lipid deposits in the smooth muscle cells underlying the PGI<sub>2</sub>-producing endothelium. Our future efforts will be directed toward studying lipid deposition in smooth muscle cell lines transfected with our PGI<sub>2</sub>-producing hybrid enzyme.

In conclusion, our array data suggests that PGI<sub>2</sub> regulates miRNA expression that inhibits insulin-mediated lipid deposition in cells (Figure 28a). This is relevant because peripheral lipid deposition (obesity) and atherosclerosis which is uncontrolled sub-endothelial lipid deposition in smooth muscle cells could be directly related to impaired PGI<sub>2</sub> production as hypothesized (Figure 28b).

The cell based method that was used to study the autocrine and paracrine effect of PGI<sub>2</sub> in the primary culture of adipocytes is novel in that it allows us to study endogenous PGI<sub>2</sub>, which has a very short half-life. This method allows us to closely mimic the *in vivo* effect of PGI<sub>2</sub> produced by endothelial cells and predicts the pathway involved in lipid deposition. The findings of the study have unravelled some of the unknown signaling mechanisms involved in the PGI<sub>2</sub> vascular protective effect.

#### **5.4. Generation of the transgenic mice overexpressing COX-1-10aa-PGIS**

Global overexpression of human COX-1-10aa-PGIS in the transgenic mice was accomplished by pronuclear microinjection of the cDNA construct directed by pCMV promoter in FVB/N mice. The vascular protective effect of PGI<sub>2</sub> is well demonstrated by studies that have shown an increase in the risk of heart attack associated with the use of COX-2 inhibitors, such as Vioxx. For decades, increasing PGI<sub>2</sub> level to prevent and treat vascular diseases, such as pulmonary arterial hypertension has been documented. Our results presented here are based on the hypothesis that the approach of increasing PGI<sub>2</sub> biosynthesis constantly in vivo could be a genetic and fundamental solution to reduce the risk for vascular and heart diseases. Encouraged by our PGI<sub>2</sub>-PSFC study results, we were able to generate transgenic mice overexpressing COX-1-10aa-PGIS and overproducing PGI<sub>2</sub>. Homozygous line of the transgenic mice was generated by breeding and all the animals had normal phenotype appearance as well as behaviour. Also LC/MS analysis of urine collected from the transgenic mice showed a 5 fold increase in PGI<sub>2</sub> compared to the wild type mice (Figure 22). This indicated that overexpression of COX-1-10aa-PGIS in mice had the functional triple catalytic activity.

In photochemical carotid artery injury model, both laser beam and rose bengal induce thrombosis in WT mice due to increase in the production of TXA<sub>2</sub>. Thus this model was a very good way to study the functional activity of COX-1-10aa-PGIS overexpression in transgenic mice. Transgenic mice (TG) induced with the carotid injury

protected themselves from thrombosis compared to the WT mice which showed a complete block in blood flow by the end of 2 hrs (Figure 27). The mechanism of action whereby COX-1-10aa-PGIS overexpression provides protection against the development of thrombogenesis are likely to be multifactorial. We propose here that the overexpressed COX-1-10aa-PGIS in the TG were able to divert and metabolize most of the AA released during injury towards production of PGI<sub>2</sub>. This in turn was able to inhibit the platelet aggregation and vasoconstriction effect of TXA<sub>2</sub>. Not only the actions of TXA<sub>2</sub> might be inhibited but its synthesis also might be decreased as indicated by an increase in perfusion. After studying the vascular protective effect of COX-1-10aa-PGIS overexpression in TG mice, it was also necessary to study the risks of the permanent upregulation of PGI<sub>2</sub> biosynthesis *in vivo*.

Bleeding time measurement indicated that the TG mice had an increase in bleeding time (Figure 23i) which indicated PGI<sub>2</sub> inhibitory function on platelets activation but also indicated caution in cases of surgery where excessive bleeding can take place during the process. Generation of transgenic mice are several times associated with embryonic lethality. However homozygous colony of TG mice producing PGI<sub>2</sub> rather showed an increase in the number of litters when compared to the wild types (Figure 25). This also further confirmed the reports that PGI<sub>2</sub> supports embryonic development. PGI<sub>2</sub> is a potent endogenous vasodilator and therefore it can cause lowering of blood pressure. Therefore it was necessary to measure blood pressure in the

transgenic mice. It was observed that both the systolic and diastolic blood pressure were similar to that of the wild type mice when measured using the tail cuff method (Figure 23ii). The reason behind no change may be either due to the variation involved with using the non invasive tail cuff method or due to any compensatory mechanism that regulated the blood pressure to normal in TG mice.

It was interesting to observe that PCR analysis and immunoblot analysis showed a wide expression of COX-1-10aa-PGIS in several organs like heart, kidney, lung, brain, and uterus (Figure 24). This indicated that the triple catalytic enzyme had the ability to express in several organs. Also the expression of COX-1-10aa-PGIS in the adipose tissue further confirmed our previous results in which we expressed this enzyme in the fat cells. Thus we propose in future to study the effect on miRNA expression regulation *in vivo* due to overexpression in adipose tissue and thus can confirm our miRNA results.

## 6. SUMMARY AND CONCLUSIONS

- 1) The adipose tissue derived mature adipocytes were successfully cultured and differentiated into cells producing predominantly PGE<sub>2</sub> and PGI<sub>2</sub> endogenously as analysed by LC/MS analysis. Therefore these cells were referred to as prostanoid synthesizing fat cells (PSFC).
- 2) PSFCs showed endogenous protein expression of COX-1, cPGES and PGIS. Thus enzyme activity assay by HPLC showed that exogenous AA was metabolized to PGE<sub>2</sub> and PGI<sub>2</sub>.
- 3) Stable expression of the triple catalytic enzyme (COX-1-10aa-PGIS) in PSFCs was achieved and these cells were capable of redirecting the endogenous and exogenous AA metabolism towards a stable and dominant production of PGI<sub>2</sub>. Therefore these cells were referred to as PGI<sub>2</sub> producing fat cells (PGI<sub>2</sub>-PSFCs).
- 4) The PGI<sub>2</sub>-PSFCs demonstrated superior anti-platelet aggregation in vitro and also protected the mice from thrombosis induced by photochemical vascular injury.

- 5) Transplantation of PGI<sub>2</sub>-PSFCs in mice with hindlimb ischemia increased reperfusion in the ischemic limb and subsequent increase in mobility and decrease in autoamputation of the mice.
  
- 6) MicroRNA microarray analysis revealed a significant upregulation (711, 148b and 744) and downregulation of miRNAs in PGI<sub>2</sub>-PSFCs as compared to PSFCs. Treating the PGI<sub>2</sub>-PSFCs with IP and PPAR $\gamma$  receptors antagonists reversed this effect.
  
- 7) Quantitative RT-PCR analysis to confirm the upregulation of miRNA 711 was performed and indicated a 6-fold increase in miRNA-711 in PGI<sub>2</sub>-PSFCs when compared with the PSFCs.
  
- 8) Insulin mediated lipid deposition was inhibited in the PGI<sub>2</sub>-PSFCs whereas PSFC showed significant lipid accumulation as indicated by red oil staining.
  
  
  
  
  
  
  
  
  
  
- 9) RNA illumina gene expression assay showed more than 2 fold increase and decrease in several mRNAs and one of them was Akt1, the predicted target of miRNA-711 which was decreased by 4 fold in PGI<sub>2</sub>-PSFCs.

- 10) Immunoblot analysis further confirmed that Akt1 protein expression is comparatively low with respect to PSFCs.
- 11) Transgenic mice overexpressing COX-10aa-PGIS were successfully generated by using pronuclear microinjection and were genotyped by tail clip PCR analysis.
- 12) The transgenic mice were successfully bred to get a colony of homozygous mice which showed no phenotypic physical change or anatomical changes.
- 13) Increase in the biosynthesis of PGI<sub>2</sub> and decrease in synthesis of other prostanoids was confirmed by performing LC/MS analysis of urine collected from the transgenic mice.
- 14) The transgenic mice showed an increase in bleeding time as well as increase in the number of litters produced after breeding the transgenic mice.
- 15) PCR analysis and immunoblot analysis of the different organs showed expression of COX-1-10aa-PGIS in heart, kidney, brain, uterus and adipose tissue of the transgenic mice

16) Transgenic mice significantly reversed the decrease in blood flow induced by photochemical carotid artery injury to normal whereas the wild type mice showed no recovery over time.

## 7. REFERENCES

- Ambros, V. (2004). "The functions of animal microRNAs". *Nature* 431: 350–355.
- Arehart E, Gleim S, Kasza Z, Fetalvero KM, Martin KA, Hwa J. (2007). "Prostacyclin, atherothrombosis, and cardiovascular disease". *Curr Med Chem* 14:2161–2169.
- Barst, R. J., Gibbs, J. S., Ghofrani, H. A., Hoeper, M. M., Mclaughlin, V. V., Rubin, L. J., Sitbon, O., Tapson, V. F., and Galie, N. (2009). "Updated evidence-based treatment algorithm in pulmonary arterial hypertension". *J. Am. Coll. Cardiol.* 54: S78–S84.
- Barst RJ, Rubin LJ, Long WA, *et al.* (1996). " A comparison of continuous intravenous epoprostenol (prostacyclin) with conventional therapy for primary pulmonary hypertension". *N Engl J Med.* 334:296–301.
- Becker, J., Delayre-Orthez, C., Frossard, N., and Pons, F. (2006). " Regulation of inflammation by PPARs: a future approach to treat lung inflammatory diseases?". *Fundam. Clin. Pharmacol.* 20, 429–447.
- Berman S, Quick R, Yoder P, Voigt S, Strootman D, Wade M. "Treprostinil sodium (Remodulin), a prostacyclin analog, in the treatment of critical limb ischemia: open-label study". *Vascular* 2006; **14**:142–148.
- Blenkiron, C., and Miska, E.A. (2007). " miRNAs in cancer: approaches, aetiology, diagnostics and therapy". *Hum. Mol. Genet.* 16: R106–R113.

- Boie Y, Rushmore TH, Darmongoodwin A et al.,(1994). "Cloning and expression of a Cdna for the human prostanoid Ip receptor". *J Biol Chem.* 269:12173-8
- Bombardier C, Laine L, Reicin A, et al. (2000). " Comparison of upper gastrointestinal toxicity of rofecoxib and naproxen in patients with rheumatoid arthritis. VIGOR Study Group". *N Engl J Med* 343:1520–1528.
- Braissant, O., Foufelle, F., Scotto, C., Dauca, M., and Wahli, W. (1996). "Differential expression of peroxisome proliferator-activated receptors (PPARs): tissue distribution of PPAR-alpha, -beta, and -gamma in the adult rat". *Endocrinology* 137, 354–366
- Brannon, T. S.; North, A. J.; Wells, L. B.; Shaul, P. W. (1994). "Prostacyclin synthesis in bovine pulmonary artery is developmentally regulated by changes in cyclooxygenase-1 gene expression". *J. Clin. In- vest.*, 93: 2230-2235.
- Bresalier RS, Sandler RS, Quan H, et al., (2005). "Cardiovascular events associated with rofecoxib in a colorectal adenoma chemoprevention trial". *N Engl J Med*, 352:1092–1102
- Bunting S, Gryglewski R, Moncada S, Vane JR. (1976). "Arterial walls generate from prostaglandin endoperoxide a substance (prostaglandin X) which relaxes strips of mesenteric and coeliac arteries and inhibits platelet aggregation". *Prostaglandins* 12: 897-913
- Cheng Y, Austin SC, Rocca B, (2002). "Role of prostacyclin in the cardiovascular response

to thromboxane A<sub>2</sub>". *Science* 296: 539-541

Christman, B. W., Mcpherson, C. D., Newman, J. H., King, G. A., Bernard, G. R., Groves, B. M., and Loyd, J. E. (1992). "An imbalance between the excretion of thromboxane and prostacyclin metabolites in pulmonary hypertension". *N. Engl. J. Med.* 327: 70–75.

Della Bella, S., Molteni, M., Mocellin, C., Fumagalli, S., Bonara, P., and Scorza, R. (2001). "Novel mode of action of iloprost: *in vitro* down-regulation of endothelial cell adhesion molecules". *Prostaglandins Other Lipid Mediat.* 65: 73–83.

Deng H, Wu J, So SP, Ruan KH.(2003). Identification of the residues in the helix F/G loop important to catalytic function of membrane-bound prostacyclin synthase". *Biochemistry* 42:5609–5617.

Denizot Y, Dulery C, Trimoreau F, Desplat V, Praloran V.(1998). "Arachidonic acid and human bone marrow stromal cells". *Biochim Biophys Acta* 1402:209–215.

DeWitt DL, Smith WL (1983). "Purification of prostacyclin synthase from bovine aorta by immunoaffinity chromatography. Evidence that the enzyme is a hemoprotein". *J. Biol. Chem.* 258 (5): 3285–93.

Dewitt DL (1991). "Prostaglandin endoperoxide synthase: Regulation of enzyme expression". *Biochim. Biophys. Acta* 1083: 121-134.

Du, T., and Zamore, P.D. (2007). "Beginning to understand microRNA function". *Cell Res.* 17: 661–663

- Egan KM, Lawson JA, Fries S, Koller B, Rader DJ, Smyth EM, Fitzgerald GA (2004). "COX-2-derived prostacyclin confers atheroprotection on female mice". *Science* 10;306(5703):1954-7.
- Esau, C., Davis, S., Murray, S.F., Yu, X.X., Pandey, S.K., Pear, M., Watts, L., Booten, S.L., Graham, M., McKay, R., Subramaniam, A., Propp, S., Lollo, B.A., Freier, S., Bennett, C.F., Bhanot, S., and Monia, B.P. (2006). "miR-122 regulation of lipid metabolism revealed by *in vivo* antisense targeting". *Cell Metab.* 3: 87–98.
- Fajas, L., Auboeuf, D., Raspé, E., Schoonjans, K., Lefebvre, A.M., Saladin, R., Najib, J., Laville, M., Fruchart, J.C., Deeb, S., Vidal-Puig, A., Flier, J., Briggs, M.R., Staels, B., Vidal, H., and Auwerx, J. (1997). "The organization, promoter analysis, and expression of the human PPAR $\gamma$  gene". *J. Biol. Chem.* 272: 18779–18789.
- Falcetta, E., Flavell, D.M., Staels, B., Tinker, A., Haworth, S.G., and Clapp, L.H. (2007). "IP receptor-dependent activation of PPAR $\gamma$  by stable prostacyclin analogues". *Biochem Biophys Res Commun.* 360: 821–827.
- Farber, H. W., and Loscalzo, J. (2004). "Pulmonary arterial hypertension". *N. Engl. J. Med.* 351:1655–1665.
- Farh, K.K., Grimson, A., Jan, C., Lewis, B.P., Johnston, W.K., Lim, L.P., Burge, C.B., and Bartel, D.P. (2005). "The widespread impact of mammalian microRNAs on mRNA repression and evolution". *Science* 310: 1817–1821.
- Fetalvero KM, Shyu M, Nomikos AP, et al (2006). "The prostacyclin receptor induces

- human vascular smooth muscle cell differentiation via the protein kinase A pathway. *Am J Physiol Heart Circ Physiol* 290:H1337–46.
- Fetalvero, K. M., Martin, K. A., and Hwa, J. (2007). “Cardioprotective prostacyclin signaling in vascular smooth muscle”. *Prostaglandins Other Lipid Mediat.* 82: 109–118.
- FitzGerald GA.(1991).”Mechanisms of platelet activation—thromboxane-A<sub>2</sub> as an amplifying signal for other agonists”. *Am J Cardiol* 68:B11–5.
- Forman BM, Chen J, Evans RM. (1997). “Hypolipidemic drugs, polyunsaturated fatty acids, and eicosanoids are ligands for peroxisome proliferator-activated receptors alpha and delta”. *Proc Natl acad Sci USA* 94:4312-7
- Fritzius, T., and Moelling, K. (2008). “Akt- and Foxo1-interacting WD-repeat-FYVE protein promotes adipogenesis”. *Embo J.* 27: 1399–1410.
- Funk C, Funk ME, Kennedy, GA Fitzcerald. (1991). “Human platelet/erythro leukemia cell prostaglandin G/H synthase: cDNA cloning, expression, and gene chromosomal assignment”. *Faseb j.* 5: 2304-23 12.
- Funk CD.(2001).” Prostaglandins and leukotrienes: advances in eicosanoid biology”. *Science* 294, 1871–1875.
- Galie, N., M. Humbert, J. L. Vachiery, et al. (2002). “Effects of beraprost sodium, an oral

prostacyclin analogue, in patients with pulmonary arterial hypertension: a randomized, double-blind, placebo-controlled trial". *J Am Coll Cardiol* 39: 1496-502

Georges Vassaux, Danielle Gaillard, Gerard Ailhaud, and Raymond Negrel. (1992).

"Prostacyclin Is a Specific Effector of Adipose Cell Differentiation". *The Journal of biological Chemistry*. 267: 16: 11092-11097

Geraci MW, Gao B, Shepherd DC, *et al.* (1999). "Pulmonary prostacyclin synthase overexpression in transgenic mice protects against development of hypoxic pulmonary hypertension". *J Clin Invest* 103:1509–1515.

Gimble, J., Guilak, F., (2003). "Adipose-derived adult stem cells: isolation, characterization, and differentiation potential". *Cytotherapy* 5 :5: 362-369.

Gomberg-Maitland M, Olschewski H.(2008) "Prostacyclin therapies for the treatment of pulmonary arterial hypertension". *Eur Respir J* 31:891–901.

Hajjar, D. P., and Weksler, B. B. (1983). "Metabolic activity of cholesteryl esters in aortic smooth muscle cells is altered by prostaglandins I<sub>2</sub> and E<sub>2</sub>". *J. Lipid Res*. 24:1176–1185.

Hansson GK, Libby P. (2006). "The immune response in atherosclerosis: a double-edged sword". *Nat Rev Immunol* 6:508–519.

Hara S, Miyata A, Yokoyama C (1995). "Molecular-cloning and expression of prostacyclin synthase from endothelial-cells". *Prostaglandins Relat Compd* 23:121–3.

- Hara S, Morishita R, Tone Y, et al.(1995). "Overexpression of prostacyclin synthase Inhibits growth of vascular smooth muscle cells". *Biochem Biophys Res Commun* 216:862-7
- Hatae N, Yamaoka K, Sugimoto Y, Negishi M, Ichikawa A (2002). "Augmentation of receptor-mediated adenylyl cyclase activity by Gi-coupled prostaglandin receptor subtype EP3 in a G betagamma subunit-independent manner". *Biochem Biophys Res Commun* 290:162–168.
- Hatae T, Wada M, Yokoyama C, Shimonishi M, Tanabe T.(2001). "Prostacyclin dependent apoptosis mediated by PPAR $\delta$ ". *J Biol Chem* 276:46260–46267
- He T, Lu T, D'Uscio LV.(2008). "Angiogenic function of prostacyclin biosynthesis in human endothelial progenitor cells". *Circ Res* 103(1):80–8.
- Heng Lin, Teng-Nan Lin, Wai-Mui Cheung, Gau-Ming Nian, Ping-Hui Tseng, Shu-Fen Chen, Jean-Ju Chen, Song-Kun Shyue, Jun-Yang Liou, Cheng-Wen Wu, and Kenneth K. Wu. (2002). "Cyclooxygenase-1 and Bicistronic Cyclooxygenase-1/Prostacyclin Synthase Gene Transfer Protect Against Ischemic Cerebral Infarction" . *Circulation* ;105:1962-1969.
- Herschman, H. R.(1999). "Function and regulation of prostaglandin synthase 2". *Adv. Exp. Med. Biol.*, 469: 3-8.
- Hinderliter AL, Willis PW, Barst RJ, Rich S, Rubin LJ, Badesch DB, Groves BM, McGoon MD, Tapson VF, Bourge RC, Brundage BH, Koerner SK, Langleben D, Keller CA,

- Murali S, Uretsky BF, Koch G, Li S, Clayton LM, Jöbsis MM, Blackburn SD, Crow JW, Long WA. (1997). "Effects of long-term infusion of prostacyclin (epoprostenol) on echocardiographic measures of right ventricular structure and function in primary pulmonary hypertension". *Circulation*. 95:1479–1486
- Hinz B, Brune K. (2002). "Cyclooxygenase-2: 10 years later". *J Pharmacol Exp Ther* 300:367-375.
- Hodnett, B.L., Dearman, J.A., Carter, C.B., and Hester, R.L. (2009). "Attenuated PGI<sub>2</sub> synthesis in obese Zucker rats". *Am. J. Physiol. Regul. Integr. Comp. Physiol.* 296: R715–R721.
- Hoepfer MM, Schwarze M, Ehlerding S, Adler-Schuermeyer A, Spiekerkoetter E, Niedermeyer J, Hamm M, and Fabel H (2000b). "Long-term treatment of primary pulmonary hypertension with aerosolized iloprost, a prostacyclin analogue". *N Engl J Med* 342:1866–1870.
- Hwang, H.W., and Mendell, J.T. (2006). "MicroRNAs in cell proliferation, cell death, and tumorigenesis". *Br. J. Cancer*. 94, 776–780.
- Hyun Jung Lim and Sudhansu K. Dey. (2002). "Minireview: A Novel Pathway of Prostacyclin Signaling—Hanging Out with Nuclear Receptors". *Endocrinology* 143(9):3207–3210
- Hyun Jung Lim, Rajnish A.Gupta, Wen-ge Ma, Bibhash C. Paria, David E. Moller, Jason D.

- Morrow, Raymond N. DuBois, James M.Trzaskos, and Sudhansu K. Dey. (1999). "Cyclo-oxygenase-2-derived prostacyclin mediates embryo implantation in the mouse via PPAR $\delta$ ". *Genes & Dev.* 13: 1561-1574
- Idzko, M., Hammad, H., Van Nimwegen, M., Kool, M., Vos, N., Hoogsteden, H. C., and Lambrecht, B. N. (2007). "Inhaled iloprost suppresses the cardinal features of asthma via inhibition of airway dendritic cell function". *J. Clin. Invest.* 117, 464–472.
- Jaschonek K, Faul C, Schmidt H, RennW.(1988). "Desensitization of platelets to iloprost—loss of specific binding-sites and heterologous desensitization of adenylate-cyclase". *Eur J Pharmacol* 147:187–96.
- Jovanovic, M., and Hengartner, M.O. (2006). "miRNAs and apoptosis: RNAs to die for". *Oncogene.* 25:6176–6187.
- Kajimoto, K., Naraba, H., and Iwai, N. (2006). "MicroRNA and 3T3-L1 pre-adipocyte differentiation". *RNA* 12:1626–1632.
- Kasza, Z., Fetalvero, K.M., Ding, M., Wagner, R.J., Acs, K., Guzman, A.K., Douville, K.L., Powell, R.J., Hwa, J., and Martin, K.A. (2009). "Novel signaling pathways promote a paracrine wave of prostacyclin-induced vascular smooth muscle differentiation". *J. Mol. Cell. Cardiol.* 46:682–694.
- Ke-He Ruan, and Jean-Michel Dogné.(2006). "Implications of the Molecular Basis of

Prostacyclin Biosynthesis and Signaling in Pharmaceutical Designs". *Current Pharmaceutical Design*, 12: 925-941

Kerbaul F, Brimiouille S, Rondelet B, Dewachter C, Hubloue I, Naeije R. (2007). "How prostacyclin improves cardiac output in right heart failure in conjunction with pulmonary hypertension". *Am J Respir Crit Care Med* 175:846–850.

Kleiveland CR, Kassem M, Lea T.(2008). "Human mesenchymal stem cell proliferation is regulated by PGE<sub>2</sub> through differential activation of cAMP-dependent protein kinase isoforms". *Exp Cell Res* 314:1831–1838.

Kliewer SA, Umesono K, Noonan DJ, Heyman RA, Evans RM. (1992). "Convergence of 9-*cis* retinoic acid and peroxisome proliferator signalling pathways through heterodimer formation of their receptors". *Nature* 358:771–774

Kliewer, S.A., Forman, B.M., Blumberg, B., Ong, E.S., Borgmeyer, U., Mangelsdorf, D.J., Umesono, K., and Evans, R.M. (1994). "Differential expression and activation of a family of murine peroxisome proliferator-activated receptors". *Proc Natl Acad Sci USA*. 91: 7355–7359

Kurumbail, R.G., et al.(1996). "Structural basis for selective inhibition of cyclooxygenase-2 by anti-inflammatory agents". *Nature* 384: 644-648

Lefebvre, P., Chinetti, G., Fruchart, J.C., and Staels, B. (2006). "Sorting out the roles of PPAR $\alpha$  in energy metabolism and vascular homeostasis". *J. Clin. Invest.* 116: 571–580.

- Lewis P.J. and Drollery C.T. (1983). "Clinical pharmacology and potential of prostacyclin".  
*Br.Med. Bull.* 39:281-284
- Lim H, Gupta RA, Ma WG, Paria BC, Moller DE, Morrow JD, DuBois RN, Trzaskos JM, Dey SK. (1999). "Cyclo-oxygenase-2-derived prostacyclin mediates embryo implantation in the mouse via PPAR $\delta$ ". *Genes Dev* 13:1561–1574
- Liou, J. Y., Shyue, S. K., Tsai, M. J., Chung, C. L., & Wu, K. K. (2000). "Colocalization of prostacyclin synthase with prostaglandin H synthase-1 (PGHS-1) but not phorbol ester-induced PGHS-2 in cultured endothelial cells". *J Biol Chem* 275(20): 15314–15320.
- Majerus, P.W. (1983). "Arachidonate metabolism in vascular disorders". *J. Clin. Invest.* 72: 1521–1525.
- Massiera, F., Saint-Marc, P., Seydoux, J., Murata, T., Kobayashi, T., Narumiya, S., Guesnet, P., Amri, E.Z., Negrel, R., and Ailhaud, G. (2003). "Arachidonic acid and prostacyclin signaling promote adipose tissue development: a human health concern?" *J.Lipid Res.* 44: 271–279.
- Melanie Wosnitza, Karsten Hemmrich, Andreas Groger, Steffen Graber and Norbert Pallua.(2007). "Plasticity of human adipose stem cells to perform adipogenic and endothelial differentiation". *Differentiation* 75:12–23
- Min-Chen Tsai, Lihong Chen, Jing Zhou, Zhihui Tang, Tzu-Fang Hsu, Ying Wang, Yu-Tsung

Shih, Hsin-Hsin Peng, Nanping Wang, Youfei Guan, Shu Chen, Jeng-Jiann Chiu.(2009). "Shear stress induces synthetic-to-contractile phenotypic modulation in smooth muscle cells via peroxisome proliferator-activated receptor  $\alpha/\delta$  activations by prostacyclin released by sheared endothelial cells". *Circulation Research* 105:471-480

Miranville A, Heeschen C, Sengenès C, Curat CA, Busse R, Bouloumie A. "Improvement of postnatal neovascularization by human adipose tissue-derived stem cells". *Circulation* 110 (3):349-355

Miyahara Y, Nagaya N, Kataoka M, Yanagawa B, Tanaka K, Hao H, Ishino K, Ishida H, Shimizu T, Kangawa K, Sano S, Okano T, Kitamura S, Mori H., (2006). "Monolayered mesenchymal stem cells repair scarred myocardium after myocardial infarction". *Nature Medicine* 12 (4): 459-465.

Miyamoto K, Nishigami K, Nagaya N, et al. (2006). "Unblinded pilot study of autologous transplantation of bone marrow mononuclear cells in patients with thromboangiitis obliterans". *Circulation* 114(24): 2679–84.

Moncada, S., Herman, A.G., Higgs, E.A., and Vane, J.R. (1997). "Differential formation of prostacyclin (PGX or PGI<sub>2</sub>) by layers of the arterial wall. An explanation for the anti-thrombotic properties of vascular endothelium" *Thromb. Res.* 11: 323–344.

Moncada,S. & Amezcua, J. L. (1979). "Prostacyclin, thromboxane A<sub>2</sub> interactions in haemostasis and thrombosis". *Haemostasis* 8: 252-265

- Moncada, S., Gryglewski, R., Bunting, S. & Vane, J. R. (1976a). "An enzyme isolated from arteries transforms prostaglandin endoperoxides to an unstable substance that inhibits platelet aggregation". *Nature* 263: 663–665.
- Morita I. (2002). "Distinct functions of COX-1 and COX-2". *Prostaglandins Other Lipid Mediators* 68/69: 165-175
- Mroske, C.; Plant, M. H.; Franks, D. J.; Laneuville, O. (2000). "Characterization of prostaglandin endoperoxide H synthase-1 enzyme expression during differentiation of the megakaryocytic cell line MEG- 01". *Exp. Hematol* 28: 411-421.
- Murata, T., Ushikubi, F., Matsuoka, T., Hirata, M., Yamasaki, A., Sugimoto, Y., Ichikawa, A., Aze, Y., Tanaka, T., Yoshida, N., Ueno, A., Oh-Ishi, S., and Narumiya, S. (1997). "Altered pain perception and inflammatory response in mice lacking prostacyclin receptor." *Nature* 388: 678-682
- Nagaya N, Yokoyama C, Kyotani S, *et al.* (2000). "Gene transfer of human prostacyclin synthase ameliorates monocrotaline-induced pulmonary hypertension in rats. *Circulation* 102:2005–2010.
- Nakae, J., Kitamura, T., Kitamura, Y., Biggs, W.H. 3rd, Arden, K.C., and Accili, D. (2003). "The forkhead transcription factor Foxo1 regulates adipocyte differentiation". *Dev. Cell.* 4: 119–129.

Narumiya, S., Sugimoto, Y., and Ushikubi, F. (1999). "Prostanoid receptors: structures, properties, and functions,". *Physiol Rev.* 79: 1193–1226.

Needleman, P., Turk, J., Jackschik, B. A., Morrison, A. R. and Leflowithz, J.B. (1986). "Arachidonic acid metabolism". *Ann.Rev. Biochem.*55: 69-102

Nithipatikom K, Laabs ND, Isbell MA, Campbell WB. (2003). "Liquid chromatographic-mass spectrometric determination of cyclooxygenase metabolites of arachidonic acid in cultured cells". *J Chromatogr B Analyt Technol Biomed Life Sci* 785:135–145.

Noritoshi Nagaya, Chieko Yokoyama, Shingo Kyotani, Manabu Shimonishi, Ryuichi Morishita, Masaaki Uematsu, Toshio Nishikimi, Norifumi Nakanishi, Toshio Ogihara, Masakazu Yamagishi, Kunio Miyatake, Yasufumi Kaneda, Tadashi Tanabe. (2000). "Gene Transfer of Human Prostacyclin Synthase Ameliorates Monocrotaline-Induced Pulmonary Hypertension in Rats". *Circulation.* 102:2005-2010

Olschewski H, Simonneau G, Galie N, *et al.* (2002). "Inhaled iloprost for severe pulmonary hypertension". *N Engl J Med* 347:322–329.

Owens GK, Kumar MS, Wamhoff BR. (2004). "Molecular regulation of vascular smooth muscle cell differentiation in development and disease". *Physiol Rev* 84:767–801.

Páramo, J.A., Orbe, J., Beloqui, O., Colina, I., Benito, A., Rodríguez, J.A., and Díez, J.

- (2008). "Association of age, inflammatory markers and subclinical atherosclerosis in subjects free from cardiovascular disease". *Med Clin (Barc)*. 131: 361–366.
- Pasquinelli, A.E., Hunter, S., and Bracht, J. (2005). "MicroRNAs: a developing story". *Curr Opin Genet Dev*. 15: 200–205.
- Pavel Poredos. (2000). "Possibilities for clinical use of prostacyclin in vascular disease". *Pflügers Arch - Eur J Physiol* 440 [Suppl]: R137-R138
- Planat-Benard, V, Menard C, Andre M, Puceat M, Perez A, Garcia-Verdugo JM, Penicaud L, Casteilla L, (2004). "Spontaneous cardiomyocyte differentiation from adipose tissue stromal cells". *Circulation Research* 94 (2), 223-229.
- Planat-Benard V, Silvestre JS, Cousin B, *et al.* (2004). "Plasticity of human adipose lineage cells toward endothelial cells: physiological and therapeutic perspectives". *Circulation* 109:656–663
- Pomerantz, K. B., Fleisher, L. N., Tall, A. R., and Cannon, P. J. (1985). "Enrichment of endothelial cell arachidonate by lipid transfer from high density lipoproteins: relationship to prostaglandin I<sub>2</sub> synthesis". *J. Lipid Res*. 26: 1269–1276.
- Poy, M.N., Eliasson, L., Krutzfeldt, J., Kuwajima, S., Ma, X., Macdonald, P.E., Pfeffer, S., Tuschl, T., Rajewsky, N., Rorsman, P., and Stoffel, M. (2004). "A pancreatic islet-specific microRNA regulates insulin secretion". *Nature* 432: 226–230.
- Rane, S., Sayed, D., and Abdellatif, M. (2007). "MicroRNA with a MacroFunction". *Cell Cycle* .6: 1850–1855.

- Robyr D, Wolffe AP, Wahli W. (2000). "Nuclear hormone receptor coregulators in action: diversity for shared tasks". *Mol Endocrinol* 14:329–347
- Rodriguez, A., Vigorito, E., Clare, S., Warren, M.V., Couttet, P., Soond, D.R., van Dongen, S., Grocock, R.J., Das, P.P., Miska, E.A., Vetrie, D., Okkenhaug, K., Enright, A.J., Dougan, G., Turner, M., and Bradley, A. (2007). "Requirement of bic/microRNA-155 for normal immune function". *Science* 316: 608–611.
- Ruan KH, Deng H, So SP. (2006). Engineering of a protein with cyclooxygenase and prostacyclin synthase activities that converts arachidonic acid to prostacyclin". *Biochemistry* 45:14003–14011.
- Ruan, K.H., So, S.P., Cervantes, V., Wu, H., Wijaya, C., and Jentzen, R.R. (2008). "An active triple-catalytic hybrid enzyme engineered by linking cyclo-oxygenase isoform-1 to prostacyclin synthase that can constantly biosynthesize prostacyclin, the vascular protector". *Febs J* 275: 5820–5829.
- Ruan KH, Deng H, Wu J, So SP. (2005). „The N-terminal membrane domain of the membrane-bound prostacyclin synthase involved in the substrate presentation in the coupling reaction with cyclooxygenase". *Arch Biochem Biophys* 435:372–381.
- Ruan, K.H., So, S.P., Wu, H., and Cervantes, V. (2008). "Large-scale expression, purification, and characterization of an engineered prostacyclin-synthesizing enzyme with therapeutic potential". *Arch. Biochem. Biophys.* 480: 41–50

- Samuelsson B, Goldyne M, Granstrom E, Hamberg M, Hammarstrom S, Malmsten C. (1978). "Prostaglandins and thromboxanes". *Annu Rev Biochem* 47:997–1029.
- Santhanam AV, Smith LA, He T, Nath KA, Katusic ZS. (2007). "Endothelial progenitor cells stimulate cerebrovascular production of prostacyclin by paracrine activation of cyclooxygenase-2". *Circ Res* 100(9):1243–5.
- Schmidt P, Youhnovski N, Daiber A, Balan A, Arsic M, Bachschmid M, Przybylski M, Ullrich V. (2003). "Specific nitration at tyrosine 430 revealed by high resolution mass spectrometry as basis for redox regulation of bovine prostacyclin synthase". *J Biol Chem* 278 : 12813 –12819
- Shyue SK, Tsai MJ, Liou JY, et al. (2001). "Selective augmentation of prostacyclin production by combined prostacyclin synthase and cyclooxygenase-1 gene transfer". *Circulation*. 103:2090 –2095.
- Simonneau G, Barst RJ, Galie N, et al. (2002). "Continuous subcutaneous infusion of treprostinil, a prostacyclin analogue, in patients with pulmonary arterial hypertension: a double-blind, randomized, placebo-controlled trial". *Am J Respir Crit Care Med* 165:800–804.
- Sitbon O, Humbert M, Nunes H, Parent F, Garcia G, Herve P, Rainisio M, Simonneau G. (2002). "Long-term intravenous epoprostenol infusion in primary pulmonary hypertension: prognostic factors and survival". *J Am Coll Cardiol*. 40(4): 780-8.

- Smith WL, DeWitt DL, Allen ML .(1983). "Bimodal distribution of the prostaglandin I<sub>2</sub> synthase antigen in smooth muscle cells". *J Biol Chem* 258:5922–5926
- Smith WL, Song I. (2002). "The enzymology of prostaglandin endoperoxide H synthases-1 and -2". *Prostaglandins Other Lipid Mediat* 68- 69: 115-28.
- Smith, W. L.; Dewitt, D. L. (1996). "Prostaglandin endoperoxide H synthases-1 and -2". *Adv. Immunol* 62: 167-215.
- Smith, W. (1997). "Molecular biology of prostanoid biosynthetic enzymes and receptors". *Adv. Exp. Med. Biol.* 400B: 989-1011.
- Smith, C. J.; Morrow, J. D.; Roberts, L. J., Marnett, L. J. (1993). "Differentiation of monocytoid THP-1 cells with phorbol ester induces expression of prostaglandin endoperoxide synthase-1 (COX-1)". *Biochem. Biophys. Res. Commun.*, 192: 787-793.
- Smyth, E.M, and FitzGerald, G.A. (2002). "Human prostacyclin receptor". *Vitam.Horm.*65: 149-165
- Smyth, E. M., Grosser, T., Wang, M., Yu, Y., and Fitzgerald, G. A. (2009). "Prostanoids in health and disease". *J. Lipid Res.* 50(Suppl.), S423–S428
- Stryer, H.C. (2003). "Atlas of Atherosclerosis: Progression and Regression". 2<sup>nd</sup> ed. Parthenon Publishing Group. New York, NY.
- Stitham J, Stojanovic A, Ross LA, Blount AC, Hwa J. (2004). "Clusters of transmembrane

residues are critical for human prostacyclin receptor activation". *Biochemistry* 43:8974-86

Strong, J.P., Malcom, G.T., McMahan, C.A., Tracy, R.E., Newman, W.P. and Herderick, E.E., (1999). "Prevalence and extent of atherosclerosis in adolescents and young adults: implications for prevention from the Pathobiological Determinants of Atherosclerosis in Youth Study" *JAMA*. 281: 727–735.

Suhara H, Sawa Y, Fukushima N, *et al.* (2002). "Gene transfer of human prostacyclin synthase into the liver is effective for the treatment of pulmonary hypertension in rats". *J Thorac Cardiovasc Surg* 123:855–861.

Tahara N, Kai H, Niiyama H, *et al.* (2004). "Repeated gene transfer of naked prostacyclin synthase plasmid into skeletal muscles attenuates monocrotaline-induced pulmonary hypertension and prolongs survival in rats". *Hum Gene Ther* 15:1270–1278.

Tang, Q.Q., Zhang, J.W., and Daniel Lane, M. (2004). "Sequential gene promoter interactions by C/EBPbeta, C/EBPalpha, and PPARgamma during adipogenesis". *Biochem. Biophys. Res. Commun.* 318: 213–218.

Tateishi-Yuyama E, Matsubara H, Murohara T. (2002). "Therapeutic Angiogenesis using Cell Transplantation (TACT) Study Investigators. Therapeutic angiogenesis for patients with limb ischaemia by autologous transplantation of bone-marrow cells: a pilot study and a randomised controlled trial". *Lancet* 360(9331):427–35.

- Tateson JE, Moncada S, Vane JR. (1977). "Effects of prostacyclin (Pgx) on cyclic-Amp concentrations in human platelets". *Prostaglandins* 13:389–97.
- Taylor L, Foxall T, Auger K, Heinsohn C, Polgar P. (1987). "Comparison of prostaglandin synthesis by endothelial cells from blood vessels originating in the rat, baboon, calf and human". *Atherosclerosis* 65:227–236.
- Thomas CE, Ehrhardt A, Kay MA. (2003). "Progress and problems with the use of viral vectors for gene therapy". *Nat Rev Genet.* 4(5):346-58.
- Todaka T, Yokoyama C, Yanamoto H, et al. (1999). "Gene transfer of human prostacyclin synthase prevents neointimal formation after carotid balloon injury in rats". *Stroke* 30:419–26.
- Tuder, R M, Cool, C.D., Geraci, M.W., Wang J, Abman SH., Wright L, Badesch, D, and Voelkel, N. F (1999). "Prostacyclin synthase expression is decreased in lungs from patients with severe pulmonary hypertension." *Am.J. Respir.Crit.Care Med.* 159: 1925-1932.
- Ullrich V, Castle L, Weber P. (1981). "Spectral evidence for the cytochrome p450 nature of prostacyclin synthase". *Biochem Pharmacol* 30: 2033-6.
- Van Rooij, E., and Olson, E.N. (2007). "MicroRNAs: powerful new regulators of heart disease and provocative therapeutic targets". *J. Clin. Invest.* 117: 2369–2376.
- Vane, J., and Corin, R.E. (2003). "Prostacyclin: a vascular mediator". *Eur. J. Vasc.*

- Endovasc. Surg* 26: 571–578.
- Wise, H. (2003). “Multiple signaling options for prostacyclin”. *Acta Pharmacol. Sin.* 24: 625–630.
- Wong DR, Wang MA, Cheng Y, FitzGerald GA.(2005). “Cardiovascular hazard and non-steroidal anti-inflammatory drugs”. *Curr Opin Pharmacol* 5:204–10.
- Wu, K. K., & Liou, J. Y. (2005). “Cellular and molecular biology of prostacyclin synthase”. *Biochem Biophys Res Commun* 338(1), 45–52.
- Xiao, C.Y.Hara, A., Yuhki Ki K., Fujino, T., Ma, H., Okada, Y., Takahata, O., Yamada, T., Murata, T., Narumiya, S., and Ushikubi, F. (2001). “Roles of prostaglandin I(2) and thromboxane A(2) in cardiac ischemia-reperfusion injury: a study using mice lacking their respective receptors”. *Circulation* 104: 2210-2215
- Xie W, Merrill JR, Bradshaw WS, Simmons DL. (1993). “Structural determination and promoter analysis of the chicken mitogen-inducible prostaglandin G/H synthase gene and genetic mapping of the murine homolog. *Arch Biochem Biophys* 300:247–52.
- Yamada M, Numaguchi Y, Okumura K, et al. (2002). “Prostacyclin synthase gene transfer modulates cyclooxygenase-2-derived prostanoid synthesis and inhibits neointimal formation in rat balloon-injured arteries”. *Arterioscler Thromb Vasc Biol* 22:256–62
- Yang P, Felix E, Madden T, Fischer SM, Newman RA. (2002). “Quantitative high-

performance liquid chromatography/electrospray ionization tandem mass spectrometric analysis of 2- and 3-series prostaglandins in cultured tumor cells". *Anal Biochem* 308:168–177.

Yasushi Numaguchi; Keiji Naruse; Mitsunori Harada; Hiroyuki Osanai; Shinji Mokuno; Kichiro Murase; Hideo Matsui; Yukio Toki; Takayuki Ito; Kenji Okumura; Tetsuo Hayakawa.(1999).“Prostacyclin Synthase Gene Transfer Accelerates Reendothelialization and Inhibits Neointimal Formation in Rat Carotid Arteries After Balloon Injury”. *Arteriosclerosis, Thrombosis, and Vascular Biology*. 19:727-733.

Yatrik M Shah, Keiichirou Morimura, Qian Yang, Tomotaka Tanabe, Mitsuhiro Takagi, and Frank J.Gonzalez. (2007). “Peroxisome Proliferator-Activated Receptor  $\alpha$  Regulates a MicroRNA-Mediated Signaling Cascade Responsible for Hepatocellular Proliferation”. *Molecular and Cellular Biology* 27:12

Yokoyama, C.; Yabuki, T.; Shimonishi, M.; Wada, M.; Hatae, T.; Ohkawara, S.; Takeda, J.; Kinoshita, T.; Okabe, M.; Tanabe, T. (2002). “Prostacyclin-deficient mice develop ischemic renal disorders, including nephrosclerosis and renal infarction” *Circulation*, 106: 2397.

Yue H, Jansen SA, Strauss KI, *et al.* (2007). “A liquid chromatography/mass spectrometric method for simultaneous analysis of arachidonic acid and its endogenous eicosanoid metabolites prostaglandins, dihydroxyeicosatrienoic acids,

hydroxyeicosatetraenoic acids, and epoxyeicosatrienoic acids in rat brain tissue".

*J Pharm Biomed Anal* 43:1122–1134.

Yun, S.J., Kim, E.K., Tucker, D.F., Kim, C.D., Birnbaum, M.J., and Bae, S.S. (2008).

"Isoform-specific regulation of adipocyte differentiation by Akt/protein kinase Balpha". *Biochem. Biophys. Res. Comm.* 371: 138–143.

Zhang J, Fu M, Zhu X, Xiao Y, Mou Y, Zheng H, Akinbami MA, Wang Q, Chen YE. (2002).

"Peroxisome proliferator- activated receptor $\delta$  is upregulated during vascular lesion formation and promotes post-confluent cell proliferation in vascular smooth muscle cells". *J Biol Chem* 277:11505–11512

Zoldhelyi P, McNatt J, Xu XM, et al. (1996). "Prevention of arterial thrombosis by adenovirus-mediated transfer of cyclooxygenase gene". *Circulation.* 93:10 –17